

Characterization of a LRRK2 (PARK8) Homologue in Drosophila melanogaster

by

Michael Craig Nightingale, B.Sc.

A thesis submitted to the

School of Graduate Studies

in partial fulfillment of the requirements for the degree of

Master of Science

Department of Biology

Memorial University of Newfoundland

2023

St. John's

Newfoundland and Labrador

Abstract

Parkinson Disease is the second-most common neurodegenerative disorder and is caused by a loss of dopamine-producing neurons in the *substantia nigra* region of the brain. The disease is characterized by symptoms of involuntary tremors, weakness, and a characteristic posture in which the trunk of the body is bent forward. Variations in the *LRRK2* gene may be responsible for up to 13% of monogenic and 5% of sporadic cases of the disease, which would make it one of the most common causes of Parkinson Disease. Despite the prevalence of *LRRK2*-linked cases of Parkinson Disease, the role that *LRRK2* plays in Parkinson Disease pathogenesis is still unclear. This study focuses on the examination of the *Drosophila melanogaster Lrrk* gene, a homologue of the human *LRRK2* gene, in order to gain a better understanding of *LRRK2* and its role in Parkinson Disease. Bioinformatic comparison of the human *LRRK2* and *Drosophila Lrrk* protein suggests that the functions of these proteins are similar in both humans and *Drosophila*. Examination of a *Drosophila Lrrk* loss-of-function mutation was found to result in loss of climbing ability at eclosion, which indicates the possibility of abnormalities in dopamine-producing neurons, as well as other phenotypes that suggest an upregulation of dopamine synthesis. A P-element insertion into the promoter region of the *Lrrk* gene was found to induce the sporadic formation of melanotic tumors in *Drosophila* larvae, further supporting a possible link between dopamine synthesis and the *Lrrk* gene. As dopamine-producing neurons are at risk of cell death in Parkinson Disease, these results suggest a possible link between *LRRK2* and regulation of dopamine synthesis in Parkinson Disease pathogenesis. In addition to links to dopamine synthesis, the phenotypes suggest the possibility of changes in Notch signalling. Finally, *Drosophila Lrrk* was found to interact with Gal4-induced toxicity when Gal4 was expressed through use of the *Ddc:Gal4* driver, which supports a possible role for *Lrrk* in protein degradation.

Acknowledgements

When I started this Masters project in 2006, I never expected its completion would extend to 2023. During this lengthy journey, I have received invaluable support from many people that has enabled me to finally finish this work. I am grateful to my thesis supervisor, Dr. Brian Staveley, for his guidance throughout the process. Without his support I would not have had the opportunity to return to the program to complete this thesis. My time in Dr. Staveley's lab was a formative experience, helping me develop critical research skills and deepening my understanding of the scientific process - lessons that continue to shape my career as an educator today. I also wish to thank my committee members, Dr. Andrei Igamberdiev and Dr. Tom Chapman, for lending their expertise and thoughtful feedback to strengthen my work. Additionally, I am thankful to Meghann Kenkel for her tireless assistance in reviewing my drafts and providing helpful editing advice, as well as for cheering me on towards the finish line. I would also like to thank my family for their support during times when I was struggling with my mental health. Without their care and understanding, I may not have emerged from those challenges successfully, let alone been able to complete this work. Although the journey has been longer than anticipated, I am happy to have had this opportunity to finish what I started so long ago. Thank you to everyone that helped me to reach this goal. You have helped in making this achievement possible. I am deeply appreciative.

Table of Contents

Abstract.....	i
Acknowledgements.....	ii
Table Contents	iii
List of Figures.....	vi
List of Tables	viii
List of Common Abbreviations	ix
Introduction and Overview	
Purpose of study.....	1
Introduction to Parkinson Disease	1
Overview of the genetic causes of Parkinson Disease.....	2
Structure and evolution of LRRK2.....	3
Effects of Parkinson-linked mutations on kinase function	5
Effects of Parkinson-linked mutations ROCO domain function	6
Role of LRRK2 in the regulation of cytoskeletal structure and neurite morphology.....	7
Role of LRRK2 in vesicle trafficking and autophagy	8
Protein misfolding in Parkinson Disease	9
The <i>Drosophila melanogaster</i> model of Parkinson Disease.....	13
Gene expression through use of the UAS/Gal4 system.....	14
Goals and Objectives	16
Materials and Methods	
Bioinformatic analysis of LRRK1, LRRK2, and Lrrk proteins.....	19
Transcription factor prediction	19
Experimental genotypes.....	20
Drosophila medium.....	21

Climbing assay.....	24
Aging assay.....	26
Measurement of ommatidial number, area, and bristle number	26
Fecundity assay.....	27
Quantifying the penetrance of wing vein and abdominal cuticle phenotype.....	27
 Results	
Domain and sequence analysis of <i>Drosophila melanogaster</i> Lrrk and its homologues.....	28
Prediction of upstream transcription factors for <i>Lrrk</i> , <i>LRRK1</i> , and <i>LRRK2</i>	38
Influence of <i>Lrrk</i> ^{e03680} mutation on climbing index.....	39
Influence of <i>Lrrk</i> ^{e03680} mutation on longevity.....	41
Penetrance of <i>Lrrk</i> ^{e03680} cuticle defects.....	42
Influence of <i>Lrrk</i> ^{e03680} mutation on female fecundity.....	43
The <i>Lrrk</i> ^{e03680} mutation affects development of posterior wing vein	44
The <i>Lrrk</i> ^{e03680} mutation affects development of the eye	45
The <i>EPgy2</i> ^{EY06588} insertion causes sporadic melanotic tumors	50
Interaction of <i>SOD</i> and <i>TH</i> overexpression with climbing index and survival	51
Interaction of <i>SOD</i> and <i>TH</i> overexpression with climbing index and survival in <i>Lrrk</i> ^{e03680} mutant background.....	54
The <i>Lrrk</i> ^{e03680} mutation suppresses <i>Ddc:Gal4</i> -induced loss of lifespan.....	57
 Discussion	
Similar domain structure of LRRK2, LRRK1, and <i>Drosophila melanogaster</i> Lrrk suggest shared structure and function.....	60
The <i>LRRK1</i> and <i>Drosophila Lrrk</i> genes may have similar transcriptional regulation.....	62
Climbing impairment in <i>Lrrk</i> ^{e03680} mutants may be caused by changes in neuronal development.....	62
<i>Drosophila Lrrk</i> and human LRRK2 may regulate dopamine synthesis	63

<i>TH</i> overexpression and the <i>Lrrk^{e03680}</i> mutation have similar climbing phenotypes	67
<i>SOD</i> overexpression has a negative effect on climbing ability	68
LRRK2 may cause oxidative stress through regulation of dopamine synthesis	69
Comparison of <i>Lrrk^{e03680}</i> eye phenotype to research on the role of <i>Lrrk</i> and <i>LRRK2</i> in Drosophila eye development	72
Drosophila <i>Lrrk</i> may regulate Notch signalling	74
The <i>Lrrk^{e03680}</i> mutation may cause maternal effects on climbing index.....	77
The <i>Lrrk^{e03680}</i> mutation suppresses Gal4-induced toxicity	78
Conclusion	79
References.....	80

List of Figures

Figure 1: The UAS/Gal4 system in <i>Drosophila melanogaster</i>	15
Figure 2: Climbing apparatus	25
Figure 3: Diagrammatic representation of the domain structure of <i>D. melanogaster</i> Lrrk, <i>C. elegans</i> Lrk-1, and vertebrate LRRK1 and LRRK2 proteins	28
Figure 4: Clustal alignment of the armadillo-like domain of the LRRK2 protein and its homologues	29
Figure 5: Clustal alignment of the ankyrin repeat region of the <i>Drosophila melanogaster</i> Lrrk protein and its homologues	30
Figure 6: Diagrammatic representation of the leucine-rich repeat structure of <i>Drosophila melanogaster</i> Lrrk, <i>C. elegans</i> Lrk-1, and vertebrate LRRK1 and LRRK2 proteins	31
Figure 7: Clustal alignment of the leucine rich repeat region of the <i>Drosophila melanogaster</i> Lrrk protein and its homologues	32
Figure 8: Clustal alignment of the ROC domain of the <i>Drosophila melanogaster</i> Lrrk protein and its homologues	34
Figure 9: Clustal alignment of the COR domain of the <i>Drosophila melanogaster</i> Lrrk protein and its homologues	35
Figure 10: Clustal alignment of the kinase domain of the <i>Drosophila melanogaster</i> Lrrk protein and its homologues	36
Figure 11: Clustal alignment of the QPL domain of the <i>Drosophila melanogaster</i> Lrrk protein with the WD40-like domain of its homologues.....	37
Figure 12: Effect of <i>Lrrk</i> ^{e03680} mutation on climbing ability	39
Figure 13: Effect of <i>Lrrk</i> ^{e03680} mutation on longevity.....	41
Figure 14: Examples of <i>Lrrk</i> ^{e03680} incomplete abdominal cuticle phenotype and percentage of males and females that express the phenotype	42
Figure 15: Effect of <i>Lrrk</i> ^{e03680} mutation on female fertility in <i>Drosophila</i>	43
Figure 16: Incomplete formation of posterior cross vein in <i>Lrrk</i> ^{e03680} homozygotes	44
Figure 17: Percentage of <i>Lrrk</i> ^{e03680} flies expressing the incomplete posterior cross vein phenotype.....	45
Figure 18: Example of black ommatidia in a fly homozygous for the <i>Lrrk</i> ^{e03680} mutation	46

Figure 19: Analysis of ommatidia number (A), area (B), and bristle number (C) for the eyes of <i>Lrrk^{e03680}</i> mutant females	47
Figure 20: Analysis of ommatidia number (A), area (B), and bristle number (C) for the eyes of <i>Lrrk^{e03680}</i> mutant males	48
Figure 21: The <i>EPgy2^{EY06588}</i> insertion induces the formation of melanotic tumors in third instar larvae.....	50
Figure 22: Effect of <i>SOD</i> and <i>TH</i> overexpression in dopamine-producing neurons on climbing ability	51
Figure 23: Effect of <i>SOD</i> and <i>TH</i> overexpression on longevity.....	53
Figure 24: Effect of <i>SOD</i> and <i>TH</i> overexpression in dopamine producing neurons on climbing ability in <i>Lrrk^{e03680}</i> mutants.....	54
Figure 25: Effect of <i>SOD</i> and <i>TH</i> overexpression expression on longevity in <i>Lrrk^{e03680}</i> mutant background.....	56
Figure 26: The <i>Lrrk^{e03680}</i> mutation suppresses <i>Ddc:Gal4</i> -induced loss of lifespan	58

List of Tables

Table 1: Description and source of fly stocks	21
Table 2: Parental and critical-class genotypes of test subjects used in <i>Lrrk</i> ^{e03680} experiments	22
Table 3: Parental and critical-class genotypes of test subjects used in <i>Lrrk</i> ^{e03680} genetic interaction experiments	23
Table 4: Predicted transcription factors upstream of <i>Lrrk</i>	38
Table 5: Predicted transcription factors upstream of human <i>LRRK2</i>	38
Table 6: Predicted transcription factors upstream of human <i>LRRK1</i>	38
Table 7: Comparison of the Y-intercept of the non-linear fitted curves for the <i>Lrrk</i> ^{e03680} climbing assays	40
Table 8: Comparison of rate-constant of the non-linear fitted curves for the <i>Lrrk</i> ^{e03680} climbing assays	40
Table 9: Log-rank statistical analysis of longevity curve for <i>Lrrk</i> ^{e03680} mutant <i>Drosophila</i>	41
Table 10: Comparison of the slopes for the <i>Lrrk</i> ^{e03680} fecundity assay	43
Table 11: Summary of unpaired t-test comparing <i>Lrrk</i> ^{e03680} mutant ommatidia area, size, and bristle number to <i>w/+</i> controls for female flies	49
Table 12: Summary of unpaired t-test comparing <i>Lrrk</i> ^{e03680} mutant ommatidia area, size, and bristle number to <i>w/+</i> controls for male flies	49
Table 13: Comparison of Y-intercept for non-linear fitted curves for expression of <i>GFP</i> and overexpression of <i>SOD</i> or <i>TH</i>	52
Table 14: Comparison of rate constant of fitted curves for expression of <i>GFP</i> and overexpression of <i>SOD</i> or <i>TH</i>	52
Table 15: Log-rank statistical analysis of longevity of <i>Drosophila</i> with expression of <i>GFP</i> and overexpression of <i>SOD</i> or <i>TH</i>	53
Table 16: Comparison of Y-intercept of non-linear fitted curves for expression of <i>GFP</i> and overexpression of <i>SOD</i> or <i>TH</i> in a <i>Lrrk</i> ^{e03680} background	55
Table 17: Comparison of rate constant of non-linear fitted curves for expression of <i>GFP</i> overexpression of <i>SOD</i> or <i>TH</i> in a <i>Lrrk</i> ^{e03680} background	55
Table 18: Log-rank statistical analysis of longevity of <i>Drosophila</i> with expression of <i>GFP</i> and overexpression of <i>SOD</i> or <i>TH</i> in a <i>Lrrk</i> ^{e03680} background	56
Table 19: Log-Rank statistical analysis of longevity of <i>Lrrk</i> ^{e03680} mutant <i>Drosophila</i> compared to <i>w/+</i> and <i>GFP</i> controls	59

List of Common Abbreviations

Catsup – Catecholamines-up

COR - C-Terminal of ROC

Ddc - Dopa decarboxylase

Gal4 – Galactose-responsive transcription factor

GCH-1 - GTP cyclohydrolase I

GFP – Green fluorescent protein

GTP – Guanosine triphosphate

Lrk-1 – Leucine-rich repeat serine/threonine-protein kinase 1

Lrrk – Leucine-rich repeat kinase

LRRK1 – Leucine-rich repeat kinase 1

LRRK2 – Leucine-rich repeat kinase 2

PINK1 – PTEN-induced kinase 1

QPL – Quinoprotein-like

Rab - Ras-related in brain

ROC - Ras of complex proteins

ROS – Reactive oxygen species

SNCA - Alpha-synuclein

SOD – Superoxide dismutase

TH – Tyrosine hydroxylase

VPS35/Vps35 – Vacuolar protein sorting 35

VPS26/Vps26 – Vacuolar protein sorting 26

UCHL1 – Ubiquitin C-terminal hydrolase L1

Introduction and Overview

Purpose of study

Parkinson Disease is the second-most common age-related neurodegenerative disorder after Alzheimer Disease and causes a dysfunction of motor control that can greatly impact a person's ability to function in their daily life [1, 2]. Despite considerable research efforts, the exact mechanisms of pathogenesis remain elusive. Continued research is crucial for the development of new treatments to alleviate the suffering of future Parkinson Disease patients. The aim of this project was to characterize *leucine-rich repeat kinase (Lrrk)*, a *Drosophila melanogaster* homologue of the Parkinson Disease-linked gene *leucine rich repeat kinase 2 (LRRK2)*. Detailed research on the *Drosophila* homologue could deepen our understanding of the human *LRRK2* gene and the pathogenic processes involved in Parkinson Disease.

Introduction to Parkinson Disease

Parkinson Disease was first characterized by James Parkinson in 1817, when he described a group of patients with the following locomotor abnormalities: involuntary tremors, weakness, and a characteristic posture in which the trunk of the body is bent forward [3]. Parkinson was able to differentiate the disease from other conditions with similar locomotor symptoms due to the absence of severe cognitive decline in affected patients. Later studies found a loss of pigmented dopamine-producing neurons in the *substantia nigra* region of the brain [4]. As these neurons regulate voluntary motor control, this finding provided an explanation for the locomotor impairment present in individuals afflicted with Parkinson Disease.

Overview of the genetic causes of Parkinson Disease

Parkinson Disease has both dominant and recessive monogenic causes that involve genetic mutations associated with a variety of functions in the cell [5]. Several monogenic recessive mutations have been linked to mitochondrial homeostasis, such as those in the genes *parkin (PRKN)*, *PTEN-induced putative kinase 1 (PINK1)*, *ubiquitin C-terminal hydrolase L1 (UCHL1)*, *DJ-1*, and *vacuolar protein sorting homolog 3 (VPS13C)*, *peptidyl-tRNA hydrolase domain containing 1 (PTRHD1)*, *phospholipase A2 group VI (PLA2G6)*, and *F-box protein 7 (FBXO7)*. Other monogenic recessive forms have been linked to synaptic function such as those caused by mutations in *podocalyxin like (PODXL)*, *DnaJ heat shock protein family (Hsp40) member C6 (DNAJC6)*, *synaptojanin 1 (SYNJ1)*, and *ATPase cation transporting 13A2 (ATP13A2)*. Monogenic dominant forms of Parkinson Disease have been linked to mutations in several genes, including *LRRK2*, *vacuolar protein sorting 35 (VPS35)*, *alpha-synuclein (SNCA)*, *GTP cyclohydrolase 1 (GCH-1)*, and *ataxin 2 (ATXN2)*. The *LRRK2* and *SNCA* genes are involved in vesicular trafficking, *GCH-1* is involved with synthesis of dopamine, and *ATXN2* contributes to mRNA transport and regulation. The *LRRK2* gene has been reported to be responsible for 13% of familial and 5% of sporadic cases of Parkinson Disease [6]. This gene may be responsible for up to 40% of cases of Parkinson Disease in ethnic groups such as some North African populations and Ashkenazi Jews. This would make *LRRK2* the most common genetic cause of Parkinson Disease identified thus far. It is still unclear how mutations in *LRRK2* lead to pathogenesis in cases of Parkinson Disease. Given the prevalence of *LRRK2* mutations in cases of Parkinson Disease, better knowledge of the function of this gene is essential.

Structure and evolution of LRRK2

The *LRRK2* gene is found at chromosomal locus 12q12 (PARK8) and encodes a large protein of 51 exons and 2527 amino acids [7]. The protein has a complex structure and has been found to have several different functional domains. From N-terminus to C-terminus these are the LRRK2-specific repeat domain, ankyrin repeat domain, leucine-rich repeat domain, Ras of complex proteins (ROC) domain, C-terminal of ROC domain (COR) domain, kinase domain, and WD40 domain. The leucine-rich repeat and WD40 domains are both important for the mediation of protein-protein interactions [8, 9], while the ROC and COR domains appear to work together to regulate activity of the kinase domain [10]. Pathogenic amino acid variants are located throughout the protein within the kinase domain (G2019S, I2020T), ROC (R1441C/G/H, N1437H), and COR domain (Y1699C) [11]. The G2019S mutation is the most common *LRRK2* variant linked to Parkinson Disease [12, 13]. These mutations suggest that the ROC domain, COR domain, and kinase domain are of particular importance in *LRRK2*-related pathogenesis.

All vertebrates for which the full genome is currently available have homologues of the *LRRK2* gene and a paralogous gene called *LRRK1* [14]. The LRRK2 protein has a similar domain structure to LRRK1, as they share an ankyrin repeat domain, leucine-rich repeat domain, ROC domain, COR domain, and kinase domain. The echinoderm *Strongylocentrotus purpuratus* possesses a homologue of both the *LRRK1* and *LRRK2* genes. This suggests that both *LRRK1* and *LRRK2* were present in the common ancestor of vertebrates and echinoderms. The most notable difference between the LRRK1 and LRRK2 proteins is the N-terminal LRRK2-specific repeat domain, which is found in LRRK2 but not LRRK1. Furthermore, LRRK2 has a WD40 domain at its C-terminus, while evidence in support of the presence of a WD40 domain in LRRK1 remains weak [15]. As the WD40 domain and LRRK2-specific repeat domain are key

differences between LRRK1 and LRRK2, these domains may be important to Parkinson Disease pathogenesis.

In contrast to vertebrates, most invertebrate species have only one gene similar to the vertebrate *LRRK1* and *LRRK2* genes [14]. In the roundworm *Caenorhabditis elegans*, this gene is called *leucine-rich repeat serine/threonine-protein kinase 1 (lrk-1)*. The *lrk-1* and *Lrrk* proteins share a closer structural similarity to LRRK1 than LRRK2, as these proteins lack the N-terminal LRRK2-specific repeats and there is weak evidence for a WD40-like domain. Initially, it was proposed that an ancestral *Lrrk* gene had been duplicated in the common ancestor of vertebrates and echinoderms to give rise to the *LRRK1* and *LRRK2* genes. However, the genome of the cnidarian *Nematostella vectensis* challenges this idea. Studies have found that this species has genes similar to both *LRRK1* and *LRRK2*, as well as two additional genes called *LRRK3* and *LRRK4*. Based on sequence similarity, the *N. vectensis* *LRRK1* and *LRRK2* genes were found to be homologous to vertebrate *LRRK1* and *LRRK2* respectively. The *N. vectensis* LRRK2 protein possesses LRRK2-specific repeats and there is strong evidence for a C-terminus WD40 domain. The *C. elegans* and *D. melanogaster* genes are more similar to the *N. vectensis* *LRRK3* compared to the *LRRK1*, *LRRK2*, and *LRRK4* genes. This suggests that an ancestral gene had split early in the evolution of metazoans with several members of this family of genes being lost in different groups. Therefore, researchers that utilize invertebrate models like *D. melanogaster* or *C. elegans* should be mindful of the possibility these organisms may not possess a direct homologue of the *LRRK1* and *LRRK2* genes.

Effects of Parkinson-linked mutations on kinase function

The LRRK2 protein, through its kinase domain, has been found to phosphorylate a number of protein substrates involved in regulation of the cytoskeleton and neuronal morphogenesis such as moesin, ezrin, radixin, 4E-binding protein (4E-BP), and mitogen-activated kinase kinase (MKK) proteins [16]. Notably, LRRK2 has been found to phosphorylate itself [17]. One hypothesis is that autophosphorylation may allow the protein to self-regulate through phosphorylation of the ROC domain which then increases activation of the kinase domain [18]. Once activated, LRRK2 may act in a feed forward process to activate further LRRK2 proteins. Two mutations linked to Parkinson Disease, G2019S and I2020T, are located within the kinase domain of the protein [7]. Both of these mutations are part of an amino acid sequence called a DYG-like motif, found within a region of the kinase domain called the activation loop [19]. Phosphorylation of amino acid residues within the activation loop can alter the conformation of the kinase domain and regulate its enzymatic activity. The DYG-like motif is of particular importance to the function of the kinase domain since it participates in binding of the ATP substrate and Mg^{2+} cofactor. In the wild-type LRRK2 protein, the threonine residue at position 2035 must be phosphorylated for normal kinase function [20]. However, in the G2019S variant, phosphorylation at this site is no longer required for kinase activity, which leads to an increase in kinase activity [21]. Furthermore, the replacement of glycine (G) with serine (S) adds an additional phosphorylation site which may further increase the kinase activity of the protein. The I2020T mutation increases affinity of the protein for ATP and decreases the ability of ATP-competitive inhibitors to suppress kinase activity, which suggests that it may increase kinase activity [22]. However, several studies have revealed that I2020T can either increase, decrease, or not affect kinase activity at all [23-26]. Therefore, while the G2019S mutation may lead to

pathogenesis through increased kinase activity, it is unclear if this is true for the I2020T mutation.

Effects of Parkinson-linked mutations ROCO domain function

The ROCO domain of LRRK2 is composed of two adjacent smaller domains called the ROC domain and COR [27]. The first ROCO proteins were studied in the social slime mold *Dictyostelium discoideum*, and are involved in cytokinesis, cell polarity, and chemotaxis [28]. The close association of the COR domain and ROC domain in ROCO proteins suggests that the two domains work together as a functional unit. One function of the ROCO domain in LRRK2 seems to be the promotion of protein dimerization [29], as structural prediction of the domain suggests that ROC domains from two LRRK2 proteins can interact to form a stable dimer. However, when the R1441C mutation was introduced into the model, the predicted dimer interface was disrupted [30]. This prediction has been supported by experiments that show that the R1441C mutation inhibits the formation of LRRK2 dimers in vitro [31]. The ROC domain, as a Ras-like domain, binds guanosine triphosphate (GTP), which can activate cell signaling pathways by altering the conformation of the protein [32]. GTPase activity of Ras-like domains later hydrolyzes this bound GTP, which deactivates the signalling function. In LRRK2, GTP binding changes the dimerization interface of the ROCO domain. This alteration causes dimers to convert into monomers, which may increase the phosphorylation of other proteins by the kinase domain. This idea is supported by the fact that mutant forms of the LRRK2 protein that do not bind GTP have significantly reduced kinase activity in vitro [29]. Notably, the R1441C mutation has been reported to decrease the GTPase activity of LRRK2 and to inhibit dimerization [33]. Through a decrease in GTPase activity, monomerization might be encouraged, which could explain the rise in kinase activity observed in the R1441C variant of LRRK2 [34].

The Y1699C mutation may have a similar effect on kinase activity as it has been reported to inhibit dimerization of LRRK2 [35, 36]. Taken together, research on the R1441C variant and Y1699C variant of LRRK2 suggest the possibility that the ROCO domain may act to regulate the kinase domain, with Parkinson-linked mutations leading to an increase in the phosphorylation of other proteins by LRRK2.

Role of LRRK2 in the regulation of cytoskeletal structure and neurite morphology

The LRRK2 substrates ezrin, radixin, and moesin are part of the ERM family of proteins, and are primarily responsible for interactions between the actin cytoskeleton and cell membranes [16]. In addition, LRRK2 has been reported to interact with β -tubulin, a component of the cytoskeleton [37]. These interactions suggest that LRRK2 may be involved in cytoskeletal dynamics within the cell. The cytoskeleton is important for the development of neurites (axons and dendrites) in neurons, which may explain why *LRRK2* overexpression promotes neurite atrophy in neuronal cell culture [38, 39]. Notably, suppression of *radixin* and *moesin* expression causes a similar phenotype in rat brain cells [40]. Overexpression of *LRRK2* can induce neuronal apoptosis, which can promote neurite atrophy. However, as knockdown of *LRRK2* expression can increase neurite length, this suggests that effects of *LRRK2* overexpression on neurite morphology operate independently from its pro-apoptotic effects [41]. While there appears to be a link between *LRRK2* and neurite morphology, the implications for Parkinson Disease pathogenesis remain to be elucidated. However, the perturbation of normal neuronal signalling could play a role.

Role of LRRK2 in vesicle trafficking and autophagy

The LRRK2 protein has been reported to localize to the surfaces of endosomes within cells. Endosomes are vesicles that form as a result of the process of endocytosis, where parts of the cell membrane pinch inwards to create vesicles [42]. Endocytosis plays an important role in neurons, as it facilitates the reuptake of neurotransmitters inside of neurons, which in turn helps to prevent overactivation of neuronal signalling [43]. In addition, endocytosis can remove proteins related to cell signalling from the surface of cells to regulate cell signalling pathways [44]. Once endosomes have entered the cell these proteins are sorted and sent to various locations, a process which is regulated by the retromer protein complex [45]. Notably, a number of genes that have been linked to Parkinson Disease such as *DNAJC6*, *SYNJ1*, *ATP13A2*, and *VPS35* code for proteins that have been linked to endosomal sorting [46]. *VPS35* is of particular interest since analysis of the brain tissue of patients that carry the G2019S and I2020T *LRRK2* mutations exhibit a decrease in the amount of the VPS35 protein, as measured through the use of immunoblotting [47]. In addition, the LRRK2 protein has been found to phosphorylate members of the Rab protein family, which play a role in cell signalling processes that regulate intracellular vesicle trafficking and are known to interact with the retromer complex [48, 49]. Based on these findings, it is possible that LRRK2 may interact with proteins in the retromer complex through the phosphorylation of Rab proteins. One function of the Rab family proteins and retromer complex is to regulate the sorting of vesicles to lysosomes, where proteins are broken down by lysosomal enzymes in a process called autophagy [44, 50]. Notably, the G2019S mutation has been reported to induce lysosomal abnormalities and to increase the number of autophagic vacuoles in SH-SY5Y-derived neuronal cell cultures [51]. The evidence points towards a role for LRRK2 in vesicular transport, likely through its impact on the phosphorylation of Rab family

proteins. However, the complex nature of vesicle trafficking presents a challenge in determining precisely how *LRRK2* affects this process.

Protein misfolding in Parkinson Disease

The potential role for *LRRK2* in regulation of protein degradation via autophagy hints at a possible link with *SNCA*, another gene associated with Parkinson Disease. Notably, mutations in both *LRRK2* and *SNCA* genes have been linked to late-onset Parkinson Disease and the presence of protein aggregates called Lewy bodies [5], which suggests possible shared pathogenic mechanisms. The *SNCA* gene encodes a protein called Alpha-synuclein and is the primary component of Lewy bodies [52]. These protein aggregates are composed primarily of a misfolded conformation of alpha-synuclein called amyloid [53]. Amyloid proteins are characterized by an increased beta-sheet structure, which promotes interprotein interactions [54]. Through interaction of the beta-sheets, these misfolded proteins have been found to form amyloid fibrils and amyloid oligomers. Amyloid fibrils are roughly helical structures composed of repeated units of beta-sheets in a parallel or anti-parallel fashion. These structures are the primary component of Lewy bodies found in Parkinson Disease and are highly resistant to degradation. The formation of these structures often precedes cell death in late-onset Parkinson Disease; however, the exact relationship between cell death and amyloid aggregate formation is unclear [55]. In addition to their ability to form fibrils, amyloid proteins can assemble into oligomers composed of a small number of protein units, which resemble beta-barrels in structure and create small pores that allow ions to pass through membranes [56]. Notably, oligomers have been reported to be more toxic than the larger aggregate structures [57-59]. Oligomers may form pores that disrupt ionic gradients, which disrupts intracellular signalling. Neurons may be particularly vulnerable compared to other cell types since the function of these cells depends

heavily on ionic gradients in the form of action potentials. Loss of these gradients can result in overactivity of neurons and cause cell death. Therefore, although amyloid aggregates are more prominent when we inspect cellular structures under the microscope, the primary cause of cell death could be amyloid oligomers.

Mutations in *SNCA* and other Parkinson-linked genes suggest that protein misfolding is an important aspect of pathogenesis in Parkinson disease. It has been well established that Parkinson-linked mutations in the *SNCA* gene contribute to the generation of amyloid forms of the alpha-synuclein protein through promoting misfolding of the protein [60]. In addition, since duplication and triplication of the *SNCA* gene promotes Parkinson Disease and the formation of amyloid, it is believed that the protein is prone to misfold into an amyloid conformation and that Parkinson-linked mutations merely act to increase this propensity [61]. The importance of protein misfolding in Parkinson Disease is further supported by the fact that other Parkinson-linked genes such as *parkin* and *UCHL1* code for proteins that are important elements of the ubiquitin-proteasome system which breaks down misfolded proteins [62]. Notably, inhibition of the proteasome system has been found to increase protein aggregate formation in cell culture [63, 64]. As part of the ubiquitin-proteasome system, parkin tags proteins with a small protein called ubiquitin, signalling the proteins for degradation at cell structures by the proteasome. The relevance of this process to Parkinson Disease is supported by the fact that it has found that overexpression of *parkin* in *Drosophila* can protect against alpha-synuclein-induced cell death, possibly by targeting misfolded alpha-synuclein for degradation [65]. The UCHL1 protein performs the opposite function, by removing ubiquitin tags so that the proteins can be recycled [62]. As previously discussed, LRRK2 may have a role in guiding proteins towards autophagic degradation, a mechanism that may act to breakdown misfolded proteins such as amyloid forms

of alpha-synuclein. Therefore, impairment of protein degradation through either the proteasome or autophagy may play an important role in Parkinson Disease pathogenesis.

Dopamine-producing neurons may be particularly prone to the formation of amyloid proteins because the production of dopamine can promote oxidative stress [66]. Oxidative stress is damage to cells caused by reactive oxygen species (ROS) such as hydroxyl radical (OH^\cdot), peroxide (H_2O_2), and superoxide (O_2^\cdot) [67]. Post-mortem examinations demonstrate increased levels of oxidized fatty acids in the brain tissue of Parkinson Disease patients, supporting a potential role for oxidative stress in this disease [68]. Additionally, a potential causative relationship between Parkinson Disease and oxidative stress is indicated by the neurotoxin 1-methyl-4-phenyl-1,2,3,6-tetrahydropyridine (MPTP), which has been demonstrated to induce Parkinson-like symptoms and promotes cell death via oxidative stress [69]. In addition, a number of toxins used in animal models of Parkinson Disease such as rotenone, 6-hydroxydopamine (6-OHDA), and paraquat, promote cell death through oxidative damage to cells [70]. Dopamine may cause increased oxidative stress through a process called auto-oxidation, which forms dopamine quinones that can promote the generation of ROS [66]. In addition, ROS can promote the formation of dopamine quinones and lead to a process of positive feedback between dopamine auto-oxidation and the generation of ROS. Dopamine quinones have the potential to damage proteins such as alpha-synuclein directly through forming bonds with amino acids, which leads to the generation of dopamine adducts [71]. These adducts have been shown to induce the misfolding of alpha-synuclein and promote the formation of amyloid oligomers. As the formation of amyloid proteins may be increased by oxidative damage, this may help to explain the formation of Lewy bodies in Parkinson Disease [72]. Neurons in the *substantia nigra* may be particularly susceptible to oxidative stress because of their high free iron content, which

is known to catalyze the production of free radicals [73-75]. Therefore, the combination of dopamine and high free iron content may lead to heightened vulnerability to oxidative stress and could be the reason for the particular loss of *substantia nigra* neurons in Parkinson Disease.

Studies that have examined genes related to the monogenic-recessive forms of Parkinson Disease in *Drosophila* models further support a connection between the disease and oxidative stress. Early experiments with *parkin* mutants showed that these flies have an increased sensitivity to oxidative stress and display mitochondrial dysfunction [76]. Neurons and flight muscles degenerate with age and spermatogenesis is impaired. Significantly, flight muscle, neurons, and sperm cells all have highly active mitochondria. Therefore, the pathogenic effects on these tissues may be directly related to observed mitochondrial dysfunction. Mitochondria produce significant amounts of superoxide radicals, so increased sensitivity to oxidative stress may affect these organelles most severely. Loss-of-function mutations in the *PINK1* gene phenocopy the effects of the *parkin* mutation, and overexpression of the *parkin* gene can prevent the pathogenesis caused by *PINK1* loss-of-function mutations, which suggests that their pathogenic effects occur through a common pathogenic mechanism [77-80]. Mutations in the *DJ-1* gene have also been linked to increased sensitivity to oxidative stress and mitochondrial dysfunction in *Drosophila melanogaster* [81]. These findings indicate functional connections between *DJ-1*, *PINK1*, and *parkin*, as the three genes play a role in the protection of mitochondria against oxidative damage, which further supports an important role for oxidative stress in Parkinson Disease pathogenesis.

The *Drosophila melanogaster* model of Parkinson Disease

The current study aimed to characterize *Lrrk*, a homologue of the human *LRRK2* gene in *Drosophila melanogaster*, and to use the information gained to further our understanding of the human *LRRK2* gene. Through use of the *Drosophila* model of Parkinson Disease, we have greatly expanded our knowledge of the disease at the cellular and molecular level [82]. Despite their differences in biology, fruit flies and humans share up to 70% of disease-linked genes, thus *Drosophila* serves as a useful model for studying the genetics of human disease [83]. The highly conserved nature of these genes can be attributed to the fact that many of these genes play a role in crucial cellular processes, with their origins rooted in the earliest ancestors of modern animals.

Drosophila melanogaster has become an important model organism for a number of reasons [84]. Foremost among these is a short generation time, which allows a large sample size to be generated in a relatively short period of time. In addition, the minimal cost to house and maintain *Drosophila* stocks permits numerous experiments to be performed at a low cost. Moreover, large scale mutagenesis of *Drosophila* has led to the availability of an extensive collection of stocks that can be ordered for research. This makes the identification and procurement of mutants for a particular gene quite easy.

The first Parkinson gene to be examined in *Drosophila* was the *SNCA* gene [85]. To date, a *Drosophila* homologue of this gene has not been identified so human A53T mutant *SNCA* was expressed in these flies. The results of this initial study showed the flies experienced a loss of dopamine-producing neurons and a premature decline in climbing ability with age. Strikingly, these observations mirrored the key features of Parkinson Disease: progressive impairment of motor control and death of dopamine-producing neurons. Additionally, this behavioural

phenotype was easy to study without the necessity of expensive equipment or techniques. Due to the short lifespan of *Drosophila* the entire degenerative process can be measured in days rather than years. Therefore, Parkinson Disease research can be performed in a relatively short period of time through the use of the *Drosophila* model. The climbing phenotype has since become an important method to assay disease progression in the *Drosophila* model.

Gene expression through use of the UAS/Gal4 system

The UAS/Gal4 system is a versatile tool used in *Drosophila* research to control and study gene expression [86]. Gal4 is a transcriptional activator found in yeast (*Saccharomyces cerevisiae*), and it drives the expression of genes downstream of the upstream activator sequence (UAS) promoter sequence (Figure 1). The UAS/GAL4 system is an important tool to drive ectopic gene expression in *Drosophila*. Through the use of a variety of endogenous promoters, the expression of the Gal4 gene can be controlled, permitting its targeted expression in specific tissues. In tissues or cells where the *Gal4* gene is expressed, the Gal4 protein activates the expression of genes regulated by a UAS promoter when the two are paired together in the same fly. This system is highly useful, as a UAS gene construct can be easily maintained even if the gene expression is lethal or decreases viability, since the gene will not be expressed unless the Gal4 protein is present. UAS lines can therefore be maintained and then crossed to Gal4 lines to induce gene expression. This system is very efficient as a single UAS gene construct can be expressed in many different tissues through combination with different *Gal4* constructs. Further, a single *Gal4* construct expressed in a particular tissue can drive the expression of several different UAS genes, which permits the study of genetic interactions between various genes. The UAS/GAL4 system enables *Drosophila* researchers to create novel combinations of *Gal4* and UAS transgenes developed by different researchers. By varying the combination of Gal4

constructs, researchers can precisely control gene expression levels and explore genetic interactions through the simultaneous activation of multiple UAS genes.

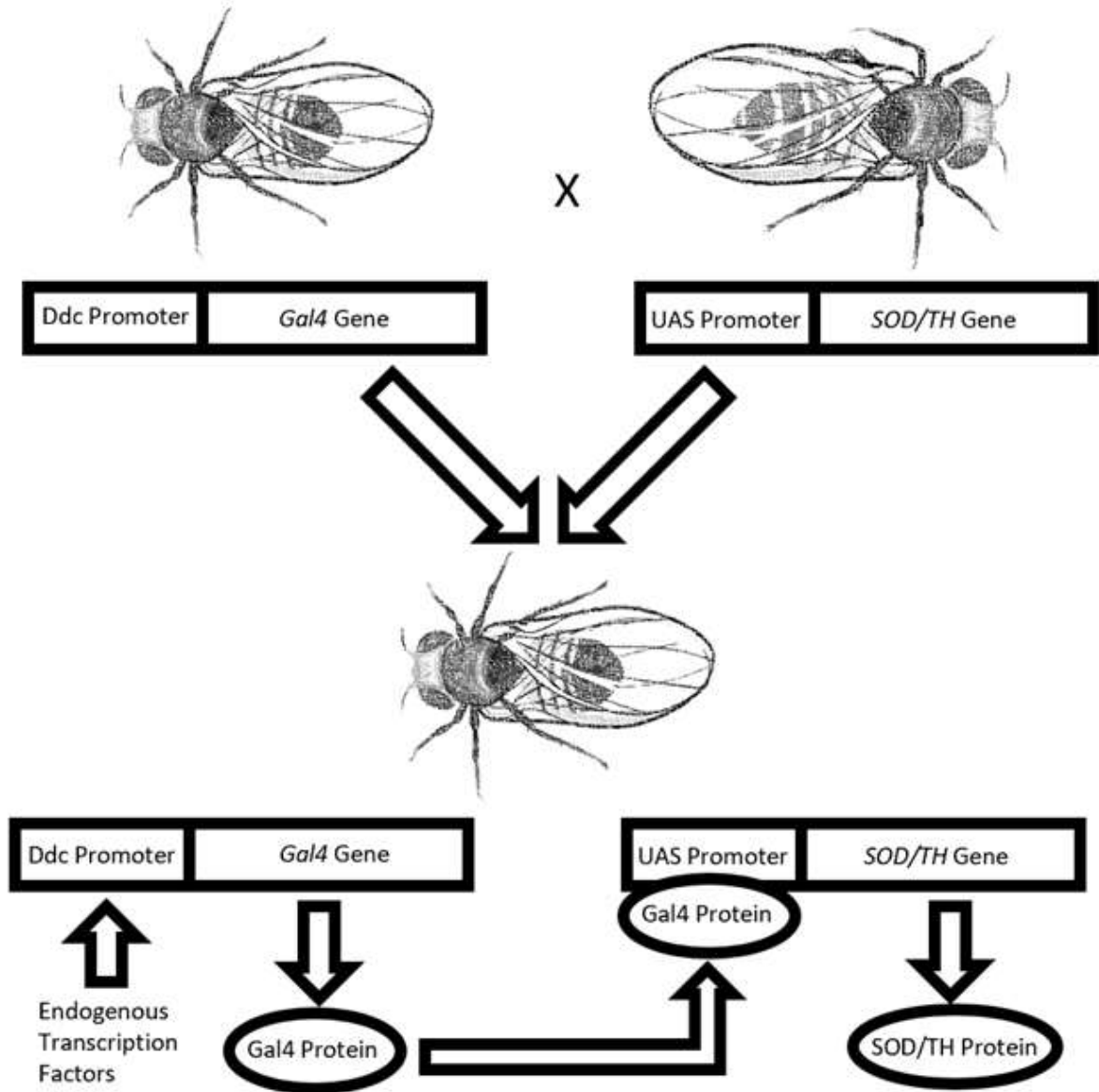


Figure 1: The UAS/Gal4 system in *Drosophila melanogaster*. The UAS/Gal4 system is a bipartite system in which the Gal4 protein is required to activate genes under the control of the UAS promoter. Generally, a driver line that expresses the Gal4 protein under the control of an endogenous promoter is crossed to a responder line that carries a responder construct gene under the control of a UAS promoter. Through crosses of these two lines, progeny can be generated in which the Gal4 protein drives the expression to the target gene in a tissue- or cell- specific manner. In the current study, the *Ddc:Gal4* line was used to drive the expression of *UAS:SOD* and *UAS:TH* in dopamine-producing neurons.

One potential concern regarding the use of the UAS/GAL4 system is the fact that Gal4 protein appears to have a pro-apoptotic role in *Drosophila*, as supported by studies of *Gal4* expression in the *Drosophila* eye [87]. Expression of *Gal4* through the use of the *dopa decarboxylase (Ddc)* promoter significantly decreases survival in *Drosophila*. Since Gal4 does not activate endogenous genes in *Drosophila*, its induction of a pathogenic effect is intriguing. Past research in our lab suggests that overexpression of *parkin* and *PINK1* can suppress Gal4-induced apoptosis [88, 89]. Overexpression of *parkin* has been found to inhibit apoptosis triggered by alpha-synuclein [90], possibly through increasing degradation of misfolded alpha-synuclein. Therefore, protein misfolding might also underlie Gal4-induced toxicity. Notably, protein misfolding is a common problem encountered when proteins are overexpressed in bacteria, and results in the formation of cytoplasmic inclusions of aggregated protein [91] – a phenomenon that is strongly reminiscent of those found in Parkinson Disease and other neurodegenerative diseases [55, 57]. However, it remains to be definitively determined whether Gal4 undergoes a similar misfolding process in *Drosophila* cells. If confirmed, this finding could carry significant implications for the use of the Gal4 system in the study of neurodegenerative diseases and cell survival. In light of the potential link between *LRRK2* and the degradation of misfolded proteins, the current study also explored a possible genetic interaction between *Lrrk* and *Gal4* expression.

Goals and Objectives

The primary objective of this study was to characterize the *Drosophila* homologue of *LRRK2*. This characterization included a detailed analysis of two *Lrrk* mutations; a P-element insertion into the promoter region of the *Lrrk* gene (*EPgy2^{EY06588}*) [92], and another with a P-element insertion into the *Lrrk* gene itself (*Lrrk^{e03680}*) which causes truncation of the protein

within the COR domain and has been confirmed to be a loss-of-function mutation [93, 94]. These flies were examined at all life-stages to discern any differences from wild-type flies. Moreover, climbing and longevity assays were conducted throughout the lifespan of adult flies. An analysis of the promoter region of *LRRK1*, *LRRK2*, and *Lrrk* was performed, and the amino acid sequence and protein domain structure were compared between the proteins to identify similarities and differences. The overarching goal of this work was to better understand the nature of the *Lrrk* gene and how it might be similar and different from human *LRRK1* and *LRRK2*. Identifying these similarities and differences is crucial to determine if the *Lrrk* gene will provide a useful model of Parkinson Disease. Furthermore, the study of *Lrrk* may provide deeper insight into human *LRRK2* and its role in Parkinson Disease.

A secondary objective in this study was to examine possible genetic interactions between *Lrrk*, dopamine production, and oxidative stress. Overexpression of the *Drosophila tyrosine hydroxylase (TH)* gene in dopamine-producing neurons was used to examine the possibility that *Lrrk* may play a role in regulating dopamine synthesis, as TH is the rate-limiting enzyme in dopamine synthesis [95]. This was done because preliminary examination of the *Lrrk*^{*e03680*} and *EPgy2*^{*EY06588*} phenotypes had indicated the possibility of increased dopamine synthesis. These phenotypes included an incomplete abdominal cuticle (Figure 14), loss of fertility in females (Figure 15), and melanotic tumors (Figure 21), which are similar to phenotypes commonly reported for mutations in the *Ddc* cluster of genes, many of which play a role in dopamine synthesis [96, 97]. The *superoxide dismutase (SOD)* gene was overexpressed in dopamine-producing neurons to explore any potential interactions between *Lrrk* and oxidative stress that might result from increased dopamine synthesis, as dopamine synthesis has been linked to sensitivity to oxidative stress [66, 98]. These genes were overexpressed through use of the

UAS/GAL4 system under the control of the *Ddc:Gal4* driver and climbing and longevity were measured across the lifespan of the adult flies. Our goal was to identify possible molecular pathways with which *Lrrk* might interact, deepening our understanding of the potential roles these pathways might play in Parkinson Disease.

A tertiary objective was to examine a possible interaction between *Lrrk* and Gal4-induced toxicity, which has been found to be rescued by overexpression of the Parkinson-linked genes *parkin* and *PINK1* [88, 89]. Overexpression of *parkin* may reduce Gal4-induced toxicity by tagging the Gal4 protein for degradation. To explore the possibility that *Lrrk* may interact with Gal4-induced toxicity, we compared *Ddc:Gal4* expressing lines with and without the *Lrrk*^{e03680} mutation. The goal here was to further examine a possible role for *Lrrk* in protein degradation and to better understand how *LRRK2* might interact with this process in Parkinson Disease.

Materials and Methods

Bioinformatic analysis of LRRK1, LRRK2, and Lrrk proteins

Homologues of the LRRK1, LRRK2, and Lrrk proteins were identified through the use of NCBI's BLAST tool (<https://blast.ncbi.nlm.nih.gov/Blast.cgi>). The vertebrate proteins selected for analysis included *Homo sapiens* LRRK2 (accession number XP_005268686.1) and LRRK1 (accession number NP_078928.3), along with *Mus musculus* LRRK2 (accession number NP_080006.3) and LRRK1 (accession number NP_666303.3). The invertebrate proteins included *Drosophila melanogaster* Lrrk (accession number NP_001097847.1) and *Caenorhabditis elegans* Lrk-1 (accession number NP_492839.4). The online utility Interproscan (<https://www.ebi.ac.uk/interpro/search/sequence/>) was used to identify the location of domains within the proteins. Lastly, the alignment of the amino acid sequences was performed with ClustalOmega (<https://www.ebi.ac.uk/Tools/msa/clustalo/>) to examine the conservation of individual amino acids and align the domain structure of the proteins.

Transcription factor prediction

Transcription factor prediction was achieved by a search of the Transfac Database using the Transfac Match tool (<https://genexplain.com/transfac/>). This tool searches query DNA sequences against a database of sequences to which particular transcription factors are known to bind. The sequences used encompassed 2000 base pairs upstream of the transcription initiation sites for the *Homo sapiens* LRRK1 and LRRK2 genes, as well as the *Drosophila melanogaster* Lrrk gene. The upstream sequences were obtained from the NCBI genome data viewer (<https://www.ncbi.nlm.nih.gov/genome/gdv/>).

Experimental genotypes

Crosses were performed as detailed in Table 1 to generate flies with the desired genotypes for the experiments. The specific crosses conducted, and the critical-class progeny used in the experiments are detailed in Table 2 and Table 3. The *TM3* and *Cyo* balancer chromosomes were used to maintain mutant alleles as they contain inversion mutations that suppress chromosomal recombination. Two mutations generated by P-element mutations were used, the *EPgy2^{EY06588}* and *Lrrk^{e03680}* mutations. The *EPgy2^{EY06588}* mutation is an insertion into the promoter region of the gene [92], but it is unclear how this mutation might affect expression of the gene. The *Lrrk^{e03680}* mutation is an insertion located within the fifth intron of the *Lrrk* gene [94]. This P-element contains a splice acceptor site, causing abnormal mRNA splicing that disrupts the protein sequence that proceeds tyrosine residue 1290. The resulting protein lacks a large portion of the COR domain, as well as the entire kinase domain, and has been confirmed to be a loss-of-function mutation [93, 94]. Because *Lrrk^{e03680}* homozygotes display a noticeable decrease in fertility (Figure 15), heterozygotes that were offspring of either wild-type or *Lrrk^{e03680}* females were compared to determine if maternal genotype impacted climbing ability.

Gene interaction experiments utilized directed gene expression, achieved through crosses of *UAS:SOD*, *UAS:TH*, and *UAS:GFP* responder lines with a *Ddc:Gal4* driver line (Table 3). *UAS:GFP*, which encodes green fluorescent protein (GFP), served as a control. Flies used for these crosses were collected on the day of eclosion, and each individual was isolated in a tube for 6 to 7 days to ensure their virgin status. Only virgins were used for crosses. After this, 4 to 6 females were placed in a vial with 2 male flies to allow the flies to mate. Critical-class progeny were collected on the day of eclosion.

Drosophila medium

The flies were maintained on a medium composed of 5.5 g/L agar, 65 g/L cornmeal, 15 g/L yeast, and 50 ml/L fancy grade molasses diluted in water. This was supplemented with 5 ml of 0.1g/ml methylparaben in ethanol and 2.5 ml of propionic acid as anti-microbial agents. Each vial was filled with approximately 7 ml of this medium. The medium was stored at a temperature of 6-7 °C until use to inhibit microbial growth.

Table 1: Description and source of fly stocks

Stock Genotype	Description	Source
<i>w¹¹¹⁸</i>	All genes are wild-type except <i>w¹¹¹⁸</i> . This gives flies a white eye colour.	H. Lipshitz, University of Toronto
<i>w¹¹¹⁸; +/+; Lrrk^{e03680/TM3}</i>	P-element Insertion into <i>Lrrk</i> gene. Removes kinase function of protein.	Bloomington Drosophila Stock Center Stock Identifier: 85160
<i>w¹¹¹⁸; +/+; EPgy2^{EY06588}</i>	Insertion into the promoter region of the <i>Lrrk</i> gene. May disrupt gene expression.	Bloomington Drosophila Stock Center Stock Identifier:17364
<i>w¹¹¹⁸; Ddc:Gal4/Cyo</i>	Drosophila Gal4 driver line with expression of the <i>Gal4</i> controlled by <i>Ddc</i> promoter.	Sheppard and Staveley, Memorial University of Newfoundland and Labrador
<i>w¹¹¹⁸; UAS:SOD^{B46}</i>	Gal4-responsive line with Drosophila <i>SOD</i> controlled by UAS promoter located on second chromosome	A.J. Hilliker and J.P. Phillips [99]
<i>w¹¹¹⁸; UAS:GFP</i>	Gal4-responsive line with <i>green fluorescent protein (GFP)</i> controlled by UAS promoter located on second chromosome	B. Dickson [100]
<i>w¹¹¹⁸; UAS:TH</i>	Gal4-responsive line with Drosophila homologue of <i>tyrosine hydroxylase (TH)</i> controlled by UAS promoter located on second chromosome	J.R. True et al. [101]

Table 2: Parental and critical-class genotypes of test subjects used in *Lrrk*^{e03680} experiments

Parental Genotypes		Critical-class Progeny	
Paternal Genotype	Maternal Genotype	Genotype	Description
<i>w</i> ¹¹¹⁸	Oregon-R (wild-type)	<i>w</i> ¹¹¹⁸ /+	Control
<i>w</i> ¹¹¹⁸ ; +/+; <i>Lrrk</i> ^{e03680} /TM3	<i>w</i> ¹¹¹⁸ ; +/+; <i>Lrrk</i> ^{e03680} /TM3	<i>w</i> ¹¹¹⁸ ; +/+; <i>Lrrk</i> ^{e03680}	<i>Lrrk</i> mutant homozygote
<i>w</i> ¹¹¹⁸	<i>w</i> ¹¹¹⁸ ; +/+; <i>Lrrk</i> ^{e03680} /TM3	<i>w</i> ¹¹¹⁸ ; +/+; <i>Lrrk</i> ^{e03680} /+	<i>Lrrk</i> mutant heterozygote with heterozygous mutant mother
<i>w</i> ¹¹¹⁸ ; +/+; <i>Lrrk</i> ^{e03680} /TM3	<i>w</i> ¹¹¹⁸	<i>w</i> ¹¹¹⁸ ; +/+; <i>Lrrk</i> ^{e03680} /+	<i>Lrrk</i> mutant heterozygote with wild-type <i>Lrrk</i> mother

Table 3: Parental and critical-class genotypes of test subjects used in *Lrrk^{e03680}* genetic interaction experiments

Parental Genotypes		Critical-class Progeny	
Paternal Genotype	Maternal Genotype	Genotype	Description
<i>w¹¹¹⁸</i> ; <i>Ddc:Gal4/Cyo</i>	<i>w¹¹¹⁸</i> ; <i>UAS:SOD^{B46}/Cyo</i>	<i>w¹¹¹⁸</i> ; <i>Ddc:Gal4/ UAS:SOD^{B46}</i>	<i>Gal4</i> expressed and <i>SOD</i> overexpressed in neurons expressing <i>Ddc</i>
<i>w¹¹¹⁸</i> ; <i>Ddc:Gal4/Cyo</i>	<i>w¹¹¹⁸</i> ; <i>UAS:TH/Cyo</i>	<i>w¹¹¹⁸</i> ; <i>Ddc:Gal4/ UAS:TH</i>	<i>Gal4</i> expressed and <i>TH</i> overexpressed in neurons expressing <i>Ddc</i>
<i>w¹¹¹⁸</i> ; <i>Ddc:Gal4/Cyo</i> ; <i>Lrrk^{e03680}/TM3</i>	<i>w¹¹¹⁸</i> ; <i>UAS:GFP/Cyo</i>	<i>w¹¹¹⁸</i> ; <i>Ddc:Gal4/UAS:GFP</i>	<i>Gal4</i> expressed and <i>GFP</i> overexpressed in neurons expressing <i>Ddc</i> (control)
<i>w¹¹¹⁸</i> ; <i>Ddc:Gal4/Cyo</i> ; <i>Lrrk^{e03680}/TM3</i>	<i>w¹¹¹⁸</i> ; <i>UAS:SOD^{B46}/Cyo</i> ; <i>Lrrk^{e03680}/TM3</i>	<i>w¹¹¹⁸</i> ; <i>Ddc:Gal4/UAS:SOD^{B46}</i> ; <i>Lrrk^{e03680}</i>	<i>Gal4</i> expressed and <i>SOD</i> overexpressed in neurons expressing <i>Ddc</i> in a <i>Lrrk</i> mutant background
<i>w¹¹¹⁸</i> ; <i>Ddc:Gal4/Cyo</i> ; <i>Lrrk^{e03680}/TM3</i>	<i>w¹¹¹⁸</i> ; <i>UAS:TH</i> ; <i>Lrrk^{e03680}/TM3</i>	<i>w¹¹¹⁸</i> ; <i>Ddc:Gal4/ UAS:TH;Lrrk^{e03680}</i>	<i>Gal4</i> expressed and <i>TH</i> overexpressed in neurons expressing <i>Ddc</i> in a <i>Lrrk</i> mutant background
<i>w¹¹¹⁸</i> ; <i>Ddc:Gal4/Cyo</i> ; <i>Lrrk^{e03680}/TM3</i>	<i>w¹¹¹⁸</i> ; <i>UAS:GFP/Cyo</i> ; <i>Lrrk^{e03680}/TM3</i>	<i>w¹¹¹⁸</i> ; <i>Ddc:Gal4/UAS:GFP</i> ; <i>Lrrk^{e03680}</i>	<i>Gal4</i> expressed and <i>GFP</i> expressed in <i>Ddc</i> expressing neurons in a <i>Lrrk</i> mutant background (control)

Climbing assay

The climbing assay, widely used in *Drosophila* studies of Parkinson Disease, is a tool that is used to indirectly track the progression of cell death in dopamine-producing cells. This study used a graded climbing assay [102]. The apparatus (Figure 2) is a 30 cm long, 1.5 cm diameter tube, supported upright in a funnel to facilitate the transference of flies into the tube. Each end of the tube is blocked with a sponge to prevent fly escape during trials. The tube is marked to divide it into five lower 2 cm levels and an upper 20 cm level. This larger upper level acts as a buffer zone, preventing flies from descending into the lower sections once they've climbed to the top. During each trial, flies are gently tapped to the bottom of the tube and allowed to climb for ten seconds. The number of flies at each level is recorded, with flies in the buffer zone being recorded as being in level 5. The climbing index is calculated based on the equation below (Equation 1).

Equation 1: Climbing index = $\Sigma(nm)/N$

Where n = the number of flies at a particular level(m); N = total number of flies

Ten trials were conducted per vial, and the climbing index was averaged. Climbing ability was assayed one day after eclosion and was repeated every five days thereafter. Each vial initially contained 10 flies and vials were discarded when three or fewer flies remained. Only male flies were used because it is difficult to collect a large number of virgin females, and if the flies are not virgins reproductive stress could affect the climbing results. Data analysis was performed with GraphPad Prism 9, plotting the change in the climbing index against age after

eclosion. A non-linear regression was performed to determine the rate of decrease in climbing ability (Equation 2).

Equation 2: Climbing index = $5 - (C_i^{Kt})$

Where C_i = Climbing index at start; K = Rate constant; t = # of days after eclosion

The rate constant (K) and the initial climbing index (C_i) were compared between experimental groups and controls to assess the rate of decline in climbing ability.

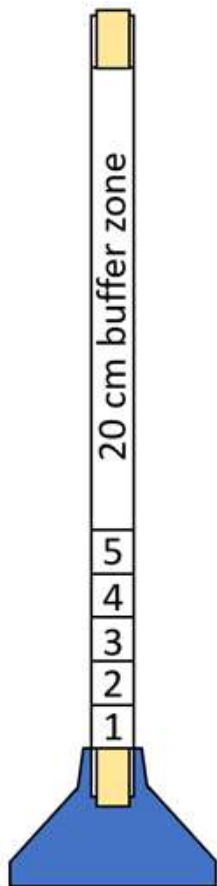


Figure 2: Climbing apparatus. This apparatus measures the vertical locomotion of *Drosophila*. It consists of a tube divided into five 2 cm sections, plus a 20 cm buffer zone at the top. Flies that reach the buffer zone are recorded as being in the fifth level. Sponges at each end of the tube prevent the escape of flies, and a funnel at the bottom supports the tube and assists with the transfer of flies into the apparatus.

Aging assay

The aging process in *Drosophila* is associated with decrease in climbing ability [103]. Therefore, it is important to determine if any changes in climbing ability could be attributed to changes in the aging process rather than death of dopamine-producing neurons. The aging analysis was performed by making a record of the number of dead flies in each vial every two days. To prevent crowding, each vial contained ≤ 20 flies, and the flies were transferred to a fresh vial every two days. Survival curves were compared and significance determined using a log-rank (Mantel-Cox) test with GraphPad Prism 9.

Measurement of ommatidial number, area, and bristle number

The *Drosophila* eye is composed of individual facets called ommatidia that form an ordered array across the entire eye, interspersed with sensory bristles. As a result of this repeated structure differences in ommatidial size or number are magnified in the eye as a whole. Consequently, the *Drosophila* eye has become an effective tool to explore genes related to cell growth, size, and death [104]. Since Parkinson Disease is a neurodegenerative disorder marked by increased neuronal cell death, *Lrrk* may alter the eye structure through interaction with cell death processes throughout eye development. The left eye of each fly was examined under the Hitachi 570 scanning electron microscope at a magnification of 150X actual size. For each eye, the number of ommatidia, bristles, and average area of ommatidia were determined. The ImageJ program (<https://www.rsweb.nih.gov/ij/>) was utilized to perform analysis of the images. Ommatidial area was estimated by measuring the area of six patches of seven ommatidia, averaging this value, and then dividing by seven to determine the average size of one ommatidium. The patches chosen were located near the centre of the eye and did not overlap.

Fecundity assay

To assess the fecundity of *Lrrk*^{e03680} mutant females wild-type flies were compared to those heterozygous and homozygous for the mutation. Ten females of each genotype were collected at eclosion and placed into separate vials. Two wild-type males were added to each vial to impregnate the females and stimulate egg laying. The next day the flies were transferred to a new vial and the number of eggs in the old vial was counted under the stereomicroscope. This process was repeated every five days and flies were transferred to a new vial at this time. GraphPad Prism 9 was used to create regression lines and to determine the level of significance.

Quantifying the penetrance of wing vein and abdominal cuticle phenotype

The *Lrrk*^{e03680} mutants displayed the phenotypes of incomplete wing vein development and incomplete abdominal cuticle development. To determine the penetrance of these phenotypes, a sample of 100 flies each of wild-type, homozygous, and heterozygous flies was selected, for both males and females. For each group, the number of flies expressing the phenotype was counted, and the percentage was calculated.

Results

Domain and sequence analysis of *Drosophila melanogaster* Lrrk and its homologues

Protein domain prediction by Interproscan revealed a highly conserved domain structure among *D. melanogaster* Lrrk, *C. elegans* Lrk-1, and LRRK1 and LRRK2. All of these proteins feature the ankyrin repeat, leucine-rich repeat domains, ROC, COR, and kinase domains. These domains maintain the same positional relationship to each other across all proteins (Figure 3). However, armadillo-like repeats, detected near the n-terminus of LRRK2, were not found in the other proteins (Figure 3 and Figure 4). Ankyrin repeat domains are found in all proteins but are shorter in LRRK1 and LRRK2 compared to Lrrk and Lrk-1 (Figure 3 and Figure 5).

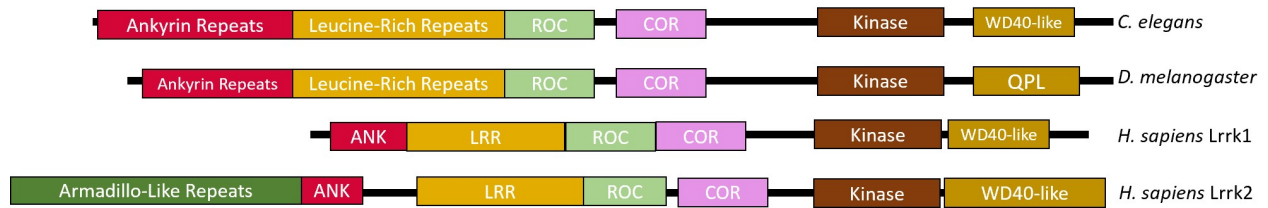


Figure 3: Diagrammatic representation of the domain structure of *D. melanogaster* Lrrk, *C. elegans* Lrk-1, and vertebrate LRRK1 and LRRK2 proteins. Conserved domains across all proteins include the ankyrin repeat (ANK), leucine-rich repeat (LRR), ROC, COR, and kinase domains. Notably, the armadillo-like repeat domain is only present in LRRK2. LRRK1, LRRK2, and *C. elegans* Lrk-1 feature a WD40 domain, whereas Lrrk hosts a quinoprotein-like (QPL) domain at the equivalent position.

H.sapiens_LRRK2	masgscqgceed--eetlkkliivrlnnvqegkqietlvqiledllvftyserasklfqgk	58
M.musculus_LRRK2	masgacqgceeeeeeaalkliivrlnnvqegkqietllqiledmlvftystrasklfdk	60
H.sapiens_LRRK1	-----	0
M.musculus_LRRK1	-----	0
D.melanogaster_Lrrk	-----	0
C.elegans_Lrk-1	-----	0
H.sapiens_LRRK2	nihvplliivldsymrvasvqgqgwsllcklievcpqtlqslmgpgdvgndweivgvhqli	118
M.musculus_LRRK2	nfhvplliivldsymrvasvqgqgwsllcklievcpqtlqslmgpgdvgndweivgihrlh	120
H.sapiens_LRRK1	-----	0
M.musculus_LRRK1	-----	0
D.melanogaster_Lrrk	-----	0
C.elegans_Lrk-1	-----	0
H.sapiens_LRRK2	lkmltvhnasvnlsvigktdlilltsgkitlilideesdifmlifdamhysfandevqk	178
M.musculus_LRRK2	lkmltvhanvnlsvigkaldlilldsgkltlilideecdiflilifdamhysandevqk	180
H.sapiens_LRRK1	-----	0
M.musculus_LRRK1	-----	0
D.melanogaster_Lrrk	-----	0
C.elegans_Lrk-1	-----	0
H.sapiens_LRRK2	lgckalhvlfervseeqltefvenkdyfillsaltnfkdeeeivhvhchlsiaipcm	238
M.musculus_LRRK2	lgckalhvlfervseeqltefvenkdyfillsfgsfrdkelvyhvlccllhslavtcsn	240
H.sapiens_LRRK1	-----	0
M.musculus_LRRK1	-----	0
D.melanogaster_Lrrk	-----	0
C.elegans_Lrk-1	-----	0
H.sapiens_LRRK2	vevlmsgnvrvcynlvveamkafpmseriqvsccllhrltlnfnfnilvlnevhefvvka	298
M.musculus_LRRK2	vevlmsgnvrvcynlvveamkafptneniqvscslfqkltlnfnfnilvlnevhefvvka	300
H.sapiens_LRRK1	-----	0
M.musculus_LRRK1	-----	0
D.melanogaster_Lrrk	-----	0
C.elegans_Lrk-1	-----	0
H.sapiens_LRRK2	vqqypenaalqisalsclalltetiflnqdleeknenqen---d--degeedkl-----	347
M.musculus_LRRK2	vqqypenaalqisalsclalltetiflnqdleersetqeq---s--eedsekl-----	349
H.sapiens_LRRK1	-----	0
M.musculus_LRRK1	-----	0
D.melanogaster_Lrrk	-----	0
C.elegans_Lrk-1	-----mdlssggpsssdvaseldnsdamqlvrqavl	32
H.sapiens_LRRK2	----fwleacy--kaltwhrknkhvqeaacwalnllmyqnslhekgidgedghfpahrev	401
M.musculus_LRRK2	----fwlepcy--kalvrhrkdkhvqeaacwalnllmyqnslhekgidgedgfpahrev	403
H.sapiens_LRRK1	-----	0
M.musculus_LRRK1	-----	0
D.melanogaster_Lrrk	-----	0
C.elegans_Lrk-1	fenvelladlfkvpwwnrvdhrgrtplmlaa-----hngkldslrti	76
H.sapiens_LRRK2	mlsmImhssskvfvqasanalstllsqnvnfrkillskgihlnvlelmqkhihs-pevae	460
M.musculus_LRRK2	mlsmImhssskdvfqaaahalstllsqnvnfrkillakgvvlnvlelmqkhaha-pevae	462
H.sapiens_LRRK1	-----	0
M.musculus_LRRK1	-----	0
D.melanogaster_Lrrk	-----mehpktgtetale-	13
C.elegans_Lrk-1	----lmlsp-----nslnlvndrgktalhmaesgetsivlvelgspmkdsne	123
H.sapiens_LRRK2	sgckmInhlfegsntslidmaavvp-kiltvmkrhets-----lpvqleal	505
M.musculus_LRRK2	sgckmInhlfegsnpdtdmaavvp-kiltvmkahgts-----lsvqleal	507
H.sapiens_LRRK1	-----magmsqrppsm-----ywcv	15
M.musculus_LRRK1	-----magtsqrppsm-----ywcv	15
D.melanogaster_Lrrk	-acdyfvdev----ieassirdareevrq--ikhgelrtavisgdertvrvl---laal	62
C.elegans_Lrk-1	ghcalelaqmagnevaaklidaiqkesedlneahmtiisacisgsadvvyeisrfrmek	183
H.sapiens_LRRK2	raihfivpgmpesred--tefhkln-----mvkqcfk-----	539
M.musculus_LRRK2	raihfvvpgllesred--sgc--rpn-----vlrkqcfr-----	539
H.sapiens_LRRK1	gpeesavcper-----ametlngagdtggkprtgdp-aarsrrtegi raayrgd	66
M.musculus_LRRK1	gteglavcpgp-----amethngaedmgskslspgss-tvqpsmeihtaykqrn	66
D.melanogaster_Lrrk	gterqilvnmmapsgantllflacqsgyesitqrlldagadgrshavtkysplvaavhshg	122
C.elegans_Lrk-1	kqsrrellfngrmeedetalliactnghieivrhlilqfeehllqshvskdtvhaavsqn	243
H.sapiens_LRRK2	ndihkvlvalnrfignpgig-----kcg-lkviissivhfpdaleml----slega	585
M.musculus_LRRK2	ndihkvlvalnrfignpgig-----kcg-lkviisslahlpdatetl----slgga	585
H.sapiens_LRRK1	rggardlee-----	76
M.musculus_LRRK1	lsrardlrg-----	76
D.melanogaster_Lrrk	lgiarlmdhfpeliqptverwplhaacinghikllellisysypdylyqtyrdeegq	182
C.elegans_Lrk-1	vevlqiclekfpqlvkstnnegstclhwaarcssecvstlnfppsefieie-idtvga	302
H.sapiens_LRRK2	mdsvlhtlqmpddqeiqc-----lglsligyilitkknvfigtghllakilvssl	635
M.musculus_LRRK2	vdsvlhtlqmpddqeiqc-----lgllmgclmtkknfcigtghllakilastl	635
H.sapiens_LRRK1	-----acdqcasqlekgqlsipaaygdlemvryllskrlv-----elpt	116
M.musculus_LRRK1	-----vceesessqekgqlsaaahgdetvqfllektkrv-----elpt	116
D.melanogaster_Lrrk	wewr---lpfdanahdvtgqtslyiasilgnkqlvgvllkqqlhcrtrlgdsassvsstpi	239
C.elegans_Lrk-1	payq---laldvnevdeqecrtamylavaeghlevvk-----	335

Figure 4: Clustal alignment of the armadillo-like domain of the LRRK2 protein and its homologues. This domain is highlighted in gray and was only detected in LRRK2. Symbols denote the degree of residue conservation: (fully conserved (*), strongly conserved (:), weakly conserved (.)).

H.sapiens_LRRK2	----fwleacy--kaltwvrknkhvqeaacwalnllmyqnslhekiqdedghfpahrev	401
M.musculus_LRRK2	----fwlepcy--kalvrhrkdkkhvqeaacwalnllmyqnslhekiqdedgqfpahrev	403
H.sapiens_LRRK1	-----	0
M.musculus_LRRK1	-----	0
D.melanogaster_Lrrk	-----	0
C.elegans_Lrk-1	fenvelladlfkvpnwvnrdrhgtrtplmlaa-----hngkldsirtl	76
H.sapiens_LRRK2	mlsmlmhssskevfqasanalstllegnvnfrkillskgihlnvlelmqkhihs-pevae	460
M.musculus_LRRK2	mlsmlmhssskdvfqaahaalstllegnvnfrkillakgvylnvlelmqkhaha-pevae	462
H.sapiens_LRRK1	-----	0
M.musculus_LRRK1	-----	0
D.melanogaster_Lrrk	-----mehpktgtetale-----	13
C.elegans_Lrk-1	----lmlsp-----nslnlvndrgktalhmaesgetsivlelvelgsdpmksdne	123
H.sapiens_LRRK2	sgckmlnhlfegsnstldimaavvp-kiltvmkrhets-----lpvqleal	505
M.musculus_LRRK2	sgckmlshlfegsnpsldtmaavvp-kiltvmkahgts-----lsvqleal	507
H.sapiens_LRRK1	-----magmsqrppsm-----ywcw	15
M.musculus_LRRK1	-----magtsqrppsm-----ywcw	15
D.melanogaster_Lrrk	-acdyfvdev----ieassirdareevrq--ikhgelrtavisgdertvrvl---laal	62
C.elegans_Lrk-1	ghcalelaqmaghnevaaklidaiqkesedlneahtmiisacisgsadvvyeisrrfmek	183
H.sapiens_LRRK2	railhfvpgmpeesred--tefhhkln-----mvkkqcfk-----	539
M.musculus_LRRK2	railhfvpgllesred--sqc--rpn-----vlrkqcf-----	539
H.sapiens_LRRK1	gpeesavcper-----ametlngagdtgkpkstrggdp-aarsrregiraayrrgd	66
M.musculus_LRRK1	gteglavcpgp-----amethngaedmgsklslpggss-tvqcpsmeeihtaykqrn	66
D.melanogaster_Lrrk	gterqiivnmapsgantllflfacqsgyesitqrlldagadgrshavtkysplyaavhsg	122
C.elegans_Lrk-1	kqsreilfngrneedetalliactngnieivrhlqfhehllqshvskdtvihaavssqn	243
H.sapiens_LRRK2	ndihklvlaalnrfignpgiq-----kcg-lkvissivhfpdaleml---slega	585
M.musculus_LRRK2	tdihklvlnrlnrfignpgiq-----kcg-lkvisslahlpadatetl---slgga	585
H.sapiens_LRRK1	rggardllee-----	76
M.musculus_LRRK1	lsrardllrg-----	76
D.melanogaster_Lrrk	lgiarlmlhdhfpeliqptverwlpphaacinghiklilellisysypdylyqtyrdeegq	182
C.elegans_Lrk-1	vevlqlclekfpqlvkstnngestclhwaarcgssecvstlnfnpsefiie-idtvg	302
H.sapiens_LRRK2	mdsvlhtlqmyppddqeiqc-----lglsliyilitkknvfigtghllakilvssl	635
M.musculus_LRRK2	vdsvlhtlqmyppddqeiqc-----lgllhmgclmtkknfcigtghllakilastl	635
H.sapiens_LRRK1	-----acdqcasklekgqllsipaaygdemvryllskrlv-----elpt	116
M.musculus_LRRK1	-----vceesssqekqgllsaaahgdletvqflltekrv-----elpt	116
D.melanogaster_Lrrk	wewr---lpfdanahdvtgtslyiasilgnkqlvlgvllkwqlhcrtrlgdsassvstpi	239
C.elegans_Lrk-1	payq---laldvnevdeqcertamylavaeghlevvk-----	335
H.sapiens_LRRK2	yrfkdvaeiq--tkgfqtilailklsasfskllvhhsfdlvifhqmsnimeqkdqqfln	693
M.musculus_LRRK2	qrfkdvaeq--ttglqttsilelsvsfskllvhysfdvviifhqmsssvveqkdeqfln	693
H.sapiens_LRRK1	eptddnpavvaayfghtavv-----qelle-----	141
M.musculus_LRRK1	eptddnpavvaahfghaevv-----relle-----	141
D.melanogaster_Lrrk	tptr---krisfgiqaim-----sklhisg-----esegpddlasqest	275
C.elegans_Lrk-1	-----amtdfkctsid	346
H.sapiens_LRRK2	lccckcfakva---mddylnvmleracdqnnsimvec-llllgadanqakegsslicqvc	749
M.musculus_LRRK2	lccckcfakva---vddelkntmleracdqnnsimvec-llllgadanqvkqatsliyqvc	749
H.sapiens_LRRK1	-----slpgpcspqrllnwmlalacqrglhgvvklvlthgadpesyavr-----	186
M.musculus_LRRK1	-----slpgpctpqrllnwmlalacqrglhlevvklvlthgadpenyavr-----	186
D.melanogaster_Lrrk	ecqrpinvnlcgaaret--allaavrgghldvvs-llqghanpnivakp-----v	325
C.elegans_Lrk-1	grqrcpfqldvycrgrtp--fmlaafn-qnlplmtl-lldagadvnlplav-----l	395
H.sapiens_LRRK2	ekesspklevllnsgsreqdvrkaltisigkqdsqiiisllrrlaldvannsiclggfc	809
M.musculus_LRRK2	ekesspklevllnngcgregdvrkaltvsigkqdsqviiisllrklaldlannsiclggfg	809
H.sapiens_LRRK1	-----knefp-----vivrplyaaiksgnediaifllrhgayfcsyill-----	226
M.musculus_LRRK1	-----knefp-----vivrplyaaiksgnediaifllrhgayfcsyill-----	226
D.melanogaster_Lrrk	edhndpkceeiyy----glsnvpiaeaackqrsmlamdlllkhgarddngtaigmaitc	379
C.elegans_Lrk-1	dte---ysveegr-----cigsgalveavrsdglhivhflldrgaldtdnkairlaaag	446

Figure 5: Clustal alignment of the ankyrin repeat region of the *Drosophila melanogaster* Lrrk protein and its homologues. The ankyrin repeat region of LRRK2 is highlighted yellow since individual repeats were not detected by Interproscan. The individual repeats are highlighted gray for LRRK1, Lrrk, and Lrk-1. Symbols denote residue conservation: (fully conserved (*), strongly conserved (:), weakly conserved (.)).

Leucine rich repeats are present in Lrk-1, Lrrk, LRRK1, and LRRK2. Analysis of the individual repeats shows that five out of seven repeats found in LRRK2 are also found in Lrrk (Figure 6 and Figure 7). Similarly, five out of seven repeats found in LRRK1 are also found in Lrrk. This suggests a similar structure for leucine-rich repeat domain in the Lrrk, LRRK1, and LRRK2 proteins.

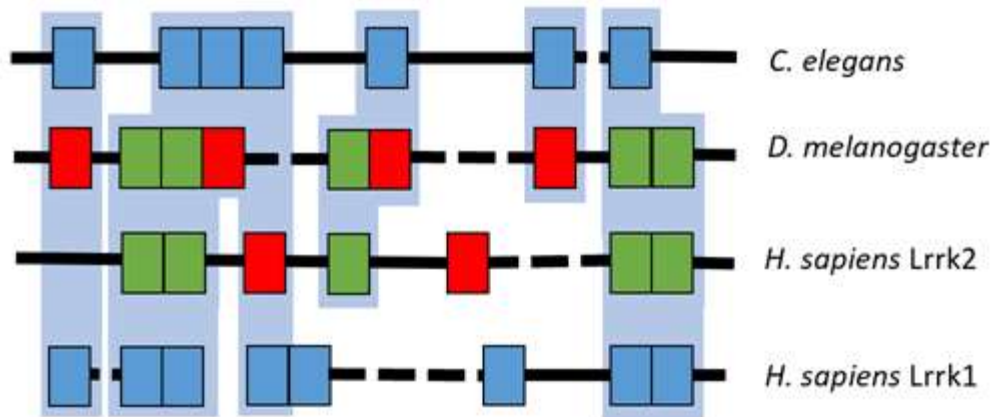


Figure 6: Diagrammatic representation of the leucine-rich repeat structure of *Drosophila melanogaster* Lrrk, *C. elegans* Lrk-1, and vertebrate LRRK1 and LRRK2 proteins. Each box represents one leucine-rich repeat. Green boxes represent repeats shared between LRRK2 and Lrrk while red boxes represent repeats that are not shared. Dotted lines represent areas where the protein backbone would need to be extended to allow the repeats to align. The clustal analysis of the leucine-rich repeat region upon which this diagram is based can be seen in Figure 7.

```

H.sapiens_LRRK2      nlqrhsnslgpfidhedllkrkrkilssddslrssklqshmrhsdsisslasereyitsl 987
M.musculus_LRRK2    naqrhsnslgpfvfdhedllrrkrkilssdeslrssrlpshmrqsdsssslaserehitsl 987
H.sapiens_LRRK1     alrvkwshl----r---lpwvdlldwldi-----scqitel 283
M.musculus_LRRK1    alrvkwshl----k---lpwvdlldwldi-----scqitel 283
D.melanogaster_Lrrk ptiidwhsmgssvq---lsvrvpvmvsgvlllnpklqshprlne-----valtatri 482
C.elegans_Lrk-1     aaqlwnsa----n---leqlqsdwfvaaahvnprlrrt----tr-----lslaaitrv 536
      .                *                :                **      :

H.sapiens_LRRK2      dlsanelrdidalsqkccisvhlhleklehqnaltsfpqqlc-e--tlkslthldlhs 1044
M.musculus_LRRK2    dlsanelkdidalsqkccslsshlehltklelhqnsaltsfpqqlc-e--tlkclihdldhs 1044
H.sapiens_LRRK1     dlsanclatlps-----vipwglinlrklnlndnhlgelpgvqssdeiicrllleidiss 338
M.musculus_LRRK1    dlsanclpslps-----iipwglinlkklnlnsnqgelpcvqssdeiicrllleidiss 338
D.melanogaster_Lrrk dfshnvltsipq-----el-fhlvslrylnvaqnkidlpapig-qtygcpvldelflqd 535
C.elegans_Lrk-1     dlsdnrlntfps-----il-fqmpslrslnlnadnsirkiepty-yi-sstsleilnlrn 588
      *:* * * :                : * * : * : * : :                * : : .

H.sapiens_LRRK2      nkftsfps-yllkmfcianldvsrndigpsvvd---ptvkcptlkqfnlsynqlsfvpe 1100
M.musculus_LRRK2    nkftsfps-fvlkmpritnldaerndigptvvd---pamkcpslkqnlslsynqlssipe 1100
H.sapiens_LRRK1     nkshlppg-fhlhsklqkltaskncleklfeenatnwigrklqeldisdnkltelpa 397
M.musculus_LRRK1    nkshlppg-fhlhsklqkltasknylerlfeenatnwigrklqeldladnrltelpv 397
D.melanogaster_Lrrk nqlttlpa-aifhlpalsildvsnnkllqqlpfd---lwr-apklrelnvafnlrdlpv 589
C.elegans_Lrk-1     ngleciaiqflsslpglqqldvsknslqlpey---iwl-cpalkeknasynrlstlpm 643
      *:: : . : : * . * :                *::: : * * : *

H.sapiens_LRRK2      nltadvvekleqlilegnkis----- 1120
M.musculus_LRRK2    nlaqvvekleqlilegnkis----- 1120
H.sapiens_LRRK1     lflhsfkslns----- 408
M.musculus_LRRK1    qfmhfsfkslts----- 408
D.melanogaster_Lrrk ppmqtssslsldklnl---q---sfeppsnkprnvtqqrllthrnslwsatlditdnd 641
C.elegans_Lrk-1     varasrgerprlnnsnnfnqtqsptqesnpivddppnvtsnplrrqnvwqasinlskvd 703

H.sapiens_LRRK2      -----gicsplrlkelkilnlsknhiisslenfleacpkvesfsarmnflaamp 1169
M.musculus_LRRK2    -----gicsplslkelkilnlsknhipsipgdflacskvesfsarmnflaamp 1169
H.sapiens_LRRK1     -----lnvsrnnlkvfpd-----pwa 424
M.musculus_LRRK1    -----lnvsrnnlksfpd-----pws 424
D.melanogaster_Lrrk mkwqheqldgdgktagvqssqslslniannlftsipa-----alp 681
C.elegans_Lrk-1     ddsif-----pdfpvtssntlttlnisfnkfhfipf-----cla 737
      : * : * : :

H.sapiens_LRRK2      flpssmtilklsqkfciscea--ilnlphlrsldmssndiqylpgp----- 1214
M.musculus_LRRK2    alpssitslklsqnsftcipea--ifslphlrsldmshnnieclpgp----- 1214
H.sapiens_LRRK1     oplk---cckasrnaeclpdkmavfwknhlkdvdfsenaakevplglfqlaldalmfl--- 478
M.musculus_LRRK1    oplk---cckasknaleslpdkmavfwkshlrdadfsenslkevplglfqlaldalmfl--- 478
D.melanogaster_Lrrk clavnltrlnmsynslrsmghv--tsyapatlkqldlshneiscwpslpritesdphlly 739
C.elegans_Lrk-1     ctcprrllilnmsnsmtslppm--acvpahlrtldlsynkiges---fieasplhvch 791
      : * * : :                * : * * * : .

H.sapiens_LRRK2      -----ahwksln--- 1221
M.musculus_LRRK2    -----ahwksln--- 1221
H.sapiens_LRRK1     -----rlqgnql-----aalppqekwtcrq--- 498
M.musculus_LRRK1    -----rlqgnql-----lslppqekwtctq--- 498
D.melanogaster_Lrrk scv-----qlpegrddyktasskgss-----ssatsfrasvlksvcrhrhr 781
C.elegans_Lrk-1     avppttsngsmplkrrnsparqhrsrsksavrqrslsvsrhhalidppqeeescvkhrr 851
      . . :

H.sapiens_LRRK2      ----lrellfshnqisildlsek-----aylwsrve 1248
M.musculus_LRRK2    ----lrelifsknqistldfsen-----phvwsrve 1248
H.sapiens_LRRK1     ----lktldlsrnqlgknedgkktkriafttrgr--qrsgteaasvlefpaflsesle 551
M.musculus_LRRK1    ----lktldlsrnqlgknedgkktkrislfttrgr--qrsgetetasmlefpaflsesle 551
D.melanogaster_Lrrk lrlealrtliladnltriqlstdd-attlfnesedadsvvgvnrs----kvifpnls 835
C.elegans_Lrk-1     dslewlktlqlagnrlrsisv-----tnaas----wllpaln 885
      * : * : * :                :                : :

H.sapiens_LRRK2      khlshnklkeippeigcLenltsldvsynlelrsfpnemgklskiwdlpdlhlhlnfdf 1308
M.musculus_LRRK2    khlshnklkeippeigcLenltsldvsynlelrsfpnemgklskiwdlpdlglhlnfdf 1308
H.sapiens_LRRK1     vlclndnhldtvppsycllkslselylgnnpglrelppelgqlgnlwqldtedltisnvp 611
M.musculus_LRRK1    vlclndnhldavppsycllknlselylgnnpglrelppelgqlgnlwqldiedlnisnvp 611
D.melanogaster_Lrrk mldmtnnclkeipaslhesslvlnisgnvnitelpphlgllsrlnwnlntgrdllqepl 895
C.elegans_Lrk-1     vmdisdnkllqappdvartltslmlnlnsgntaikelpdygmrlsrwslslkgcslkepl 945
      : : * * * * : : * * : * : * : : * : * * * * * * : .

```

Figure 7: Clustal alignment of the leucine rich repeat region of the *Drosophila melanogaster* Lrrk protein and its homologues. Individual leucine rich repeats are highlighted gray. Symbols denote the degree of residue conservation: (fully conserved (*)), strongly conserved (:), weakly conserved (.).

The ROC domain (Figure 3 and 8) is present in LRRK1, LRRK2, Lrrk, and Lrk-1. The ROC domain of the human LRRK2 protein contains the Parkinson-linked mutations R1441C/G/H and N1437H. The asparagine (N) at site 1437 is completely conserved across the proteins examined. The arginine (R) at site 1441 is conserved in the Lrk-1, Lrrk, LRRK2 proteins, while in LRRK1 lysine (L) is present. Lysine and arginine are similar in structure and both have linear positively charged side chains [105], which suggests that this change may not greatly affect protein structure and function.

The COR domain is conserved across LRRK1, LRRK2, Lrrk, and Lrk-1 proteins (Figure 3 and Figure 9). The Y1699C mutation is located within the COR domain. In LRRK2 and invertebrate proteins, this tyrosine (Y) residue is conserved. However, vertebrate LRRK1 proteins possess phenylalanine (F) at this position. Tyrosine and phenylalanine share functional similarities due to the presence of bulky benzene rings in their side chains [106]. However, tyrosine has a hydroxyl group that is absent in phenylalanine that allows it to be modified by various signalling pathways. Therefore, Lrrk, Lrk-1, and LRRK2 share a possible regulation site that is not found in LRRK1.

The kinase domain is conserved across the proteins examined and the G2019 and I2020 residue are highly conserved (Figure 3 and Figure 10). The G2019 and I2020 residues are part of a DYG regulatory motif which is critical to regulation of the enzymatic activity of the kinase domain [107]. This important function of the DYG motif may explain its high level of conservation.

Interproscan detected a WD40-like domain in LRRK1, LRRK2, and Lrk-1. A notable finding was the detection of a quinoprotein-like (QPL) domain in Lrrk (Figure 3 and Figure 11). This is significant because both the WD40-like domain and quinoprotein-like domain have a

similar propeller-like structure [9, 108]. Therefore, the detected WD40-like and QPL-like domains may represent a common domain structure that is conserved across the four proteins examined.

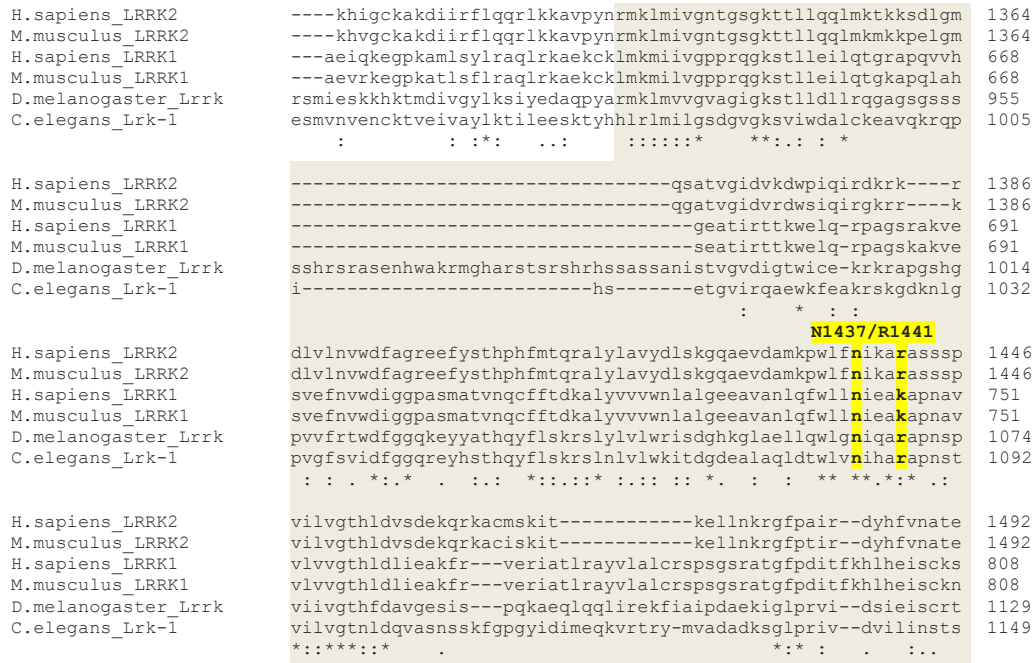


Figure 8: Clustal alignment of the ROC domain of the *Drosophila melanogaster* Lrrk protein and its homologues. ROC domain is highlighted in gray. The location of the LRRK2 residue N1437 and R1441 are highlighted in yellow. The N1437 residue is conserved across all of the proteins, while R1441 is conserved across all proteins except LRRK1. Symbols denote the degree of residue conservation: (fully conserved (*), strongly conserved (:), weakly conserved (.)).

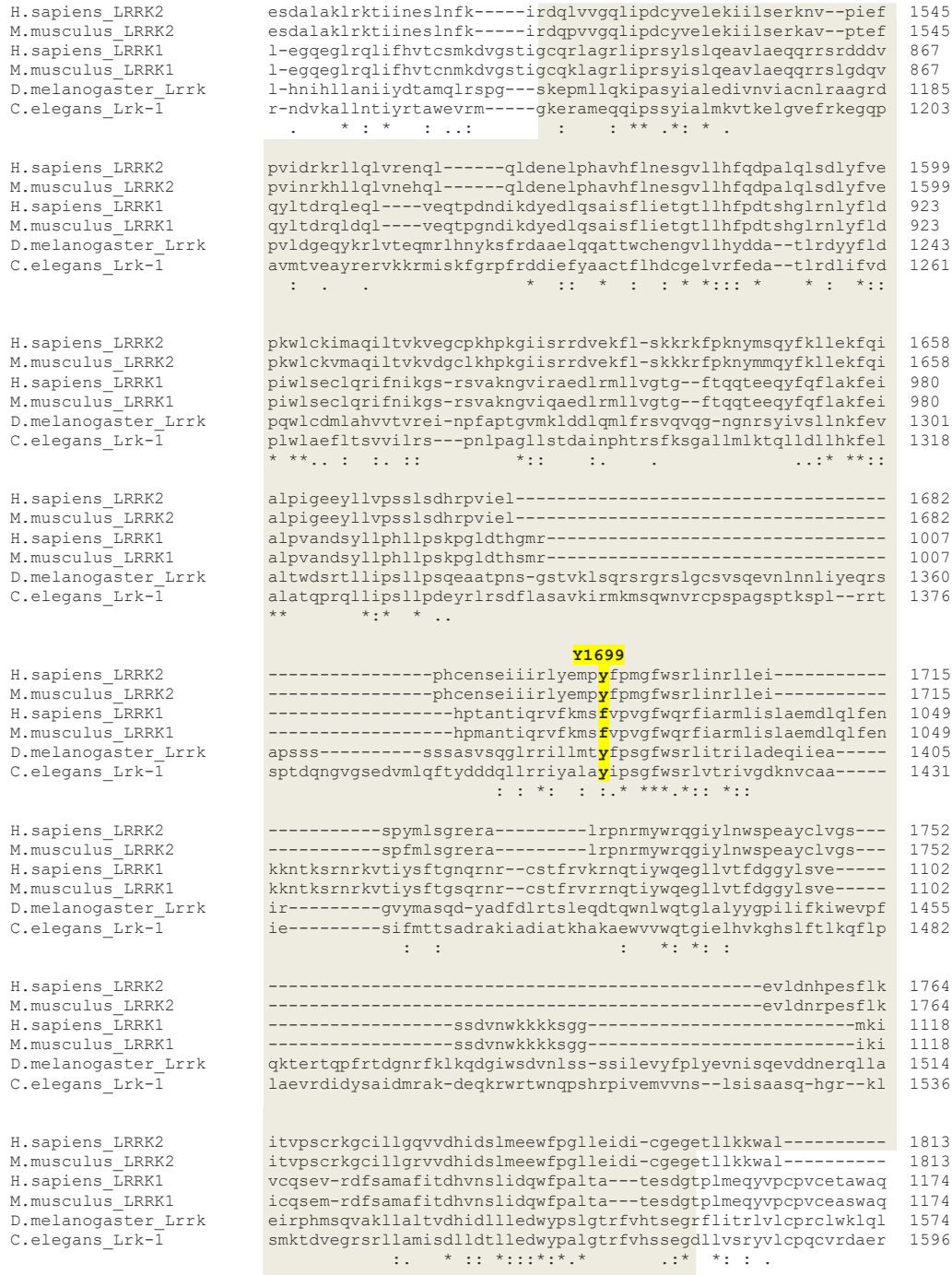


Figure 9: Clustal alignment of the COR domain of the *Drosophila melanogaster* Lrrk protein and its homologues. The COR domain is highlighted in gray. The location of the LRRK2Y1699 residue is highlighted yellow. Y1699 is conserved across all of the proteins except LRRK1. Symbols denote the degree of residue conservation: (fully conserved (*), strongly conserved (:), weakly conserved (.)).

H.sapiens_LRRK2	lvnpdqprltpisqiapdliladlprnimlnndelefefeqapefllgdgsgfsvyraaye	1899
M.musculus_LRRK2	linpdqprltpisqiapdliladlprnimlnndelefefeeapefllgdgsgfsvyraaye	1899
H.sapiens_LRRK1	iscprhpdlpvplqelvpelfmtdfparlflensklehsedegsvlggsggtviyrary	1262
M.musculus_LRRK1	iscprhpdlpvplqelvpelfmtdfparlflensklehtegensilggsggtviyqary	1262
D.melanogaster_Lrrk	iscpvhleq--smaqlapdvifadipdkhtipseci----ikgslrgagfgfvfkanck	1748
C.elegans_Lrk-1	vecpshggl--hmrelapdtvfadienaltihpdql----krsrmlrgagfgfvftratvr	1714
	: * : : : : * : : : : : : : : * * * *	
H.sapiens_LRRK2	-geev----avkifnk-----htslrllrqelvv	1923
M.musculus_LRRK2	-geev----avkifnk-----htslrllrqelvv	1923
H.sapiens_LRRK1	qgqpavkrfhikfkfnfanvp-----adtmlrhlratdamknfsefrqeasm	1310
M.musculus_LRRK1	qgqpavkrfhikfkfnfanvp-----adtmlrhlramdamknfsdfrqeasm	1310
D.melanogaster_Lrrk	vrgarsfkpvamkmlqvpvppgarakesalmafkvavgkwdrdplqhsckayctarqelav	1808
C.elegans_Lrk-1	qpn-gelcevaqkmlpevdppggrpsalaaykaaakwkrdsmevacrayctsrqelsl	1773
	* : : * * * *	
H.sapiens_LRRK2	lchlhhpslisllaagirprmlvmelaskgsldrllqqdkasl----trtlqhrialhv	1978
M.musculus_LRRK2	lchlhhpslisllaagirprmlvmelaskgsldrllqqdkasl----trtlqhrialhv	1978
H.sapiens_LRRK1	lhalqhpccivaligisihplcfalelaplsslntvlsenardssfiplghmltqkiayqi	1370
M.musculus_LRRK1	lhalqhpccivsligisihplcfalelaplsglntvlsenakdssfmplghmltqkiayqi	1370
D.melanogaster_Lrrk	lltlkhpniivplvgiciklplalvllelaplglldallrhyrsgahmgph--tfqtlvlqa	1866
C.elegans_Lrk-1	lsrmkhpniivglvgvctfplslvvelaplgalnqllgshrkagtklslg--vikesavqv	1831
	* : : * * : * : * : * * * * * : * : : *	
	G2019/I2020	
H.sapiens_LRRK2	adglrylhsamiiyrdlkphnvlfftly-----pnaaiiakadygiayccrm-gik	2030
M.musculus_LRRK2	adglrylhsamiiyrdlkphnvlfftly-----pnaaiiakadygiayccrm-gik	2030
H.sapiens_LRRK1	asglaylhkknii fcdlksdnilvwsldv-----kehiniklsdygirsqsfhe-gal	1422
M.musculus_LRRK1	asglaylhkknii fcdlksdnilvwslsa-----kehiniklsdygirsqsfhe-gal	1422
D.melanogaster_Lrrk	araieylhrrriiyrdlksenvlvwelpqptedsprnlvhikiadygirsqtaps-gak	1925
C.elegans_Lrk-1	araieylhsahiiyrdlksenvlgwrfpapfs--pqtdvllklgdygirsrvlpsggak	1888
	* . : * * * * * : * * * * * : : : : * : * * * * * : *	
H.sapiens_LRRK2	tsegtpgfrapevar--gnviynqqadvysfglllydilttggriveglkfpnefdelei	2088
M.musculus_LRRK2	tsegtpgfrapevar--gnviynqqadvysfgllldiwtgtsrimeglrfpnefdelai	2088
H.sapiens_LRRK1	gvegtpgyqapeirp---rivydekvdmsfygmvllyellsgqrpa-lghhql-qiakkls	1477
M.musculus_LRRK1	gvegtpgyqapeirp---rivydekvdmsfygmvllyellsgqrpa-lghhql-qivkkls	1477
D.melanogaster_Lrrk	gfggtegfmapeiiryngееeytekvdcfsfgmfyenislrqpf-eghesi---kecil	1981
C.elegans_Lrk-1	gfggtegfmapeivrfngееeytqkvdcfsfgmflyelltlkfpf-eseehv---kerml	1944
	* * * * * : * * * * * : * * * * * : : : : * : * * * * * : *	
H.sapiens_LRRK2	qgklpdpvkeygcapwpmveklkqclkenqerptsaqvfdilnsaelvcltrillpk	2148
M.musculus_LRRK2	qgklpdpvkeygcapwpmveklitkclkenqerptsaqvfdilnsaeliclmrhilipk	2148
H.sapiens_LRRK1	kgirpvlggpeevqfrr-lqalmmecwdtkpekrplalsvsvsqmkdptfatfmyelcc--	1534
M.musculus_LRRK1	kgirpvlggpeevqfhr-lqalmmecwdtkpekrplalsvsvsqmkdptfatfmymlpc--	1534
D.melanogaster_Lrrk	egsrpaltqretqfptc-cldlmvlwheqprrrrtasqivsilsapecihlldvvamph	2040
C.elegans_Lrk-1	dgarpvllphelllptp-mldllvhcwsahpesrpsssqvlgfcaapefthlldvcelge	2003
	. * * * * * : * * * * * : * * * * * : : : : * : * * * * * : *	

Figure 10: Clustal alignment of the kinase domain of the *Drosophila melanogaster* Lrrk protein and its homologues. The kinase domain is highlighted in gray. The G2019 and isoleucine I2020 residue are highlighted yellow and are highly conserved. Symbols denote the degree of residue conservation: (fully conserved (*), strongly conserved (:), weakly conserved (.)).

H.sapiens_LRRK2	nvi----vecmva-----thhnsrnasiwlgcgh-----tdrgqlsflfd-----	2183
M.musculus_LRRK2	nii----vecmva-----tnlnsksatlwlgcgn-----tekgqlsflfd-----	2183
H.sapiens_LRRK1	-----gkqtaff-ssggqeytvvfdgkkeesrnytvvntekglm-----	1572
M.musculus_LRRK1	-----gkqsaff-ssqsqeytvvfdgkkeesrnytvvntekgll-----	1572
D.melanogaster_Lrrk	s----ekivcgvfqslvgmgddercglelwlpsfgsridildcpspsgllqcnisiscspq	2096
C.elegans_Lrk-1	alpptqlmavgitd---eiddpddfeaqflwsg--remvvmgctqygfvdq-----	2049
	. : : * : * :	
H.sapiens_LRRK2	-----lntegyts-----eevadsrilclalvhlvpkeswivsgtqsgtllvinted	2231
M.musculus_LRRK2	-----lnterysy-----eevadsrilclalvhlhlaeakeswvvcgtqsgallvinvee	2231
H.sapiens_LRRK1	-----evqrmccpgmkvscqlq---vqrlwt--atedqkiyiyltkg	1610
M.musculus_LRRK1	-----evqrmccpgmkvscqlq---vqrlwt--atedqkiyiyltkg	1610
D.melanogaster_Lrrk	pqvappktpengansrarsaqrllpkmmmlccl---vgeaiwm--gdvsgnlhaystst	2150
C.elegans_Lrk-1	ksielp---hrqk-----yvsk---vrdsvws--cdecgqvtvygisl	2084
	. : *	
H.sapiens_LRRK2	gkkrrt---lekmdsvtclcyncsfskqskqknfllvgtadgklaifedktvklkgaap-	2287
M.musculus_LRRK2	etkrrt---lekmdsvtclhcnslakqskqsnfllvgtadgnlmifedkavkckgaap-	2287
H.sapiens_LRRK1	mcplntppqaldtpavvtcflavpvi--kknsvlvalagladglvavfpvrgtpkdsesy	1668
M.musculus_LRRK1	mcplsvppqaldtpavvtcflavpvi--kknsvlvalagladglvavfpvrgtpkdsesy	1668
D.melanogaster_Lrrk	yahlfs---ymldpniksavislvym--ekia-rvavgthngrvflvdat--qmpsncaf	2202
C.elegans_Lrk-1	hetg----hlqlpslngtlicapel--isn--dvlilisdqkivllkls--es-----	2127
	. : : :	
H.sapiens_LRRK2	-----lkilnig---nvstplmcls-estnsternvmwggcgtkifsfndftiqkli	2336
M.musculus_LRRK2	-----lktlhig---dvstplmcls-eslnsaserhitwggcgtkvfsfndftiqkli	2336
H.sapiens_LRRK1	lcshtanrskfsiadedarqnpypvkam--evvnsqsevwsngpgllvid-----cas	1720
M.musculus_LRRK1	lcshtanrskfciapededarqnpypvkam--evvnsqsevwsngpgllvid-----cti	1720
D.melanogaster_Lrrk	aeg-----sfvlt---eicsgfvlhaacsvvvdgiyelwcgeiagkinvf-----pln	2247
C.elegans_Lrk-1	-ns-----vshlg---tidspyeirtatflngstrqiwaghsegrisih-----hia	2171
	. : * . :	
H.sapiens_LRRK2	etrtsqlf-syaafsdnsniitvfv-----dtalyiakqnsppvevwdkkteklcgliid	2388
M.musculus_LRRK2	etktnqlf-syaafsdnsniialav-----dtalyiaknspvvevwdkkteklceliid	2388
H.sapiens_LRRK1	----leicrrlepymapsmvtsvvcssegrgeevvclddkanslvmyhsttyqlcaryf	1776
M.musculus_LRRK1	----ldisrrlepypaapsmvtslvcsdcrgeemvclddkanclvmyhsatyqlcaryf	1776
D.melanogaster_Lrrk	engvsgghqa-lchseepnliedvkvarmacsneshvfsclypgcmvyqwdviskrieklid	2306
C.elegans_Lrk-1	sndsfsfsssllylpddkciivrqlv---gskdaqkwialeksskvqmvvekrqvtgslid	2228
	:: : : . . ::	
H.sapiens_LRRK2	cvhflrevmvke-----nkeskh---kmsysgrvktlclqkntalwigtggghilll	2437
M.musculus_LRRK2	cvhflkevkvkl-----nkeskh---qlsysgrvkalclqkntalwigtggghilll	2437
H.sapiens_LRRK1	cgvpsplrdmfpvrpldteppaashtanpkvpegdsia----dvsimy-seelgtqili	1830
M.musculus_LRRK1	cgdpnplrdtfsvqpsvletpgs-hkttskgpveecia----dvsimy-seelgtqilt	1829
D.melanogaster_Lrrk	csklplpcseslqsi--aide---h-----vnlikcqisalaahnselyigtwtwgcлива	2355
C.elegans_Lrk-1	irkvmpgsetihti--dmem----as----qnyvtcigllernrdgdglyigtsgkllvia	2278
	. : . * ::	
H.sapiens_LRRK2	dlstrrlirviynfcnsrvmmtaqlgslknvmlvlgynrknte-----eigscltvwd	2491
M.musculus_LRRK2	dlstrrvirtihnfcdsvramataqlgslknvmlvlgynrknte-----eigsclsiwd	2497
H.sapiens_LRRK1	hgesltdycsmssyssprrqaarspslpspa--sssvpf----stdcedsdmlht	1883
M.musculus_LRRK1	hqsldtdycsmssyssprrqdprpslpsl--syssvpf-----sanyedsdrlqe	1882
D.melanogaster_Lrrk	elhtlrpivsf-----rpy-----eneiksiitlslk	2381
C.elegans_Lrk-1	hattlqplsac-----rpf-----egditsicilee	2304
	. : : . :	
H.sapiens_LRRK2	inlphev----q-----nlekhievrkelakmrrtsve-----	2521
M.musculus_LRRK2	inlphev----q-----nlekhievrteadkmrrtsve-----	2527
H.sapiens_LRRK1	pgaasdrsehdltpm-----dge----tfsqhlqavkila-vrdliwvprrggdvivi	1931
M.musculus_LRRK1	psvtsdrtehdlspm-----dge----tfsqhlqavkila-vkdliwvprhggdvivi	1930
D.melanogaster_Lrrk	dnpvliatigriry-----slisryvdsaesst-kssavstpthgaa---	2422
C.elegans_Lrk-1	psreeentrgkattlstassesglgwvrevsetvdrf----rsspavvetqgaalvvc	2359
	. . . : :	

Figure 11: Clustal alignment of the QPL domain of the *Drosophila melanogaster* Lrrk protein with the WD40-like domain of its homologues. Note that that a WD40 domain was detected in LRRK1, LRRK2, and Lrk-1, while in Lrrk a QPL domain was detected in the same location. The WD40-like and quinoprotein-like domains are highlighted gray. Symbols denote the degree of residue conservation: (fully conserved (*), strongly conserved (:), weakly conserved (.)).

Prediction of upstream transcription factors for *Lrrk*, *LRRK1*, and *LRRK2*

Transfac Match predictions suggest that *Drosophila Lrrk* expression is regulated by the transcription factors cut, nubbin, PDP1, and the broad-complex Z1 and Z4 isoforms (Table 4). Notably, the *EPgy2^{EY06588}* insertion disrupts the predicted broad-complex binding site [92]. The transcription factor cut, which plays a role in dendrite development [109], is of interest since *LRRK2* has been found to affect dendrite morphology [110]. Human *LRRK2* expression was predicted to be regulated by hepatocyte nuclear factor 1 (HNF1) and forkhead fox D3 (FOX D3) (Table 5). Human *LRRK1* expression was predicted to be regulated by C/EBP homologous protein (CHOP), pax4, POU2F1, and pax6 (Table 6). POU2F1 is a homologue of the transcription factor nubbin [111], which was predicted to regulate expression of *Drosophila Lrrk*. This indicates a possible conserved transcriptional regulation between human *LRRK1* and *Drosophila Lrrk*. In *Drosophila*, nubbin has been found to be involved with neuronal development [112], wing development [111], and immune response [113].

Table 4: Predicted transcription factors upstream of *Lrrk*

Transcription Factor	Known Functions
cut	Sensory bristle development [114], dendrite development [115]
broad-Z1 and -Z4	Dopamine synthesis [116]
nubbin	Neuronal differentiation [112], wing development [111], immune response [113]
PDP1	Mitosis and DNA replication, circadian rhythm [117]

Table 5: Predicted transcription factors upstream of human *LRRK2*

Transcription Factor	Known Functions
HNF1	Expression liver genes, linked to diabetes and cancer [118]
FOX D3	Tumor suppressor gene [119]

Table 6: Predicted transcription factors upstream of human *LRRK1*

Transcription Factor	Known Functions
CHOP	Regulates cell cycle and apoptosis [120], role in regulating body weight [121]
pax4	Pancreatic beta-cell development [122]
POU2F1	T-cell differentiation [123], oncogenesis [124], neuronal differentiation and stress response [125]
pax6	Eye and neuronal development [126]

Influence of *Lrrk*^{e03680} mutation on climbing index

Lrrk^{e03680} homozygotes had a significantly lower climbing index of 3.2200 at eclosion compared to 4.7425 for *w*/+ controls ($p < 0.0001$; Figure 12 and Table 7). Additionally, the flies exhibited a lower rate of decline in climbing ability, with a rate constant of 0.01305 compared to a rate constant of 0.04201 for *w*/+ controls (Figure 12 and Table 8). The lower rate of decline might be attributed to the lower initial climbing index of these flies, rather than any protective effect. Heterozygotes that were the progeny of homozygous *w*¹¹¹⁸ females had a significantly lower climbing index at eclosion of 4.5040 compared to 4.7425 for *w*/+ controls ($p < 0.0001$; Figure 12 and Table 7). There was a lower rate of decline in climbing index with a rate constant of 0.03076 compared to 0.04201 for controls ($p < 0.0001$; Figure 12 and Table 8). In contrast, those that were the progeny of *Lrrk*^{e03680} heterozygotes did not show a significant alteration in climbing index throughout their lifespan.

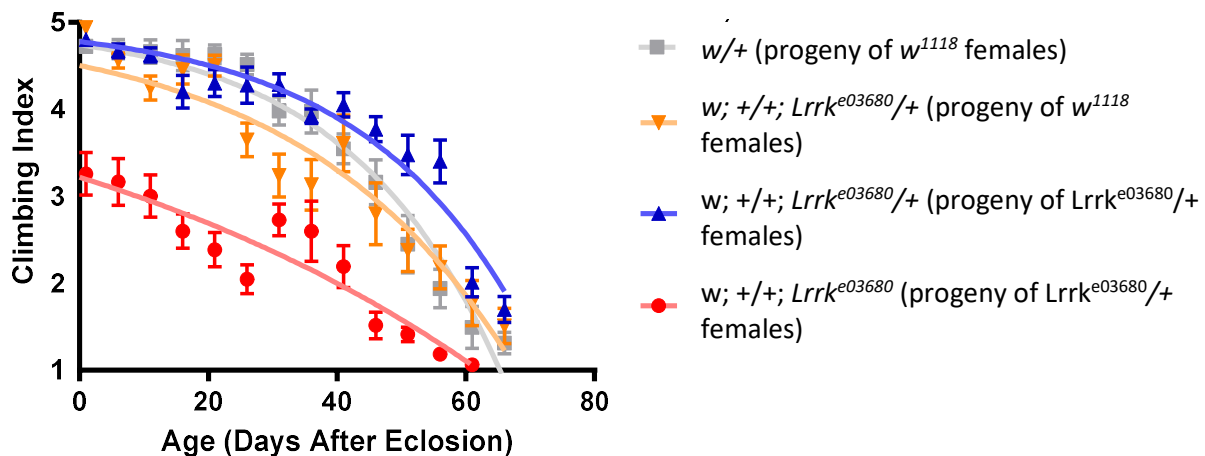


Figure 12: Effect of *Lrrk*^{e03680} mutation on climbing ability. Error bars represent standard error. *Lrrk*^{e03680} homozygotes had significantly lower climbing index at eclosion ($p < 0.0001$) and a lower rate of decline in climbing index ($p < 0.0001$). *Lrrk*^{e03680} heterozygotes that were offspring of homozygous *w*¹¹¹⁸ females had significantly lower climbing index at eclosion ($p < 0.0001$) and a lower rate of decline in climbing index ($p < 0.0001$). See tables 7 and 8 for a full analysis of the data. Data from 8 vials was used to calculate the curves. Vials started with 10 flies and were discarded when three or fewer flies remained.

Table 7: Comparison of the Y-intercept of the non-linear fitted curves for the *Lrrk^{e03680}* climbing assays

Genotype	Y-Intercept	Standard Error	95% Confidence Intervals	R ²	P-Value	Significance
w/+	4.7425	0.03521	4.6726 to 4.8123	0.8423	N/A	N/A
w/+; +/+; <i>Lrrk^{e03680}</i>/+ (w¹¹¹⁸ mother)	4.5040	0.06298	4.3791 to 4.6289	0.7019	<0.0001	Yes
W/+; +/+; <i>Lrrk^{e03680}</i> /+ (<i>Lrrk^{e03680}</i> heterozygote mother)	4.7774	0.03298	4.7120 to 4.8428	0.7408	0.4697	No
w/+; +/+; <i>Lrrk^{e03680}</i>	3.2200	0.1035	3.014 to 3.426	0.4575	<0.0001	Yes

Table 8: Comparison of rate-constant of the non-linear fitted curves for the *Lrrk^{e03680}* climbing assays

Genotype	Rate Constant	Standard Error	95% Confidence Intervals	R ²	P-Value	Significance
w/+	0.04201	0.002378	0.03729 to 0.04673	0.8423	N/A	N/A
w/+; +/+; <i>Lrrk^{e03680}</i>/+ (w¹¹¹⁸ mother)	0.03076	0.002371	0.02605 to 0.03546	0.7019	<0.0001	Yes
w/+; +/+; <i>Lrrk^{e03680}</i> /+ (<i>Lrrk^{e03680}</i> heterozygote mother)	0.03988	0.002708	0.03450 to 0.04526	0.4575	0.5568	No
w/+; +/+; <i>Lrrk^{e03680}</i>	0.01305	0.001526	0.01001 to 0.01609	0.7408	<0.0001	Yes

Influence of *Lrrk*^{e03680} mutation on longevity

Male *Lrrk*^{e03680} homozygotes have a decreased lifespan with a median survival of 56 days compared to a median survival of 72 days for controls ($p < 0.0001$; Figure 13 and Table 9). The lifespan of flies heterozygous for the *Lrrk*^{e03680} mutation is not significantly different regardless of the maternal genotype.

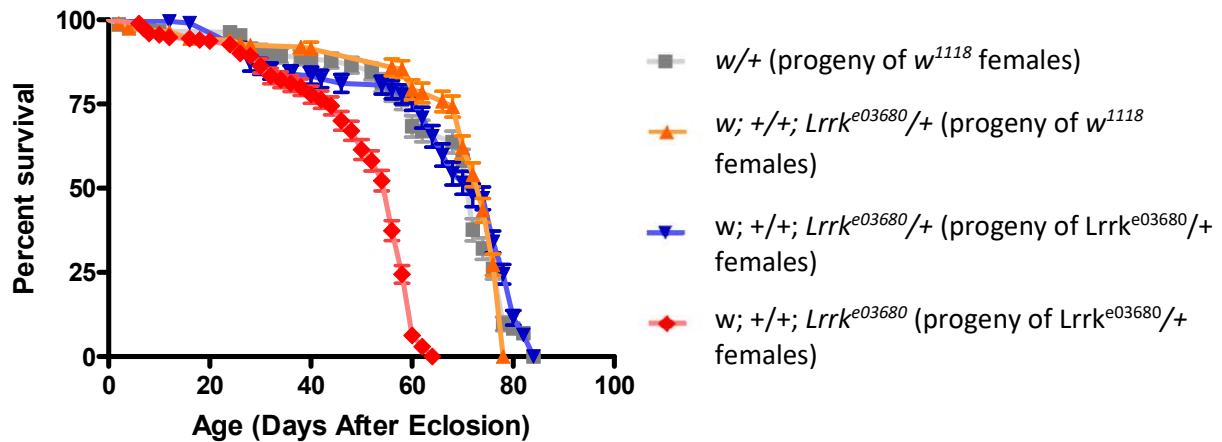


Figure 13: Effect of *Lrrk*^{e03680} mutation on longevity. Error bars represent standard error. Male *Lrrk*^{e03680} homozygotes that are progeny of *Lrrk*^{e03680} heterozygous females have decreased life span (median survival 56) compared to *w/+* controls (median survival 72). See table 9 for full data analysis.

Table 9: Log-rank statistical analysis of longevity curve for *Lrrk*^{e03680} mutant *Drosophila*

Genotype	Number of Flies	Median Survival (Days)	Chi-Square Value	P-Value	Significance
<i>w/+</i>	215	72	N/A	N/A	N/A
<i>w/+; +/+; Lrrk</i> ^{e03680} / <i>+</i> (<i>w</i> ¹¹¹⁸ mother)	212	74	0.05699	0.8113	No
<i>w/+; +/+; Lrrk</i> ^{e03680} / <i>+</i> (<i>Lrrk</i> ^{e03680} heterozygote mother)	217	72	2.040	0.1532	No
<i>w/+; +/+; Lrrk</i> ^{e03680}	270	56	228.9	<0.0001	Yes

Penetrance of *Lrrk*^{e03680} cuticle defects

Some flies with the *Lrrk*^{e03680} mutation were found to have missing patches of cuticle (Figure 14, left). These flies were afflicted at eclosion and the phenotype did not change throughout their lifespan. Counts of the number of female homozygotes that expressed this phenotype indicated that 32% were afflicted compared to controls which did not express the phenotype at all (Figure 14, right). The phenotype was expressed in 4% of both heterozygous females and homozygous males, and 1% of heterozygous males. Therefore, for both sexes homozygotes exhibited a greater penetrance for this phenotype. When the sexes are compared, females were more commonly affected than males for heterozygotes and homozygotes. None of the *w/+* control flies were found to express this phenotype.

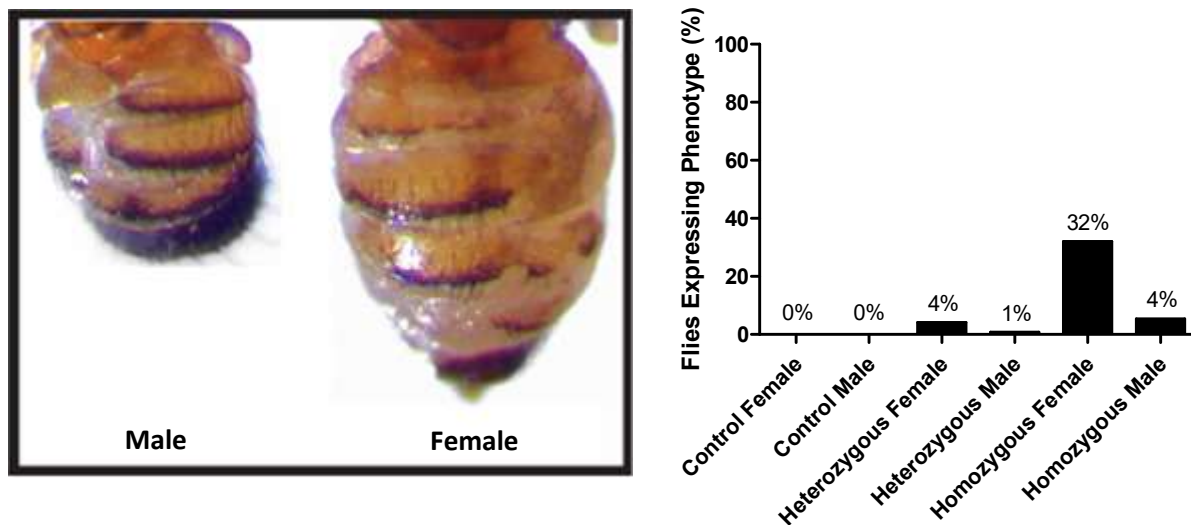


Figure 14: Examples of *Lrrk*^{e03680} incomplete abdominal cuticle phenotype and percentage of males and females that express the phenotype. A large percentage of homozygous females express the phenotype (32%; N = 100), while only a small percentage of males and heterozygous females express it (1%-4%). Counts of *w/+* controls found that no flies expressed this phenotype.

Influence of *Lrrk*^{e03680} mutation on female fecundity

Egg laying in female flies homozygous for the *Lrrk*^{e03680} mutation was severely depressed across the entire life span (Figure 15 and Table 10). In most cases no eggs were laid at all and at most eight eggs were laid per day. In contrast, a comparison of the 95% confidence interval of the linear regression lines revealed an increased number of eggs laid by heterozygotes from day 5 to day 26 post-eclosion.

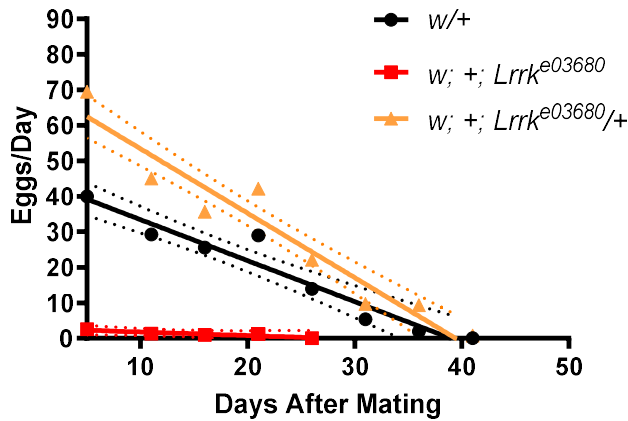


Figure 15: Effect of *Lrrk*^{e03680} mutation on female fertility in *Drosophila*. Dotted lines represent the 95% confidence interval of the linear regression line. Homozygotes had severely decreased egg laying throughout their lifespan compared to controls. Heterozygotes laid a significantly greater numbers of eggs compared to controls up to 26 days after eclosion. See table 10 for statistical analysis of the regression lines (N=10).

Table 10: Comparison of the slopes for the *Lrrk*^{e03680} fecundity assay

Genotype	Slope	Standard Error	95% Confidence Intervals	R ²	P-Value	Significance
w/+	-1.154	0.1343	-1.426 to -0.8815	0.6721	N/A	N/A
w/+; +/+; <i>Lrrk</i> ^{e03680} /+	-1.814	0.1550	-2.124 to -1.504	0.6882	0.0043	Yes
w/+; +/+; <i>Lrrk</i> ^{e03680}	-0.09998	0.06728	-0.2378 to 0.03785	0.07309	<0.0001	Yes

The *Lrrk^{e03680}* mutation affects development of posterior wing vein

Among the *Lrrk^{e03680}* mutants, a fraction displayed an incomplete posterior wing vein phenotype (Figure 16). This phenotype was present at eclosion in afflicted flies and the phenotype was not weakened or enhanced with age. Counts of affected flies revealed a penetrance of 24% for the phenotype in homozygous males and 0% penetrance in both heterozygous males and homozygous females (Figure 17).



Figure 16: Incomplete formation of posterior cross vein in *Lrrk^{e03680}* homozygous males. Incomplete cross vein is indicated by red circle. Normal wings are shown on the right. Females did not display this phenotype.

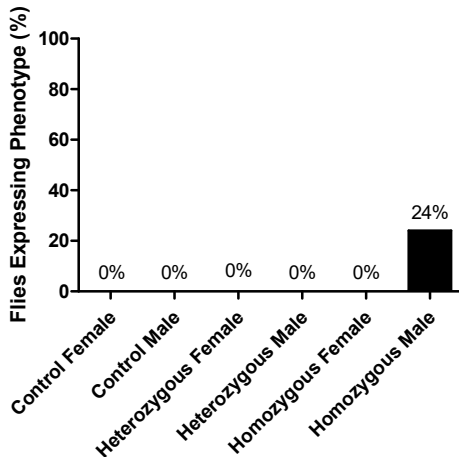


Figure 17: Percentage of *Lrrk*^{e03680} flies expressing the incomplete posterior cross vein phenotype. Approximately 24% (N=100) of homozygous males expressed this phenotype. Counts of other genotypes found no flies that expressed this phenotype.

The *Lrrk*^{e03680} mutation affects development of the eye

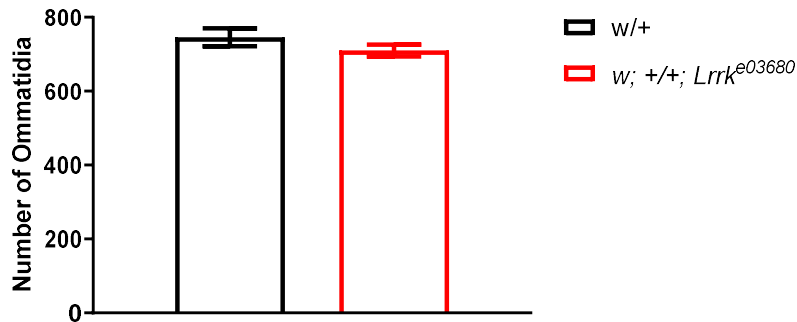
Some *Lrrk*^{e03680} homozygous flies were found to have black ommatidia (Figure 18).

When the eyes were examined with the scanning electron microscope it was found that there was no significant disruption to the structure, size, or number of the ommatidia in these mutants (Figure 19A-B and 20A-B). However, the number of bristles was lower in *Lrrk*^{e03680} homozygous females with a mean score 498.1 bristles compared to 564.8 bristles for *w/+* controls ($p=0.0007$; Figure 19C and Table 11). The number of bristles was lower in *Lrrk*^{e03680} homozygous males with a mean score of 495.6 bristles compared to 510.4 bristles for *w/+* controls, although the difference was not statistically significant ($p=0.1823$; Figure 20C and Table 12).

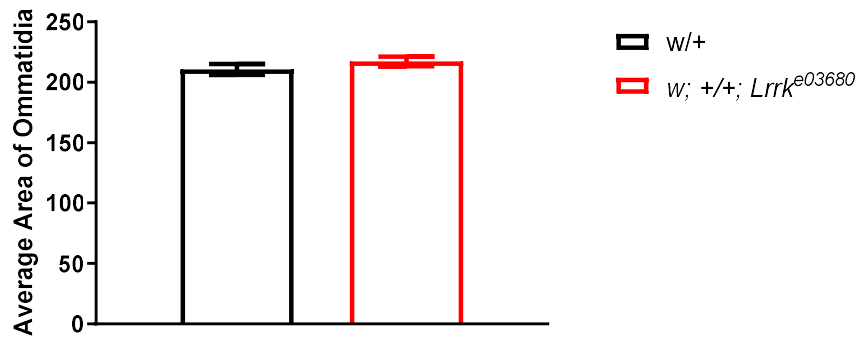


Figure 18: Example of black ommatidia in a fly homozygous for the *Lrrk*^{e03680} mutation. Patches of ommatidia were found to be black in *Lrrk*^{e03680} homozygotes. Despite these black spots, the structure and pattern of the ommatidia was not visibly disrupted.

A



B



C

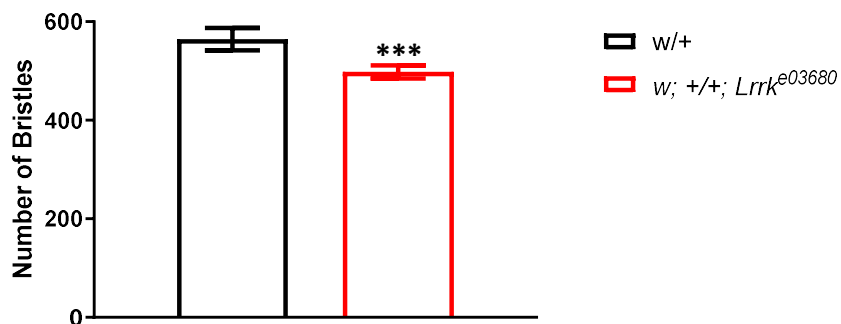
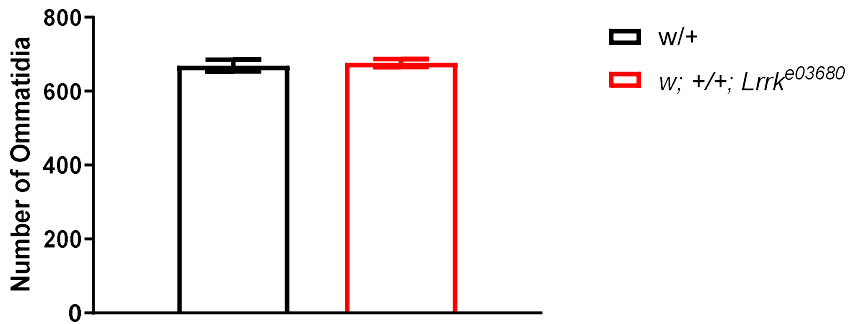
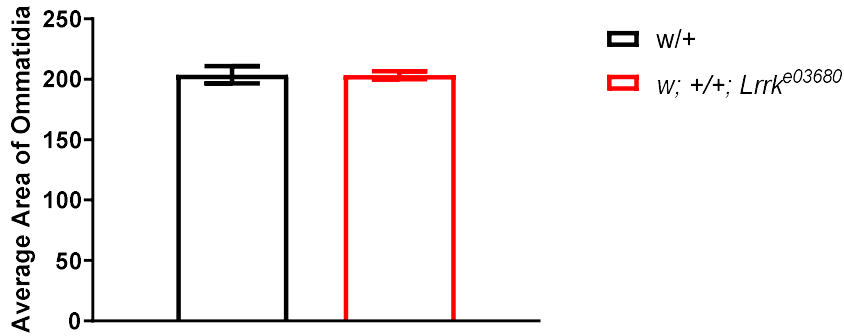


Figure 19: Analysis of ommatidia number (A), area (B), and bristle number (C) for the eyes of *Lrrk^{e03680}* mutant females. Error bars represent the 95% confidence interval. The number of bristles in *Lrrk^{e03680}* homozygotes (498.1) was significantly lower than for controls (564.8; $p=0.0007$). See table 11 for statistical analysis.

A



B



C

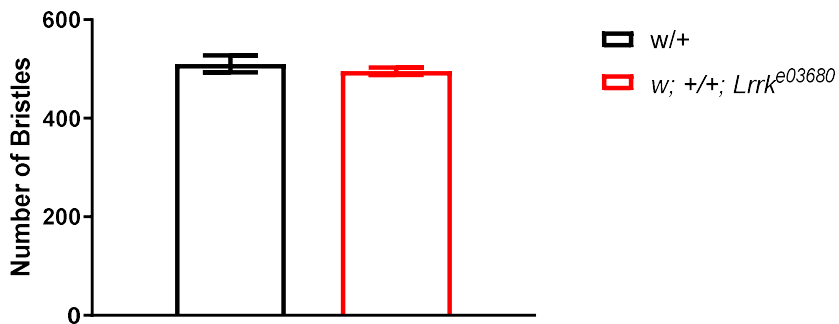


Figure 20: Analysis of ommatidia number (A), area (B), and bristle number (C) for the eyes of *Lrrk*^{e03680} mutant males. Error bars represent the 95% confidence interval. There was no significant difference between the eyes of wild-type and mutant flies for the variables analyzed. See table 12 for statistical analysis.

Table 11: Summary of unpaired t-test comparing *Lrrk*^{e03680} mutant ommatidia area, size, and bristle number to *w*/+ controls for female flies

Genotype	Sample Size	Mean ± SEM	P-Value	Significance
Ommatidia Number				
<i>w</i> /+	10	710.1 ± 10.84	N/A	N/A
<i>w</i> /+; +/+; <i>Lrrk</i> ^{e03680}	9	746.1 ± 16.30	0.0799	No
Ommatidia Area				
<i>w</i> /+	10	210.6 ± 1.944 μm	N/A	N/A
<i>w</i> /+; +/+; <i>Lrrk</i> ^{e03680}	9	217.2 ± 3.950 μm	0.1411	No
Bristle Number				
<i>w</i> /+	10	564.8 ± 9.896	N/A	N/A
<i>w</i> /+; +/+; <i>Lrrk</i> ^{e03680}	9	498.1 ± 13.12	0.0007	Yes

Table 12: Summary of unpaired t-test comparing *Lrrk*^{e03680} mutant ommatidia area, size, and bristle number to *w*/+ controls for male flies

Genotype	Sample Size	Mean ± SEM	P-Value	Significance
Ommatidia Number				
<i>w</i> /+	10	669.2 ± 7.144	N/A	N/A
<i>w</i> /+; +/+; <i>Lrrk</i> ^{e03680}	12	676.2 ± 10.70	0.6099	No
Ommatidia Area				
<i>w</i> /+	10	203.7 ± 3.142 μm	N/A	N/A
<i>w</i> /+; +/+; <i>Lrrk</i> ^{e03680}	12	203.4 ± 3.420 μm	0.9485	No
Bristle Number				
<i>w</i> /+	10	510.4 ± 7.671	N/A	N/A
<i>w</i> /+; +/+; <i>Lrrk</i> ^{e03680}	12	495.6 ± 7.311	0.1823	No

The *EPgy2^{EY06588}* insertion causes sporadic melanotic tumors

Observations of *EPgy2^{EY06588}* mutant larvae showed sporadic development of black spots within the bodies of third instar larvae (Figure 21). These spots are consistent with melanotic tumors that have been reported in a number of previous studies [127, 128]. Some tumors developed around specific organs, which include the lymph nodes near the anterior end and the fat bodies at the posterior end of the larvae. In some cases, melanotic tumors formed in other regions of the body that were not associated with any particular part of the larval anatomy.

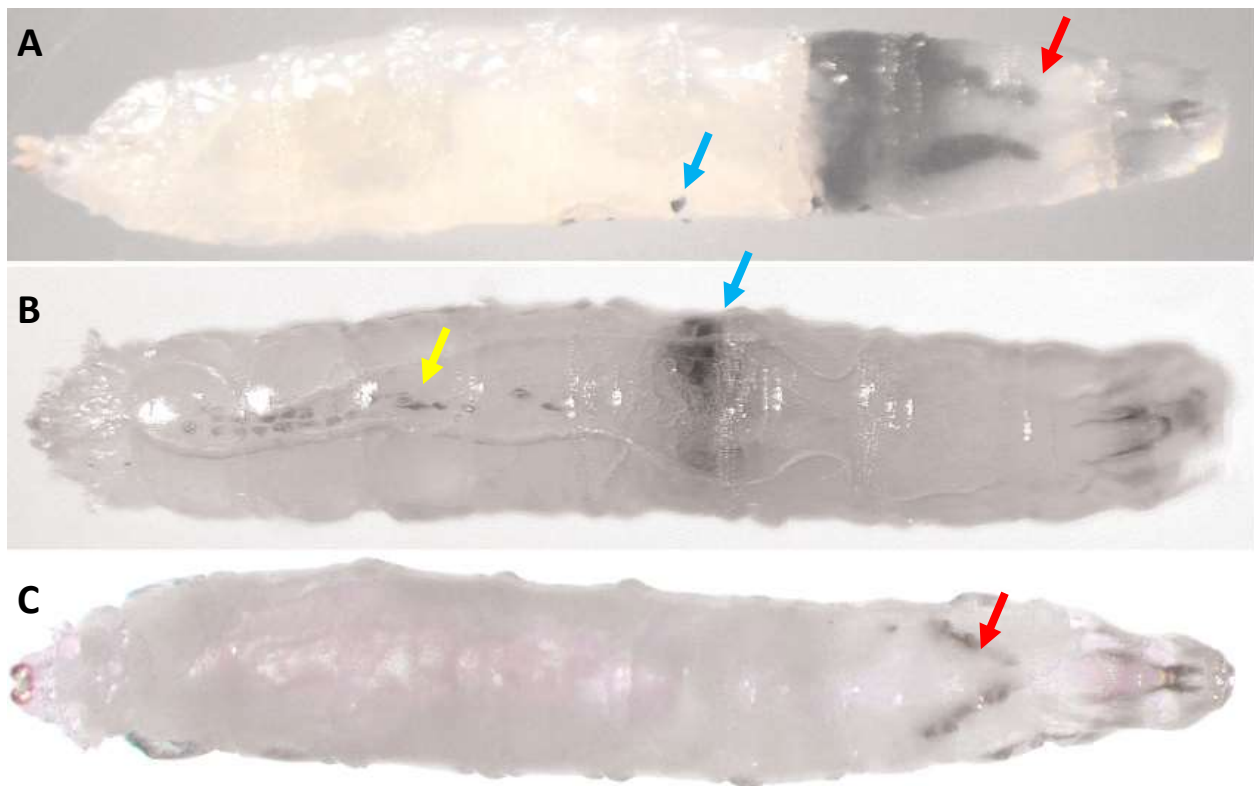


Figure 21: The *EPgy2^{EY06588}* insertion induces the formation of melanotic tumors in third instar larvae. Tumors are associated with specific structures, which include the lymph nodes (red arrows), fat bodies (yellow arrow). Other tumors are not associated with any particular body structures (blue arrows).

Interaction of *SOD* and *TH* overexpression with climbing index and survival

Flies that overexpressed *SOD* had a lower climbing index at eclosion of 3.4700 compared to controls that expressed *GFP*, with an index of 4.0818 ($p = 0.0037$; Figure 22 and Table 13). The rate of decline in climbing index was lower than for controls, with a score of 0.3502 and 0.01922 respectively ($p < 0.0001$; Figure 22 and Table 14). Similarly, overexpression of *TH* resulted in a lower climbing index at eclosion of 2.8830 compared to controls ($p < 0.0001$; Figure 22 and Table 13). The rate of decline in climbing index for *TH* overexpression was lower than controls, with a score of 0.01428 ($p < 0.0001$; Figure 22 and Table 14). Survival of flies that overexpressed *SOD* was significantly higher, with a median survival of 34 days compared to 30 days for controls ($p < 0.0001$; Figure 23 and Table 15).

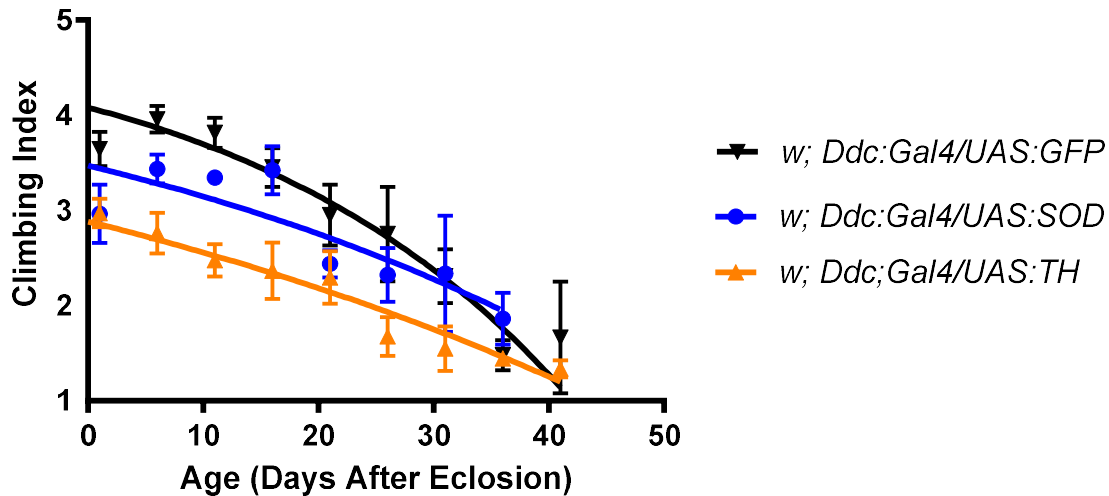


Figure 22: Effect of *SOD* and *TH* overexpression in dopamine-producing neurons on climbing ability. Error bars represent standard error. Climbing index at eclosion was lower than *GFP* controls (y-intercept = 4.0818) for flies that overexpressed *SOD* (y-intercept = 3.4700; $p < 0.0001$) and *TH* (y-intercept = 2.8830; $p = 0.0037$). Rate of decline in climbing ability was lower than *GFP* controls ($k = 0.01922$) compared to flies that overexpressed either *SOD* ($k = 0.3502$; $p < 0.0001$) and *TH* ($k = 0.01428$; $p < 0.0001$). See tables 11 and 12 for full statistical analysis. Data from 8 vials was used to calculate the curves. Vials started with 10 flies and were discarded when three or fewer flies remained.

Table 13: Comparison of Y-intercept for non-linear fitted curves for expression of *GFP* and overexpression of *SOD* or *TH*

Genotype	Y-Intercept	Standard Error	95% Confidence Intervals	R ²	P-Value	Significance
<i>w; Ddc:Gal4/UAS:GFP</i>	4.0818	0.1115	3.8590 to 4.3042	0.5082	N/A	N/A
<i>w; Ddc:Gal4/UAS:SOD</i>	3.4700	0.1621	3.1370 to 3.803	0.4519	0.0037	Yes
<i>w; Ddc:Gal4/UAS:TH</i>	2.8830	0.1134	2.6540 to 3.1120	0.6213	<0.0001	Yes

Table 14: Comparison of rate constant of fitted curves for expression of *GFP* and overexpression of *SOD* or *TH*

Genotype	Rate Constant	Standard Error	95% Confidence Intervals	R ²	P-Value	Significance
<i>w; Ddc:Gal4/UAS:GFP</i>	0.3502	0.004235	0.02657 to 0.04346	0.5082	N/A	N/A
<i>w; Ddc:Gal4/UAS:SOD</i>	0.01922	0.004127	0.007255 to 0.01886	0.4519	<0.0001	Yes
<i>w; Ddc:Gal4/UAS:TH</i>	0.01428	0.001818	0.008185 to 0.01555	0.6213	<0.0001	Yes

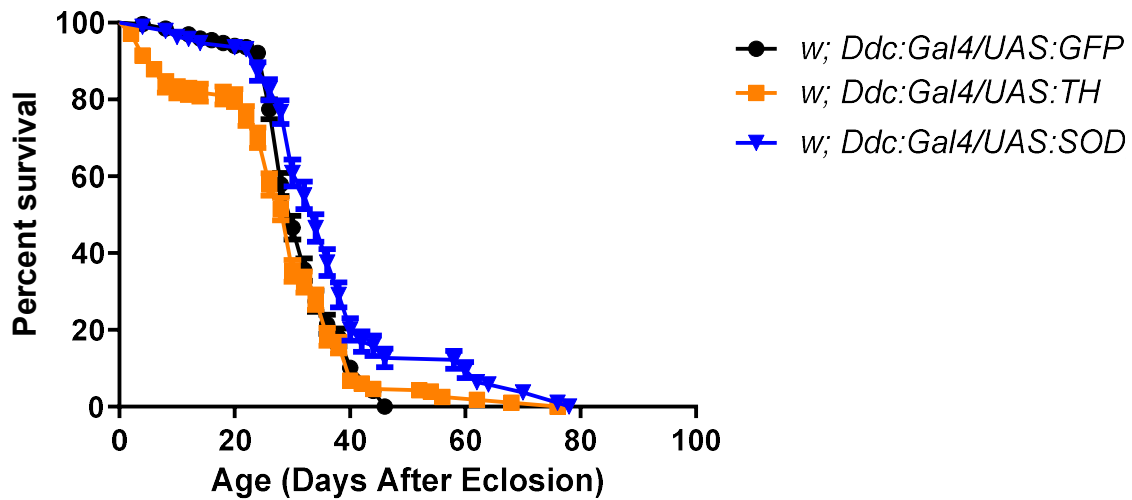


Figure 23: Effect of *SOD* and *TH* overexpression on longevity. Error bars represent standard error. Median survival was higher in flies that overexpressed *SOD* (median survival = 34 days) compared to controls (median survival = 30 days; $p < 0.0001$). See table 14 for statistical analysis.

Table 15: Log-rank statistical analysis of longevity of *Drosophila* with expression of *GFP* and overexpression of *SOD* or *TH*.

Genotype	Number of Flies	Median Survival (Days)	Chi-Square Value	P-Value	Significance
<i>w; Ddc:Gal4/UAS:GFP</i>	266	30	N/A	N/A	N/A
<i>w; Ddc:Gal4/UAS:SOD</i>	189	34	24.83	<0.0001	Yes
<i>w; Ddc:Gal4/UAS:TH</i>	280	30	2.699	0.1004	No

Interaction of *SOD* and *TH* overexpression with climbing index and survival in *Lrrk^{e03680}* mutant background

Climbing index was not significantly different for flies in *Lrrk^{e03680}* mutant background when *SOD* and *TH* were overexpressed compared to *GFP* controls (Figure 24, Tables 16 and 17). Survival of flies that overexpressed *TH* was significantly lower with a median survival of 35 days compared to 56 days for *GFP* controls ($p < 0.0001$), but survival was not significantly different for overexpression *SOD* in a *Lrrk^{e03680}* mutant background (Figure 25 and Table 18).

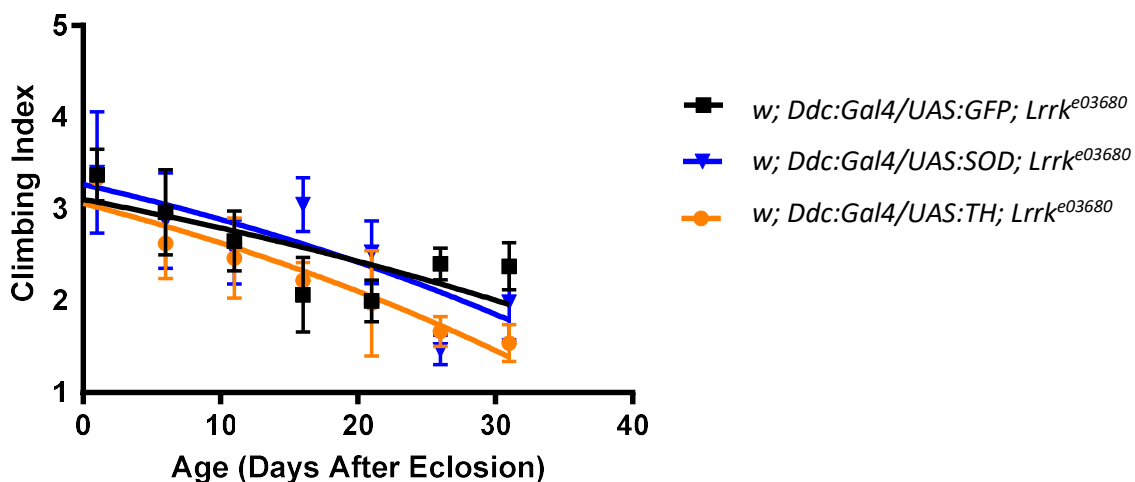


Figure 24: Effect of *SOD* and *TH* overexpression in dopamine producing neurons on climbing ability in *Lrrk^{e03680}* mutants. When *SOD* and *TH* were overexpressed, there was no significant change in climbing ability of *Lrrk^{e03680}* mutants compared to *GFP* controls. See tables 14 and 15 for statistical analysis. Data from 8 vials (10-4 flies per vial) was used to calculate the curves.

Table 16: Comparison of Y-intercept of non-linear fitted curves for expression of *GFP* and overexpression of *SOD* or *TH* in a *Lrrk^{e03680}* background

Genotype	Y-Intercept	Standard Error	95% Confidence Intervals	R ²	P-Value	Significance
<i>w; Ddc:Gal4/UAS:GFP; Lrrk^{e03680}</i>	3.1060	0.1965	2.706 to 3.506	0.3086	N/A	N/A
<i>w; Ddc:Gal4/UAS:SOD; Lrrk^{e03680}</i>	3.2690	0.2546	2.751 to 3.788	0.2731	0.6140	No
<i>w; Ddc:Gal4/UAS:TH; Lrrk^{e03680}</i>	3.0610	0.1763	2.6980 to 3.4250	0.4959	0.8686	No

Table 17: Comparison of rate constant of non-linear fitted curves for expression of *GFP* overexpression of *SOD* or *TH* in a *Lrrk^{e03680}* background

Genotype	Rate Constant	Standard Error	95% Confidence Intervals	R ²	P-Value	Significance
<i>w; Ddc:Gal4/UAS:GFP; Lrrk^{e03680}</i>	0.01525	0.004230	0.004344 to 0.02616	0.2154	N/A	N/A
<i>w; Ddc:Gal4/UAS:SOD; Lrrk^{e03680}</i>	0.01992	0.004854	0.005942 to 0.03390	0.2127	0.4708	No
<i>w; Ddc:Gal4/UAS:TH; Lrrk^{e03680}</i>	0.02009	0.004212	0.01141 to 0.02876	0.4904	0.4271	No

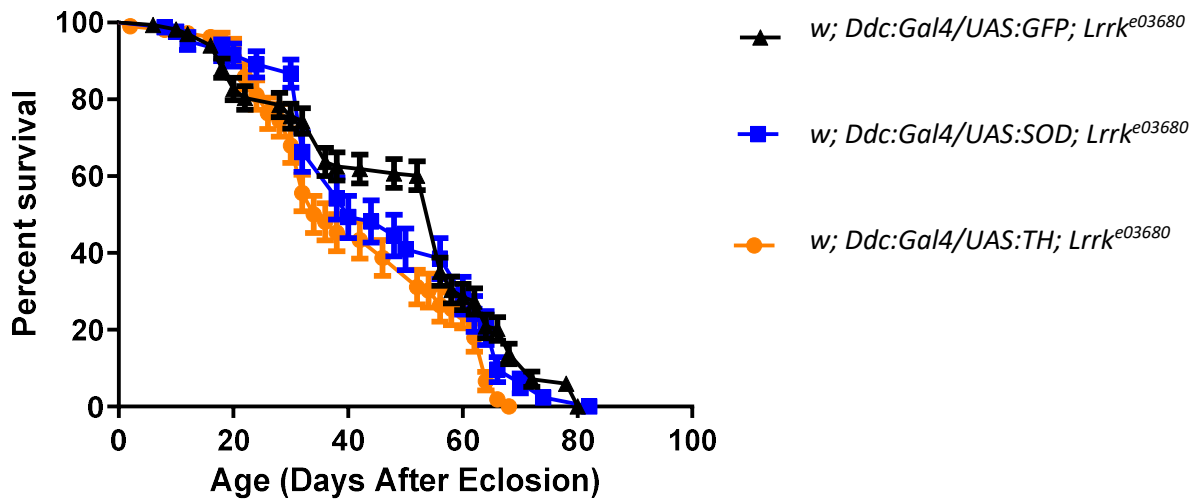


Figure 25: Effect of *SOD* and *TH* overexpression on longevity in *Lrrk^{e03680}* mutant background. When *TH* was overexpressed survival was reduced (median survival = 35 days) compared to controls (median survival = 56 days; $p < 0.0001$). See table 16 for full statistical analysis.

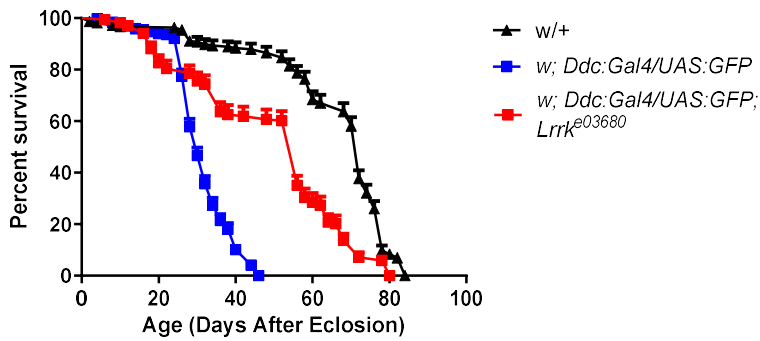
Table 18: Log-rank statistical analysis of longevity of *Drosophila* with expression of *GFP* and overexpression of *SOD* or *TH* in a *Lrrk^{e03680}* background

Genotype	Number of Flies	Median Survival (Days)	Chi-Square Value	P-Value	Significance
<i>w; Ddc:Gal4/UAS:GFP; Lrrk^{e03680}</i>	168	56	N/A	N/A	N/A
<i>w; Ddc:Gal4/UAS:SOD; Lrrk^{e03680}</i>	102	40	1.235	0.2664	No
<i>w; Ddc:Gal4/UAS:TH; Lrrk^{e03680}</i>	106	35	18.41	<0.0001	Yes

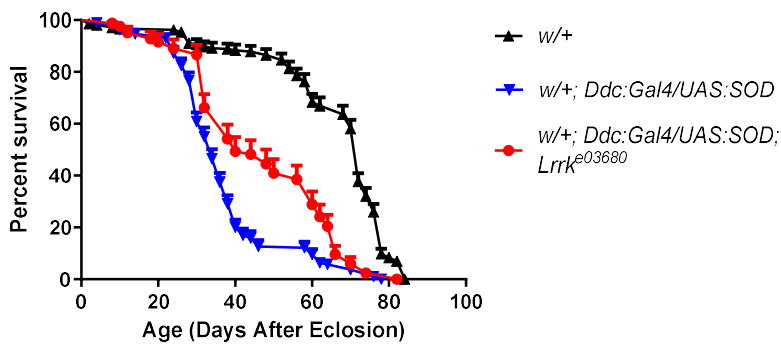
The *Lrrk^{e03680}* mutation suppresses *Ddc:Gal4*-induced loss of lifespan

Expression of *Ddc:Gal4* lowered survival of flies. While *w/+* controls had a median survival of 72 days, *UAS:GFP* flies had a median survival of 30 days, *UAS:SOD* flies had a median survival of 34 days, and *UAS:TH* flies had a median survival of 30 days ($p < 0.0001$ for all; Figure 26 and Table 17). This decrease in survival was partially rescued by the *Lrrk^{e03680}* mutation. In a *UAS:GFP* background median survival was 56 days, compared to 40 days for *UAS:SOD*, and 35 days for *UAS:TH* ($p < 0.0001$ for all; Figure 26 and Table 17).

A



B



C

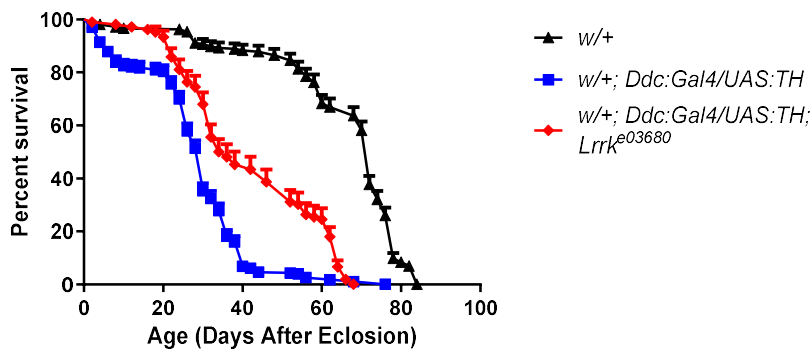


Figure 26: The *Lrrk^{e03680}* mutation suppresses *Ddc:Gal4*-induced loss of lifespan. In a *Ddc:Gal4* background, survival was decreased compared to *w/+* controls. The *Lrrk^{e03680}* mutation partially rescued this loss of survival in a *UAS:GFP*, *UAS:TH*, and *UAS:SOD* background. See table 14 for full analysis.

Table 19: Log-rank statistical analysis of longevity of *Lrrk*^{e03680} mutant *Drosophila* compared to *w*/+ and *GFP* controls

<i>UAS:GFP</i>					
Genotype	Number of Flies	Median Survival (Days)	Chi-Square Value	P-Value	Significance
<i>w; Ddc:Gal4/UAS:GFP; Lrrk</i> ^{e03680}	168	56	N/A	N/A	N/A
<i>w; Ddc:Gal4/UAS:GFP</i>	266	30	157.6	<0.0001	Yes
<i>w</i> /+	215	72	388.5	<0.0001	Yes
<i>UAS:SOD</i>					
Genotype	Number of Flies	Median Survival (Days)	Chi-Square Value	P-Value	Significance
<i>w; Ddc:Gal4/UAS:SOD; Lrrk</i> ^{e03680}	102	40	N/A	N/A	N/A
<i>w; Ddc:Gal4/UAS:SOD</i>	189	34	17.94	<0.0001	Yes
<i>w</i> /+	215	72	219.2	<0.0001	Yes
<i>UAS:TH</i>					
Genotype	Number of Flies	Median Survival (Days)	Chi-Square Value	P-Value	Significance
<i>w; Ddc:Gal4/UAS:TH; Lrrk</i> ^{e03680}	106	35	18.41	N/A	N/A
<i>w; Ddc:Gal4/UAS:TH</i>	280	30	40.93	<0.0001	Yes
<i>w</i> /+	215	72	355.0	<0.0001	Yes

Discussion

Similar domain structure of LRRK2, LRRK1, and *Drosophila melanogaster* Lrrk suggest shared structure and function

The domain structures of the human LRRK1, LRRK2, and *Drosophila* Lrrk proteins share considerable similarity to each other (Figures 3-11), with all proteins having ankyrin repeat, leucine-rich repeat, ROC, COR, and kinase domains (Figure 3). Human LRRK2 is distinct, as it has an armadillo-like domain near its N-terminus. The QPL detected in Lrrk and the WD40-like domain detected in the other proteins may represent the same conserved domain, as both domains share an eight-bladed beta-propeller structure [15, 108]. Therefore, the primary difference in the LRRK2 protein, as compared to the LRRK1 and Lrrk proteins, is the presence of the armadillo-like domain in LRRK2, which may have evolved after the divergence in evolution between LRRK1 and LRRK2.

The domain structure of these proteins indicates that protein-protein interactions are important to its function. The ankyrin repeat, leucine-rich repeat, and WD40-like domains are all known to provide scaffolds that mediate interactions between proteins [8, 9, 129]. These interactions may be important to the kinase activity of the proteins by facilitating interactions between the protein and its substrates and for interactions with proteins that might regulate the function of the proteins. The armadillo-like domain, which is found only in LRRK2 is similarly related to protein-protein interactions, in particular intracellular signalling and cytoskeletal dynamics [130]. Importantly, there is some evidence that LRRK2 interacts with cytoskeletal proteins [16]. The fact that the armadillo-like domain is not found in Lrrk suggests that LRRK2

may interact with proteins that the *Drosophila* protein does not, so not all functions of LRRK2 may be shared by Lrrk.

Amino acid residues that have been linked to Parkinson Disease are well conserved within the ROC, COR, and kinase domains. The N1437 (ROC domain), R1441 (ROC domain), Y1699 (COR domain), G2019 (kinase domain), and I2020 (kinase domain) residues were all conserved between the Lrrk, LRRK2, and Lrk-1 proteins (Figures 8-11). This suggests that Lrrk has the potential to be an effective model for the exploration of the effects of Parkinson-linked mutations that occur at these sites. Although the R1441 and Y1699 residues were not conserved between LRRK1 and the other proteins analyzed, LRRK1 has lysine (K) at site 1441 which shares a similar structure and positive charge with arginine (R) [105], and phenylalanine (F) at site 1699 which shares a similar benzene-ring structure with tyrosine (Y) [106]. However, phenylalanine cannot be phosphorylated like tyrosine, a process which can be important for regulation of protein function. Therefore, LRRK2, Lrrk, and Lrk-1 may share a regulatory site not found in LRRK1.

Despite the differences between the LRRK2 and Lrrk proteins, the overall similarity in domain structure and conservation of key amino acids in the ROC, COR, and kinase domains support *Drosophila melanogaster* as being a good model organism to improve comprehension of human LRRK2 and the role that it plays in Parkinson Disease. Although there will undoubtedly be some differences in function between the proteins, particularly due to the presence of the armadillo domain in LRRK2, there are likely to be many shared functions as indicated by the similarity in domain structure and conservation of key amino acids relevant to Parkinson Disease.

The *LRRK1* and *Drosophila Lrrk* genes may have similar transcriptional regulation

Prediction of transcription factor binding sites suggests similar transcriptional regulation between the *Lrrk* and *LRRK1* genes. Upstream of the *Lrrk* gene a predicted binding site for nubbin protein was detected by Transfac Match (Table 4), while upstream of *LRRK1* a predicted binding site for a homologous transcription factor called POU2F1 was detected (Table 6). In humans, POU2F1 is involved with the development of T-cells and in promotion of oncogenic processes. In *Drosophila*, nubbin is involved with neuronal development, wing development, and immune response. This is notable, as *Lrrk^{e03680}* mutants exhibit abnormal wing development (Figure 16), and abnormal neuronal development and structure [93, 131], and *EPgy2^{EY06588}* mutants exhibit abnormal immune response in mutants in the form of melanotic tumors (Figure 21). As discussed above, the *Lrrk^{e03680}* mutation affected neuronal development and structure. These cell types being affected by the *Lrrk^{e03680}* and *EPgy2^{EY06588}* mutations support the prediction that nubbin is a transcriptional regulator of the *Lrrk* gene in *Drosophila*. The prediction of conserved transcriptional regulation between *Drosophila Lrrk* and *LRRK1*, suggests the possibility of conserved functions between these two genes. However, further studies are required to test whether these transcription factors regulate these genes.

Climbing impairment in *Lrrk^{e03680}* mutants may be caused by changes in neuronal structure

The results of the current study show that *Lrrk^{e03680}* mutant *Drosophila* have decreased climbing index compared to wild-type *Lrrk* flies at eclosion (Figure 12 and Table 7). The fact that climbing ability was lower at eclosion suggests that the *Lrrk^{e03680}* mutation does not result in progressive death of dopamine-producing neurons as seen in Parkinson Disease. In another study, *Lrrk^{e03680}* mutant *Drosophila* displayed a lower climbing index compared to wild-type

Lrrk flies at 30 days post-eclosion [93]. However, a measure of climbing index at eclosion was not reported in that study. Notably, the study uncovered additional details that help to better characterize the *Lrrk*^{e03680} mutation. Firstly, direct counts of dopamine-producing neurons showed no difference between mutants and wild-type flies, which suggests that the climbing impairment is not due to increased age-dependent loss of dopaminergic neurons. However, there was decreased anti-TH staining found in regions of the brain that contain dopamine-producing neurons and these neurons were smaller. Secondly, the researchers investigated whether the climbing defects might be caused by muscle degeneration, but found no defects in muscle structure or degeneration of muscles in *Lrrk*^{e03680} mutant flies. Thirdly, the researchers were able to confirm that this mutation represented a loss-of-function mutation as transgenic expression of wild-type *Lrrk* rescued defects in climbing ability in *Lrrk*^{e03680} mutants. These results support the findings of the current study and help explain the climbing defects in *Lrrk*^{e03680} mutants. They suggest that climbing defects in *Lrrk*^{e03680} mutants are not a consequence of a progressive neuron loss, as seen in Parkinson Disease, but may be due to abnormalities in the development of dopamine-producing neurons, manifesting as early as eclosion, and are attributable to a loss-of-function mutation.

Drosophila Lrrk and human LRRK2 may regulate dopamine synthesis

The phenotypes exhibited by *Lrrk*^{e03680} and *EPgy2*^{EY06588} *Drosophila* are similar to those caused by mutations in genes found in the *dopa decarboxylase* (*Ddc*) cluster, a set of genes located near each other in the *Drosophila melanogaster* genome. The cluster is named for the *Ddc* gene, an important gene in dopamine synthesis, and a member of the *Ddc* cluster [128]. These genes contribute to the production of dopamine, melanin, and sclerotin, the latter two of which can be derived from dopamine. Melanin and sclerotin are pigments found in the insect

cuticle, the hardened outer shell of insects. Melanin gives the cuticle a black colour while sclerotin gives it a yellow-brown colour and forms cross-links that help to harden the cuticle. Variations in the amount of each pigment influence the overall colouration and hardness of the cuticle. Of the 18 genes in this cluster 14 have been linked to formation of the cuticle. Mutations in these 14 genes have been linked to various phenotypes, which include the formation of melanotic tumors (11 genes), incomplete cuticle formation (7 genes), female sterility (11 genes), and dysregulation or upregulation of catecholamine synthesis, such as dopamine. The incomplete cuticle phenotype occurred most commonly on the dorsal abdomen, with some other regions of the body being affected in certain mutants. One possibility is that the dorsal abdomen is most affected because this part of the cuticle forms later in development compared to other parts of the body. Notably, some *Lrrk^{e03680}* homozygotes and heterozygotes exhibited an incomplete cuticle on the dorsal abdomen (Figure 14). Although this phenotype is subtle and exhibits incomplete penetrance, it has been independently corroborated in another study [131], suggesting its reproducibility and validity beyond the specific conditions of our laboratory. Melanotic tumors are common in both the adult and larval stages of flies with mutations in *Ddc* cluster genes [128]. Similarly, *EPgy2^{EY06588}* mutants exhibited melanotic tumors in third instar larvae (Figure 21), which primarily affected the anterior lymph glands similar to the phenotype of the *Black cells* mutation, which is found in the *Ddc* cluster gene *prophenoloxidase 1 (PPO1)* [127]. This phenotype is believed to be caused by dysregulation of melanin synthesis in crystal cells. In wild-type *Drosophila*, these cells form melanotic cysts around foreign objects that enter the fly's body and seal sites of physical injury. Mutations in many *Ddc* cluster genes cause female infertility, a phenotype found in *Lrrk^{e03680}* homozygotes in this study (Figure 15) and which has been confirmed in other studies [93, 131]. The cause of female infertility in the *Ddc* cluster genes

is currently unknown, but studies indicate that the mutations somehow disrupt development of the ovaries [132]. Taken together, the phenotypic similarities suggest a link between the function of the *Ddc* cluster genes and the *Lrrk* gene.

The *catsup* (*catecholamines-up*) gene is one of the best characterized genes within the *Ddc* cluster and has considerable similarity to the phenotypes of *Lrrk* mutant flies. The *catsup* protein acts to downregulate the function tyrosine hydroxylase (TH), the rate-limiting enzyme in the synthesis of dopamine from tyrosine [96]. In flies with loss-of-function mutations in the *catsup* gene, TH becomes overactive, which leads to incomplete cuticle formation, melanotic tumors in larvae, and female infertility, similar to the phenotypes observed in *Lrrk*^{e03680} and *EPgy2*^{EY06588} mutant *Drosophila*. Drawing on the similarities, it is possible that *Lrrk* could play a similar role in downregulating dopamine synthesis. Additionally, this could account for the appearance of black ommatidia in the eyes of *Lrrk*^{e03680} mutants (Figure 18). While it is possible that these black spots represent cell death within the eye, there is little disruption to the structure of the ommatidia which would be expected if this was the cause [133]. If *Lrrk* plays a role in downregulating TH function, then it is possible that that loss-of-function in *Lrrk* has caused increased melanin synthesis within the ommatidia, which would cause the ommatidia to have a black colouration. However, further research is required to establish if the black spots are caused by increased levels of melanin in the ommatidia.

Analysis of the upstream promoter region of the *Lrrk* gene resulted in a predicted binding site from the broad-complex Z1 and/or Z4 transcription factors and lends further support for *Lrrk* in the regulation of dopamine synthesis [116, 134]. Broad-complex Z1 and Z4 are two of four known isoforms of broad-complex transcription factors, labeled as Z1-Z4. The broad-complex transcription factors are involved with metamorphosis of *Drosophila* larvae and play a role in

cuticle development (including melanin and sclerotin synthesis), central nervous system development, immune response, and oogenesis. Notably, the broad-complex transcription factor and its upstream activator ecdysone have both been found to be necessary for activation of genes involved in catecholamine synthesis such as *TH* and *Ddc*. As suggested above, *Lrrk*^{e03680} and *EPgy2*^{EY06588} mutant flies share phenotypic similarities to flies with mutations in the *Ddc* cluster of genes [128], which lends further support to the idea that the Lrrk protein plays a role in dopamine synthesis. The prediction of a broad-complex Z1 and/or Z4 binding site upstream of *Lrrk* lends further support to this idea. Notably, this predicted transcription factor binding site is the location of the *EPgy2*^{EY06588} P-element insertion [92]. The location of the *EPgy2*^{EY06588} P-element is significant because it is possible that the P-element insertion *EPgy2*^{EY06588} disrupts transcription of the *Lrrk* gene. Such disruption could potentially lead to an overproduction of dopamine in crystal cells, resulting in the spontaneous formation of melanotic tumors.

In further support of the theory that Lrrk might be involved in dopamine synthesis, one study found that *Lrrk*^{e03680} flies have increased dopamine levels in their brains compared to wild-type controls [131]. Consistent with prior research [93], it was found that there was no difference in the number of dopamine producing neurons. This suggests that the increased dopamine levels are likely due to changes in dopamine synthesis rather than an increase in the number of these neurons. Although structural changes in dopamine-producing neurons are present in *Lrrk*^{e03680} mutants [93], the climbing defects could instead be caused by alterations in dopamine synthesis, or a combination of both factors. The researchers also generated mutant forms of the *Lrrk* gene designed to functionally mimic two Parkinson's-linked mutations, Y1383C and I1915T, which correspond to the Parkinson-linked mutations Y1699C and I2020T. Interestingly, expression of these two mutant forms caused a decrease in dopamine levels while overexpression of wild-type

Lrrk did not. This suggests that Parkinson-linked forms of LRRK2 may decrease dopamine synthesis and that this may in some way be related to pathogenesis in Parkinson Disease. Taken together this research supports that possibility that *Lrrk* may play a role in regulation of dopamine synthesis and that Parkinson-linked mutations may suppress dopamine synthesis.

Studies that use transgenic animal models suggest that the proposed role for *Lrrk* in regulation of dopamine synthesis is shared by human *LRRK2*. In a *C. elegans* model it was found that expression of wild-type, R1441C, or G2019S LRRK2 proteins resulted in decreased dopamine levels [135]. The number of dopamine-producing neurons was near normal in these worms, despite an approximate 50% reduction in dopamine levels for worms that expressed wild-type LRRK2 and an approximate 72% reduction in dopamine levels in those expressing R144C or G2019S mutant forms of LRRK2. It is notable that Parkinson-linked forms of LRRK2 caused a greater decrease in dopamine levels. Further, worms expressing LRRK2 exhibited increased movement speed relative to wild-type, a phenotype similar to *cat-2(e1112)* mutants, which have decreased dopamine synthesis. Exogenous dopamine treatment successfully rescued this phenotype in *cat-2(e1112)* mutant worms and those expressing wild-type LRRK2. Similarly, in a rat model, selective expression of G2019S LRRK2 in midbrain dopamine-producing neurons resulted in a decrease in dopamine levels [136]. This was accompanied by a decrease in the expression of the *TH* gene, suggesting LRRK2 may play a role in regulation of *TH* expression. These two studies further support the idea that LRRK2 may act to downregulate the synthesis of dopamine. As this function was enhanced by Parkinson-linked mutations it may be of particular relevance to Parkinson Disease pathogenesis.

***TH* overexpression and the *Lrrk*^{e03680} mutation have similar climbing phenotypes**

As the *Lrrk*^{e03680} and *EPgy2*^{EY06588} mutant phenotypes suggest that *Lrrk* may act to decrease dopamine synthesis, the *Drosophila* homologue of the *TH* gene was overexpressed in

dopamine-producing neurons in order to explore this possibility further. The goal was to investigate whether this might exacerbate the impaired climbing ability observed in *Lrrk*^{e03680} mutants. In a wild-type *Lrrk* background *TH* overexpression resulted in decreased climbing ability at eclosion (Figure 22, Tables 13 and 14), which is similar to what was seen for *Lrrk*^{e03680} mutants (Figure 12 and Table 7). This finding supports the possibility that both *TH* overexpression and the *Lrrk*^{e03680} mutation affect the flies in a similar way, potentially via dopamine overproduction. However, further research would be required to provide more conclusive evidence. Overexpression of *TH* in a *Lrrk*^{e03680} homozygous background showed no significant effect on the loss of climbing ability (Figure 24, Tables 16 and 17), though it did reduce the survival of the flies (Figure 25 and Table 18). While a lack of interaction between the two genes could explain this observation, it is also plausible that the effects of the *Lrrk*^{e03680} mutation were already so severe that overexpression of *TH* couldn't further enhance the loss of climbing ability. Definitive conclusions are difficult to draw based on the current data. Future studies might benefit from exploring the effects of suppressing *Drosophila TH* expression to see if this could rescue the impaired climbing ability and abdominal defects observed in *Lrrk*^{e03680} mutants.

***SOD* overexpression has a negative effect on climbing ability**

It has been suggested that dopamine-producing neurons are at particular risk for oxidative stress due to the fact that dopamine production may increase susceptibility of cells to oxidative stress [66]. To investigate this possibility, we overexpressed the antioxidant gene *SOD* under the control of the *Ddc:Gal4* driver to see if it might have a protective effect. Overexpression of *SOD* did not rescue the impairment in climbing ability seen in *Lrrk*^{e03680} mutants (Figure 24, Tables 16 and 17). In addition, climbing ability was decreased at eclosion in a wild-type *Lrrk* background

(Figure 22 and Table 13). However, overexpression of *SOD* did improve survival in a wild-type *Lrrk* background (Figure 23 and Table 15). Consideration of the enzymatic functions of SOD reveals a possible explanation for the negative effects on climbing ability. SOD catalyzes a reaction that donates an electron to superoxide radical to generate hydrogen peroxide, which is a weak oxidizing agent [137]. Additionally, SOD can catalyze a mild peroxidation reaction that donates an electron to hydrogen peroxide, which results in the generation of hydroxyl radicals [138]. The hydroxyl radical is a highly reactive ROS and could cause considerable damage to cells. To prevent the production of hydroxide radicals, a second enzyme, catalase, decomposes hydrogen peroxide into water and oxygen. Overexpression of SOD may disrupt this chemical balance, as it could increase hydroxyl radical production beyond what catalase can effectively remove. Therefore, contrary to expectations, overexpression of superoxide dismutase may enhance oxidative stress. The loss of climbing ability may be related to defects during development, since the flies exhibited climbing defects at eclosion and because *Ddc:Gal4* should drive expression of *SOD* throughout the entire lifespan of the flies [139]. However, *SOD* overexpression did cause a small but significant increase in longevity in wild-type *Lrrk* flies, which indicates that this overexpression may have some protective effect. Whether *SOD* overexpression is harmful or beneficial may depend on the balance of ROS and antioxidant enzymes in different cell types or stages of development.

LRRK2 may cause oxidative stress through regulation of dopamine synthesis

Although the current study was unable to find an interaction between *SOD* and *Lrrk*, a number of studies indicate that the *Lrrk* and *LRRK2* genes may play a role in susceptibility to oxidative stress. For example, *Lrrk RNAi* knockdown or null *Lrrk* flies exposed to paraquat or H₂O₂ have been reported to reduce loss of dopamine-producing neurons and improve survival

compared to wild-type flies [140]. However, another study had conflicting results, and it was found that *Lrrk* loss-of-function resulted in decreased survival when flies were exposed to H₂O₂, while survival from exposure to paraquat or rotenone was not affected [141]. Examination of studies on *LRRK2* expression in animal models further supports a link between this gene and oxidative stress. In transgenic *Drosophila* models, expression of the G2019S or Y1699C variant of LRRK2 through use of the *Ddc:Gal4* driver resulted in increased susceptibility to rotenone, while expression of wild-type *LRRK2* did not [142]. In mouse models, the overexpression of the G2019S variant of LRRK2 showed greater susceptibility to MPTP-induced Parkinsonism compared to overexpression of wild-type *LRRK2* [143]. In contrast, *LRRK2* knockout in mice has been reported to ameliorate the negative effects of paraquat treatment [144]. In general, these studies indicate that expression of Parkinson Disease-linked forms of *LRRK2* may increase susceptibility to oxidative stress, while decreased expression of *LRRK2* and *Lrrk* may decrease susceptibility to oxidative stress. However, it should be noted that inconsistent results across different studies introduce some uncertainty regarding the relationship between *Lrrk* and oxidative stress in *Drosophila* models.

As proposed previously, *Lrrk* may function similarly to *catsup*, which decreases expression of *TH*. The suggested similarity between *Lrrk* and *catsup* could provide insight into why *Lrrk* loss-of-function mutations may confer protection against oxidative stress, as *catsup* loss-of-function mutations have been shown to yield a protective effect against hydrogen peroxide and paraquat in *Drosophila* [98]. In contrast, *TH* loss-of-function mutations resulted in greater susceptibility to paraquat. Notably, overexpression of *TH* in human neuroblastoma cell lines was found to have a protective effect against hydrogen peroxide [145]. Interestingly, *glutathione S-transferase (GSTO1)* expression was found to be increased in *catsup* loss-of-

function mutants [98]. This suggests that the possibility that elevated dopamine levels may trigger increased expression of antioxidant response genes, such as *glutathione S-transferase (GSTO1)*, thus priming cells to defend against oxidative insults from toxins that induce oxidative stress. Therefore, it is plausible that suppression of *Lrrk* may increase *TH* expression, thereby increasing dopamine synthesis and activate oxidative stress defense systems within cells.

Another possible explanation for the potential role that *Lrrk* and *LRRK2* may play in oxidative stress defense is the link between tetrahydrobiopterin (BH₄) and *TH* expression. BH₄ is a TH cofactor required for dopamine synthesis [146]. The enzyme GTP cyclohydrolase is the rate-limiting enzyme in the synthesis of BH₄. This is significant as mutations in the *GCH-1* gene, which encodes this enzyme, have been linked to Parkinson Disease [147, 148]. In addition to being a cofactor for TH, BH₄ can scavenge reactive oxygen species and protect cells against oxidative stress [149]. Importantly, BH₄ synthesis is tightly associated with dopamine synthesis, and a loss-of-function in *catsup* leads to increased synthesis of both BH₄ and dopamine [150, 151]. If *LRRK2* plays a role similar to that of *catsup*, and if Parkinson-linked variants of *LRRK2* are gain-of-function mutations, then BH₄ synthesis could be decreased in Parkinson Disease, and lead to increased susceptibility to oxidative stress. This possibility that Parkinson-linked *LRRK2* mutations are gain-of-function mutations is supported by evidence that R144C, G2019S, and Y1699C forms of *LRRK2* increase the kinase function of the protein [22, 24-26, 29, 34]. However, it should be noted that there is conflicting evidence in regard to the I2020T variant, as different studies have found it either increases or decreases kinase function [35, 36]. Despite this inconsistency, the majority of the evidence points toward an increase in kinase activity of Parkinson-linked variants of *LRRK2* and kinase inhibitors have become an active area of research on potential treatments of Parkinson Disease [152]. The connection between BH₄ and

TH activity suggests that there is a connection between dopamine synthesis and oxidative stress defense, which makes sense from an evolutionary standpoint, as enhancement of antioxidant defense in dopamine-producing cells would be adaptive. Parkinson-linked *LRRK2* variants may disrupt this balance, and potentially promote sensitivity to oxidative stress.

Comparison of *Lrrk*^{e03680} eye phenotype to research on the role of *Lrrk* and *LRRK2* in *Drosophila* eye development

Both male and female *Lrrk*^{e03680} mutants have slightly more bristles on their eyes, although this difference is only statistically significant in females (Figures 19 and 20; Tables 11 and 12). In addition, the eyes of some flies exhibit black ommatidia (Figure 13). This suggests that *Lrrk* influences development of the *Drosophila* eye. This section will review and compare these phenotypes to currently available research *LRRK2* on to the development of the *Drosophila* to determine possible explanations for the eye *Lrrk*^{e03680} phenotype.

Flies mutant for the *Rac1* gene exhibit a rough eye phenotype, which could be explained by abnormal bristle development. Both *Lrrk* and *LRRK2* have been reported to interact with this rough eye phenotype. In one study, the *Lrrk*^{e03680} mutation was shown to enhance the rough eye phenotype caused by *Rac1* overexpression [42], while in another study it was found that overexpression of *Lrrk* or human *LRRK2* was able to suppress the *Rac1* rough eye phenotype [153]. However, it should be noted that the phenotype may be caused by disruption of the normal morphology of cells rather than changes in bristle development. This idea is supported by the fact that flies with one extra copy of *Rac1* had normal eye morphology, but the eye was easily deformed when pressure was applied. Since *Rac1* has been linked to cytoskeletal dynamics, it is possible that overexpression of *Rac1* disrupts the cytoskeletal structure, which would allow the cells to easily deform. Therefore, it is possible that *Lrrk* regulates cytoskeletal structure through a

possible interaction with *Rac1*. This may help to explain abnormalities in neuronal structure reported in *Lrrk*^{e03680} mutants [141, 153]. However, it cannot explain the changes in bristle number in *Lrrk*^{e03680} mutants.

Expression of I2020T mutant LRRK2 protein in the *Drosophila* eye has also been reported to induce a rough eye phenotype [154]. This rough eye phenotype differs from that caused by *Rac1* overexpression, as evidenced by the formation of black spots on the eye. This phenotype appears to be caused by dysregulation of apoptosis throughout eye development, which causes large necrotic lesions that disrupt ommatidial structure. Although expression of both I2020T LRRK2 [154] and the *Lrrk*^{e03680} mutation (Figure 18) cause the formation of black spots on the eye, there is no disruption of ommatidial structure in *Lrrk*^{e03680} mutants. This suggests that the black ommatidia may be the result of necrotic lesions, as is the case with expression of I2020T LRRK2. Notably, overexpression of either *Vps35* or *Vps26* can partially rescue this I2020T eye phenotype [155]. The interaction between *Vps35* and *LRRK2* is of particular interest because mutations in the *Vps35* gene have been linked to Parkinson Disease [5, 6]. *Vps35* and *Vps26* proteins are part of the retromer complex, which is involved in protein sorting and trafficking through endosomal pathways [156]. A role for *LRRK2* in this process is further supported by evidence that *LRRK2* overexpression can lead to the formation of enlarged lysosomes in rat PC12 cell lines, which may be caused by abnormalities in sorting and trafficking of proteins to lysosomes [150]. The connection between *LRRK2* and *Vps35* is further supported by the fact that it has been found that climbing defects caused by expression of I2020T, Y1699C, and I1122V *LRRK2* were ameliorated by *Vps35* overexpression [155]. In contrast, knockdown of *Vps35* and *Vps26* induced climbing defects. This suggests the possibility that

LRRK2 and *Vps35* may contribute to Parkinson pathogenesis through a common pathway that involves endosomal dynamics.

Drosophila *Lrrk* may regulate Notch signalling

The potential role that *LRRK2* plays in endosomal dynamics may explain the *Lrrk*^{e03680} bristle loss phenotype through regulation of Delta-mediated Notch signalling. In *Drosophila*, the development of bristles in the eye and other parts of the body is regulated by Notch signalling pathway [157]. Suppression of the Notch ligand Delta can either result in an increase or decrease in eye bristle number, depending on the developmental stage at which the suppression takes place [158]. The Notch protein is an extracellular receptor which, upon activation by extracellular ligands such as Delta, changes conformation to trigger the release of an intracellular domain of the protein. This domain then travels to the nucleus where it activates the expression of genes [159]. Notch is activated by Delta on adjacent cells (trans-activation) and inhibited by Delta found on the same cell (cis-inhibition). In a *Drosophila* study, it was found that flies overexpressing *LRRK2* in dopamine-producing neurons have fewer of these neurons compared to wild-type flies [160]. Moreover, it was found that overexpression of *LRRK2* increases recycling of Delta and increases Notch signalling, perhaps through cis-inhibition. Flies overexpressing *Delta* also exhibited decreased numbers of dopamine-producing neurons. Partial rescue of this phenotype was achieved by suppressing *Lrrk* expression through the use of RNAi, suggesting that *Lrrk* regulates *Delta* in a similar manner to *LRRK2*. Therefore, the results of this study suggest that *Lrrk* and *LRRK2* appear to have a function in regulating Delta-mediated Notch signalling. However, it should be noted that as Delta modulates Notch signalling through both cis-inhibition and trans-activation the exact effects of this regulation may vary by cell type.

If the *Lrrk*^{e03680} mutation increases Notch signalling, this may explain decreased egg laying in these mutants (Figure 15), as downregulation of Notch signalling has been found to be important for oogenesis in *Drosophila* [161]. Similarly, *Vps26* loss-of-function mutations have been found to lead to inhibition of oogenesis through an increase in Notch signalling [162]. This appears to be caused by a build up of Delta on the outside of nurse cells. As nurse cells border the follicle cells, Notch signalling within the follicle cells is upregulated through trans-activation. As discussed previously, *Vps26* is part of the retromer protein complex, responsible for sorting of endosomes to either recycle or degrade their contents [163]. In the case of *Vps26* loss-of-function mutations, recycling appears to be increased, resulting in a build-up of Delta on the outside of nurse cells. The role that *Vps26* plays in oogenesis is noteworthy, particularly as *LRRK2* has been demonstrated to interact genetically with both *Vps26* and *Vps35* [155], and this may be due to a common role in regulating recycling of Delta. The *Lrrk*^{e03680} mutation may act similarly to *Vps26* loss-of-function mutations and disrupt oogenesis through an increase in Notch signalling. In contrast, flies heterozygous for the *Lrrk*^{e03680} mutation laid an increased number of eggs compared to wild-type controls (Figure 15). This could be related to Notch signalling; however, currently available research cannot substantiate this claim. Therefore, further research is required to elucidate the cause of increased fecundity in *Lrrk*^{e03680} heterozygotes.

The formation of melanotic tumors in the *EPgy2*^{EY06588} larvae (Figure 21) may also be explained by increased Notch signalling, since overexpression of Notch has been shown to increase crystal cell numbers [164]. Normally these cells form in response to parasitization. However, if Notch signalling is upregulated in *EPgy2*^{EY06588} mutants, crystal cells may develop without parasites being present, which can promote the formation of melanotic tumors. Unfortunately, it is unclear exactly what effect the *EPgy2*^{EY0658} mutation has on expression of the

Lrrk gene, which makes these results difficult to interpret. Examining the effects of *Lrrk* gene overexpression and suppression in crystal cells on the melanization reaction in *Drosophila* could be a valuable direction for future studies.

Notch signalling may play a role in wing development that could help to explain the observation of incomplete wing veins in some *Lrrk*^{e03680} mutant flies (Figure 16), as the cells that become the wing veins differentiate into intervein cells when Notch receptors are activated [165]. A number of genes involved in the bone morphogenic protein (BMP)-like signalling pathway have been found to play a role in cross vein formation. These include the BMP-like protein ligands *decapentaplegic* (*dpp*) and *glass bottom boat* (*gbb*), which promotes BMP-like signalling, and *short gastrulation* (*sog*), which inhibits BMP-like signalling [166]. Taken together, this research indicates that BMP-like and Notch signalling have inverse effects, with Notch promoting and BMP-like suppressing wing vein formation. In flies with loss-of-function mutations in the *crossveinless-2* gene, which inhibits BMP-like signalling, the posterior cross vein appears to be more severely affected compared to other wing veins. Notably, in *Lrrk*^{e03680} mutant flies the posterior wing vein was observed to be affected while the other wing veins were not. As Notch signalling has an antagonistic interaction with BMP-like signalling during wing development [167, 168], the similarity in phenotype supports the possibility that *Lrrk* may play a role in the inhibition of Notch signalling. If this is the case, then the *Lrrk*^{e03680} loss-of-function mutation may enhance Notch signalling and lead to suppression of wing vein formation, with the posterior cross vein being particularly susceptible to this effect.

While the current study reveals a potential link between *Lrrk* and Delta-mediated Notch signalling, the specific mechanisms remain unclear. In *Drosophila*, suppression of *Delta* expression in dopamine-producing neurons increases dopamine synthesis and neuronal survival

over the adult lifespan [160]. In mouse models, disruption of the *Nurr1* gene prevents dopamine synthesis specifically in dopamine-producing neurons of the ventral midbrain, which would include the neurons of in the *substantia nigra* that exhibit progressive degeneration in Parkinson Disease [169]. As Notch is an upstream activator of *Nurr1* expression, Notch signalling could influence dopamine synthesis by causing increased expression of *Nurr1* [170]. This connection may explain why many of the *EPgy2^{EY0658}* and *Lrrk^{e03680}* mutant phenotypes can be linked to both Notch and dopamine synthesis. In addition, to a potential role in dopamine synthesis, it should be noted that Notch plays a role in differentiation and development of neuronal precursor cells [171], which could be relevant to the fact that climbing defects were present at eclosion, indicating the possibility of developmental defects prior to adulthood. While it is possible that *Lrrk* and *LRRK2* may act to regulate dopamine synthesis through regulation of Delta-mediated Notch signalling, further research is required to explore this potential connection.

The *Lrrk^{e03680}* mutation may cause maternal effects on climbing index

The *Lrrk^{e03680}* gene was found to play a role in the climbing ability of offspring depending on maternal genotype. This was evidenced by the lower climbing index at eclosion for offspring of *Lrrk^{e03680}* heterozygotes compared to *w/+* controls (Figure 12, Tables 7 and 8). When the mothers were *w¹¹¹⁸* females, the climbing index at eclosion was not significantly different from *w/+* controls. Given that mutations in genes involved in dopamine synthesis in female flies can affect dopamine levels of their progeny [172], it is plausible that changes in maternal dopamine levels may influence the development of the *Lrrk^{e03680}* heterozygotes. For example, if *Lrrk* suppresses TH activity as proposed, *Lrrk^{e03680}* heterozygotes have slightly higher levels of dopamine throughout development compared to *w¹¹¹⁸* flies and this may affect their progeny. Notably, increased *TH* expression has been linked to increased resistance to oxidative stress, perhaps because dopamine upregulates oxidative stress defense mechanisms

[98]. Therefore, the offspring of the *Lrrk*^{e03680} heterozygotes may potentially benefit from increased resistance to oxidative stress compared to those of *w*¹¹⁸ flies.

The *Lrrk*^{e03680} mutation suppresses Gal4-induced toxicity

Gal4 has been shown to induce apoptosis in *Drosophila melanogaster* through an unknown mechanism. Previous research in our lab suggests that this is relevant to Parkinson Disease since overexpression of *parkin* and *PINK1* suppresses this phenotype [88, 89]. Since one of the primary functions of the parkin protein is to ubiquitinate misfolded proteins and target the proteins for degradation by the proteasome, it is conceivable that Gal4-induced toxicity might arise from protein misfolding [62]. This theory gains credence from the observation that *parkin* overexpression can suppress apoptosis induced by expression of *SNCA*, a protein with a propensity to misfold into amyloid conformations [65]. In the current study, it was discovered that the *Lrrk*^{e03680} mutation mitigates the toxic effects of Gal4-induced cell death (Figure 26 and Table 19). This interaction may involve lysosomal degradation of proteins, given that abnormal lysosomes have been reported to be induced by the expression of Parkinson-linked variants of *LRRK2* [51]. Nonetheless, as the cause of Gal4-induced toxicity is currently unknown, more research is needed to determine the precise mechanism through which the *Lrrk*^{e03680} mutation suppresses Gal4-induced toxicity.

Conclusion

The analysis of the phenotype of both *Lrrk*^{*e03680*} and *EPgy2*^{*EY06588*} mutant *Drosophila* provides strong evidence for a possible role of the *Drosophila* Lrrk protein in the regulation of dopamine synthesis. Bioinformatic analysis of the structure of the Lrrk and LRRK2 proteins supports a conserved structure, and therefore function, for the two proteins. This information, combined with the fact that dopamine-producing neurons are the most susceptible cell type to cell death in Parkinson Disease, suggests the possibility that Parkinson-linked *LRRK2* mutations may promote cell death through changes in the regulation of dopamine synthesis. This may occur through disruption of cellular oxidative stress defenses which are tightly linked to dopamine synthesis. In addition, *Drosophila* *Lrrk* may interact with Delta-mediated Notch signalling to affect neuronal development, survival, and potentially regulate dopamine synthesis through changes in gene expression. The current study illuminates potential new research areas that could lead to an improved comprehension of the pathogenic processes in Parkinson Disease and possibly open avenues for novel treatments.

References

1. Reeve A, Simcox E, Turnbull D: **Ageing and Parkinson's disease: why is advancing age the biggest risk factor?** *Ageing Res Rev* 2014, **14**:19-30.
2. Tolosa E, Ebersbach G, Ferreira JJ, Rascol O, Antonini A, Foltynie T, Gibson R, Magalhaes D, Rocha JF, Lees A: **The Parkinson's Real-World Impact Assessment (PRISM) Study: A European Survey of the Burden of Parkinson's Disease in Patients and their Carers.** *J Parkinsons Dis* 2021, **11**(3):1309-1323.
3. Parkinson J: **An essay on the shaking palsy. 1817.** *J Neuropsychiatry Clin Neurosci* 2002, **14**(2):223-236; discussion 222.
4. Mettler FA: **The substantia nigra and parkinsonism.** *Trans Am Neurol Assoc* 1964, **89**:68-73.
5. Guadagnolo D, Piane M, Torrisi MR, Pizzuti A, Petrucci S: **Genotype-Phenotype Correlations in Monogenic Parkinson Disease: A Review on Clinical and Molecular Findings.** *Front Neurol* 2021, **12**:648588.
6. Monfrini E, Di Fonzo A: **Leucine-Rich Repeat Kinase (LRRK2) Genetics and Parkinson's Disease.** *Adv Neurobiol* 2017, **14**:3-30.
7. Herbst S, Lewis PA: **From structure to aetiology: a new window on the biology of leucine-rich repeat kinase 2 and Parkinson's disease.** *Biochem J* 2021, **478**(14):2945-2951.
8. Bella J, Hindle KL, McEwan PA, Lovell SC: **The leucine-rich repeat structure.** *Cell Mol Life Sci* 2008, **65**(15):2307-2333.
9. Xu C, Min J: **Structure and function of WD40 domain proteins.** *Protein Cell* 2011, **2**(3):202-214.
10. Sancho RM, Law BM, Harvey K: **Mutations in the LRRK2 Roc-COR tandem domain link Parkinson's disease to Wnt signalling pathways.** *Hum Mol Genet* 2009, **18**(20):3955-3968.
11. Refai FS, Ng SH, Tan EK: **Evaluating LRRK2 genetic variants with unclear pathogenicity.** *Biomed Res Int* 2015, **2015**:678701.
12. Tan S, Zhang Q, Wang J, Gao P, Xie G, Liu H, Yao X: **Molecular Modeling Study on the Interaction Mechanism between the LRRK2 G2019S Mutant and Type I Inhibitors by Integrating Molecular Dynamics Simulation, Binding Free Energy Calculations, and Pharmacophore Modeling.** *ACS Chem Neurosci* 2021, **13**(5):599-612.
13. Simpson C, Vinikoor-Imler L, Nassan FL, Shirvan J, Lally C, Dam T, Maserejian N: **Prevalence of ten LRRK2 variants in Parkinson's disease: A comprehensive review.** *Parkinsonism Relat Disord* 2022, **98**:103-113.
14. Marin I: **The Parkinson disease gene LRRK2: evolutionary and structural insights.** *Mol Biol Evol* 2006, **23**(12):2423-2433.
15. Jorgensen ND, Peng Y, Ho CC, Rideout HJ, Petrey D, Liu P, Dauer WT: **The WD40 domain is required for LRRK2 neurotoxicity.** *PLoS One* 2009, **4**(12):e8463.
16. Parisiadou L, Xie C, Cho HJ, Lin X, Gu XL, Long CX, Lobbstaël E, Baekelandt V, Taymans JM, Sun L *et al*: **Phosphorylation of ezrin/radixin/moesin proteins by LRRK2 promotes the rearrangement of actin cytoskeleton in neuronal morphogenesis.** *J Neurosci* 2009, **29**(44):13971-13980.
17. Athanasopoulos PS, Heumann R, Kortholt A: **The role of (auto)-phosphorylation in the complex activation mechanism of LRRK2.** *Biol Chem* 2009, **399**(7):643-647.

18. Webber PJ, Smith AD, Sen S, Renfrow MB, Mobley JA, West AB: **Autophosphorylation in the leucine-rich repeat kinase 2 (LRRK2) GTPase domain modifies kinase and GTP-binding activities.** *J Mol Biol* 2011, **412**(1):94-110.
19. Ray S, Liu M: **Current understanding of LRRK2 in Parkinson's disease: biochemical and structural features and inhibitor design.** *Future Med Chem* 2012, **4**(13):1701-1713.
20. Nguyen APT, Tsika E, Kelly K, Levine N, Chen X, West AB, Boularand S, Barneoud P, Moore DJ: **Dopaminergic neurodegeneration induced by Parkinson's disease-linked G2019S LRRK2 is dependent on kinase and GTPase activity.** *Proc Natl Acad Sci U S A* 2020, **117**(29):17296-17307.
21. Luzon-Toro B, Rubio de la Torre E, Delgado A, Perez-Tur J, Hilfiker S: **Mechanistic insight into the dominant mode of the Parkinson's disease-associated G2019S LRRK2 mutation.** *Hum Mol Genet* 2007, **16**(17):2031-2039.
22. Reichling LJ, Riddle SM: **Leucine-rich repeat kinase 2 mutants I2020T and G2019S exhibit altered kinase inhibitor sensitivity.** *Biochem Biophys Res Commun* 2009, **384**(2):255-258.
23. Anand VS, Reichling LJ, Lipinski K, Stochaj W, Duan W, Kelleher K, Pungaliya P, Brown EL, Reinhart PH, Somberg R *et al*: **Investigation of leucine-rich repeat kinase 2 : enzymological properties and novel assays.** *FEBS J* 2009, **276**(2):466-478.
24. Gloeckner CJ, Kinkl N, Schumacher A, Braun RJ, O'Neill E, Meitinger T, Kolch W, Prokisch H, Ueffing M: **The Parkinson disease causing LRRK2 mutation I2020T is associated with increased kinase activity.** *Hum Mol Genet* 2006, **15**(2):223-232.
25. Jaleel M, Nichols RJ, Deak M, Campbell DG, Gillardon F, Knebel A, Alessi DR: **LRRK2 phosphorylates moesin at threonine-558: characterization of how Parkinson's disease mutants affect kinase activity.** *Biochem J* 2007, **405**(2):307-317.
26. Ray S, Bender S, Kang S, Lin R, Glicksman MA, Liu M: **The Parkinson disease-linked LRRK2 protein mutation I2020T stabilizes an active state conformation leading to increased kinase activity.** *J Biol Chem* 2014, **289**(19):13042-13053.
27. Wauters L, Versees W, Kortholt A: **Roco Proteins: GTPases with a Baroque Structure and Mechanism.** *Int J Mol Sci* 2019, **20**(1).
28. van Egmond WN, van Haastert PJ: **Characterization of the Roco protein family in Dictyostelium discoideum.** *Eukaryot Cell* 2010, **9**(5):751-761.
29. Nguyen AP, Moore DJ: **Understanding the GTPase Activity of LRRK2: Regulation, Function, and Neurotoxicity.** *Adv Neurobiol* 2017, **14**:71-88.
30. Deng J, Lewis PA, Greggio E, Sluch E, Beilina A, Cookson MR: **Structure of the ROC domain from the Parkinson's disease-associated leucine-rich repeat kinase 2 reveals a dimeric GTPase.** *Proc Natl Acad Sci U S A* 2008, **105**(5):1499-1504.
31. Wu CX, Liao J, Park Y, Reed X, Engel VA, Hoang NC, Takagi Y, Johnson SM, Wang M, Federici M *et al*: **Parkinson's disease-associated mutations in the GTPase domain of LRRK2 impair its nucleotide-dependent conformational dynamics.** *J Biol Chem* 2019, **294**(15):5907-5913.
32. Marin I, van Egmond WN, van Haastert PJ: **The Roco protein family: a functional perspective.** *FASEB J* 2008, **22**(9):3103-3110.
33. Lewis PA, Greggio E, Beilina A, Jain S, Baker A, Cookson MR: **The R1441C mutation of LRRK2 disrupts GTP hydrolysis.** *Biochem Biophys Res Commun* 2007, **357**(3):668-671.

34. West AB, Moore DJ, Biskup S, Bugayenko A, Smith WW, Ross CA, Dawson VL, Dawson TM: **Parkinson's disease-associated mutations in leucine-rich repeat kinase 2 augment kinase activity.** *Proc Natl Acad Sci U S A* 2005, **102**(46):16842-16847.
35. Klein CL, Rovelli G, Springer W, Schall C, Gasser T, Kahle PJ: **Homo- and heterodimerization of ROCO kinases: LRRK2 kinase inhibition by the LRRK2 ROCO fragment.** *Journal of Neurochemistry* 2009, **111**(3):703-715.
36. Rudenko IN, Chia R, Cookson MR: **Is inhibition of kinase activity the only therapeutic strategy for LRRK2-associated Parkinson's disease?** *BMC Med* 2012, **10**:20.
37. Law BM, Spain VA, Leinster VH, Chia R, Beilina A, Cho HJ, Taymans JM, Urban MK, Sancho RM, Blanca Ramirez M *et al*: **A direct interaction between leucine-rich repeat kinase 2 and specific beta-tubulin isoforms regulates tubulin acetylation.** *J Biol Chem* 2014, **289**(2):895-908.
38. Tsika E, Kannan M, Foo CS, Dikeman D, Glauser L, Gellhaar S, Galter D, Knott GW, Dawson TM, Dawson VL *et al*: **Conditional expression of Parkinson's disease-related R1441C LRRK2 in midbrain dopaminergic neurons of mice causes nuclear abnormalities without neurodegeneration.** *Neurobiol Dis* 2014, **71**:345-358.
39. Kett LR, Boassa D, Ho CC, Rideout HJ, Hu J, Terada M, Ellisman M, Dauer WT: **LRRK2 Parkinson disease mutations enhance its microtubule association.** *Hum Mol Genet* 2012, **21**(4):890-899.
40. Paglini G, Kunda P, Quiroga S, Kosik K, Caceres A: **Suppression of radixin and moesin alters growth cone morphology, motility, and process formation in primary cultured neurons.** *J Cell Biol* 1998, **143**(2):443-455.
41. Häbig K, Gellhaar S, Heim B, Djuric V, Giesert F, Wurst W, Walter C, Hentrich T, Riess O, Bonin M: **LRRK2 guides the actin cytoskeleton at growth cones together with ARHGEF7 and Tropomyosin 4.** *Biochimica et Biophysica Acta (BBA) - Molecular Basis of Disease* 2013, **1832**(12):2352-2367.
42. Schreij AM, Chaineau M, Ruan W, Lin S, Barker PA, Fon EA, McPherson PS: **LRRK2 localizes to endosomes and interacts with clathrin-light chains to limit Rac1 activation.** *EMBO Rep* 2015, **16**(1):79-86.
43. Fon EA, Edwards RH: **Molecular mechanisms of neurotransmitter release.** *Muscle Nerve* 2001, **24**(5):581-601.
44. Cui Y, Yang Z, Teasdale RD: **The functional roles of retromer in Parkinson's disease.** *FEBS Lett* 2017, **592**(7):1096-1112.
45. Yoshida S, Hasegawa T: **Beware of Misdelivery: Multifaceted Role of Retromer Transport in Neurodegenerative Diseases.** *Front Aging Neurosci* 2022, **14**:897688.
46. Navarro-Romero A, Montpeyo M, Martinez-Vicente M: **The Emerging Role of the Lysosome in Parkinson's Disease.** *Cells* 2020, **9**(11).
47. Zhao Y, Perera G, Takahashi-Fujigasaki J, Mash DC, Vonsattel JPG, Uchino A, Hasegawa K, Jeremy Nichols R, Holton JL, Murayama S *et al*: **Reduced LRRK2 in association with retromer dysfunction in post-mortem brain tissue from LRRK2 mutation carriers.** *Brain* 2018, **141**(2):486-495.
48. Seol W, Nam D, Son I: **Rab GTPases as Physiological Substrates of LRRK2 Kinase.** *Exp Neurobiol* 2009, **28**(2):134-145.
49. Stenmark H: **Rab GTPases as coordinators of vesicle traffic.** *Nat Rev Mol Cell Biol* 2009, **10**(8):513-525.

50. Ao X, Zou L, Wu Y: **Regulation of autophagy by the Rab GTPase network.** *Cell Death Differ* 2014, **21**(3):348-358.
51. Plowey ED, Cherra SJ, 3rd, Liu YJ, Chu CT: **Role of autophagy in G2019S-LRRK2-associated neurite shortening in differentiated SH-SY5Y cells.** *J Neurochem* 2008, **105**(3):1048-1056.
52. Vazquez-Velez GE, Zoghbi HY: **Parkinson's Disease Genetics and Pathophysiology.** *Annu Rev Neurosci* 2021, **44**:87-108.
53. Petrou M, Dwamena BA, Foerster BR, MacEachern MP, Bohnen NI, Muller ML, Albin RL, Frey KA: **Amyloid deposition in Parkinson's disease and cognitive impairment: a systematic review.** *Mov Disord* 2015, **30**(7):928-935.
54. Sakono M, Zako T: **Amyloid oligomers: formation and toxicity of Abeta oligomers.** *FEBS J* 2010, **277**(6):1348-1358.
55. Zaman M, Khan AN, Wahiduzzaman, Zakariya SM, Khan RH: **Protein misfolding, aggregation and mechanism of amyloid cytotoxicity: An overview and therapeutic strategies to inhibit aggregation.** *Int J Biol Macromol* 2019, **134**:1022-1037.
56. Durell SR, Guy HR: **The amyloid concentric beta-barrel hypothesis: Models of synuclein oligomers, annular protofibrils, lipoproteins, and transmembrane channels.** *Proteins* 2022, **90**(2):512-542.
57. Caughey B, Lansbury PT: **Protofibrils, pores, fibrils, and neurodegeneration: separating the responsible protein aggregates from the innocent bystanders.** *Annu Rev Neurosci* 2003, **26**:267-298.
58. Lashuel HA, Hartley D, Petre BM, Walz T, Lansbury PT, Jr.: **Neurodegenerative disease: amyloid pores from pathogenic mutations.** *Nature* 2002, **418**(6895):291.
59. Sipe JD, Cohen AS: **Review: history of the amyloid fibril.** *J Struct Biol* 2000, **130**(2-3):88-98.
60. Flagmeier P, Meisl G, Vendruscolo M, Knowles TP, Dobson CM, Buell AK, Galvagnion C: **Mutations associated with familial Parkinson's disease alter the initiation and amplification steps of alpha-synuclein aggregation.** *Proc Natl Acad Sci U S A* 2016, **113**(37):10328-10333.
61. Emanuele M, Chierregatti E: **Mechanisms of alpha-synuclein action on neurotransmission: cell-autonomous and non-cell autonomous role.** *Biomolecules* 2015, **5**(2):865-892.
62. Lim KL, Tan JM: **Role of the ubiquitin proteasome system in Parkinson's disease.** *BMC Biochem* 2007, **8 Suppl 1**:S13.
63. Hyun DH, Lee M, Halliwell B, Jenner P: **Proteasomal inhibition causes the formation of protein aggregates containing a wide range of proteins, including nitrated proteins.** *J Neurochem* 2003, **86**(2):363-373.
64. Latonen L, Moore HM, Bai B, Jaamaa S, Laiho M: **Proteasome inhibitors induce nucleolar aggregation of proteasome target proteins and polyadenylated RNA by altering ubiquitin availability.** *Oncogene* 2011, **30**(7):790-805.
65. Haywood AFM, Staveley BE: **parkin counteracts symptoms in a Drosophila model of Parkinson's disease.** *BMC Neuroscience* 2004, **5**(1):14.
66. Meiser J, Weindl D, Hiller K: **Complexity of dopamine metabolism.** *Cell Commun Signal* 2013, **11**(1):34.
67. Betteridge DJ: **What is oxidative stress?** *Metabolism* 2000, **49**(2 Suppl 1):3-8.

68. Burte F, Houghton D, Lowes H, Pyle A, Nesbitt S, Yarnall A, Yu-Wai-Man P, Burn DJ, Santibanez-Koref M, Hudson G: **metabolic profiling of Parkinson's disease and mild cognitive impairment.** *Mov Disord* 2017, **32**(6):927-932.
69. Mustapha M, Mat Taib CN: **MPTP-induced mouse model of Parkinson's disease: A promising direction of therapeutic strategies.** *Bosn J Basic Med Sci* 2020, **21**(4):422-433.
70. Wen S, Aki T, Unuma K, Uemura K: **Chemically Induced Models of Parkinson's Disease: History and Perspectives for the Involvement of Ferroptosis.** *Front Cell Neurosci* 2020, **14**:581191.
71. Mor DE, Tsika E, Mazzulli JR, Gould NS, Kim H, Daniels MJ, Doshi S, Gupta P, Grossman JL, Tan VX *et al*: **Dopamine induces soluble alpha-synuclein oligomers and nigrostriatal degeneration.** *Nat Neurosci* 2017, **20**(11):1560-1568.
72. Cheignon C, Tomas M, Bonnefont-Rousselot D, Faller P, Hureau C, Collin F: **Oxidative stress and the amyloid beta peptide in Alzheimer's disease.** *Redox Biol* 2018, **14**:450-464.
73. Berg D, Gerlach M, Youdim MB, Double KL, Zecca L, Riederer P, Becker G: **Brain iron pathways and their relevance to Parkinson's disease.** *J Neurochem* 2001, **79**(2):225-236.
74. Dexter DT, Wells FR, Lees AJ, Agid F, Agid Y, Jenner P, Marsden CD: **Increased nigral iron content and alterations in other metal ions occurring in brain in Parkinson's disease.** *J Neurochem* 1989, **52**(6):1830-1836.
75. Sofic E, Riederer P, Heinsen H, Beckmann H, Reynolds GP, Hebenstreit G, Youdim MB: **Increased iron (III) and total iron content in post mortem substantia nigra of parkinsonian brain.** *J Neural Transm* 1988, **74**(3):199-205.
76. Pesah Y, Pham T, Burgess H, Middlebrooks B, Verstreken P, Zhou Y, Harding M, Bellen H, Mardon G: **Drosophila parkin mutants have decreased mass and cell size and increased sensitivity to oxygen radical stress.** *Development* 2004, **131**(9):2183-2194.
77. Tan JM, Dawson TM: **Parkin blushed by PINK1.** *Neuron* 2006, **50**(4):527-529.
78. Clark IE, Dodson MW, Jiang C, Cao JH, Huh JR, Seol JH, Yoo SJ, Hay BA, Guo M: **Drosophila pink1 is required for mitochondrial function and interacts genetically with parkin.** *Nature* 2006, **441**(7097):1162-1166.
79. Park J, Lee SB, Lee S, Kim Y, Song S, Kim S, Bae E, Kim J, Shong M, Kim JM *et al*: **Mitochondrial dysfunction in Drosophila PINK1 mutants is complemented by parkin.** *Nature* 2006, **441**(7097):1157-1161.
80. Yang Y, Gehrke S, Imai Y, Huang Z, Ouyang Y, Wang JW, Yang L, Beal MF, Vogel H, Lu B: **Mitochondrial pathology and muscle and dopaminergic neuron degeneration caused by inactivation of Drosophila Pink1 is rescued by Parkin.** *Proc Natl Acad Sci U S A* 2006, **103**(28):10793-10798.
81. McCoy MK, Cookson MR: **DJ-1 regulation of mitochondrial function and autophagy through oxidative stress.** *Autophagy* 2011, **7**(5):531-532.
82. Rahul, Siddique YH: **Drosophila: A Model to Study the Pathogenesis of Parkinson's Disease.** *CNS Neurol Disord Drug Targets* 2022, **21**(3):259-277.
83. Fortini ME, Skupski MP, Boguski MS, Hariharan IK: **A survey of human disease gene counterparts in the Drosophila genome.** *J Cell Biol* 2000, **150**(2):F23-30.
84. Yamaguchi M, Yoshida H: **Drosophila as a Model Organism.** *Adv Exp Med Biol* 2018, **1076**:1-10.

85. Feany MB, Bender WW: **A Drosophila model of Parkinson's disease.** *Nature* 2000, **404**(6776):394-398.
86. Klueg KM, Alvarado D, Muskavitch MA, Duffy JB: **Creation of a GAL4/UAS-coupled inducible gene expression system for use in Drosophila cultured cell lines.** *Genesis* 2002, **34**(1-2):119-122.
87. Kramer JM, Staveley BE: **GAL4 causes developmental defects and apoptosis when expressed in the developing eye of Drosophila melanogaster.** *Genet Mol Res* 2003, **2**(1):43-47.
88. Haywood AFM: **The analysis of parkin in Drosophila melanogaster.** Memorial University of Newfoundland; 2006.
89. Todd AM, Staveley BE: **Pink1 Rescues Gal4-Induced Developmental Defects in the Drosophila Eye.** *Advances in Parkinson's Disease* 2015, **4**(03):43.
90. Haywood AF, Staveley BE: **Mutant alpha-synuclein-induced degeneration is reduced by parkin in a fly model of Parkinson's disease.** *Genome* 2006, **49**(5):505-510.
91. Schramm FD, Schroeder K, Jonas K: **Protein aggregation in bacteria.** *FEMS Microbiology Reviews* 2020, **44**(1):54-72.
92. Bellen HJ, Levis RW, Liao G, He Y, Carlson JW, Tsang G, Evans-Holm M, Hiesinger PR, Schulze KL, Rubin GM *et al*: **The BDGP gene disruption project: single transposon insertions associated with 40% of Drosophila genes.** *Genetics* 2004, **167**(2):761-781.
93. Lee SB, Kim W, Lee S, Chung J: **Loss of LRRK2/PARK8 induces degeneration of dopaminergic neurons in Drosophila.** *Biochem Biophys Res Commun* 2007, **358**(2):534-539.
94. Thibault ST, Singer MA, Miyazaki WY, Milash B, Dompe NA, Singh CM, Buchholz R, Demsky M, Fawcett R, Francis-Lang HL *et al*: **A complementary transposon tool kit for Drosophila melanogaster using P and piggyBac.** *Nat Genet* 2004, **36**(3):283-287.
95. Nagatsu T, Nakashima A, Ichinose H, Kobayashi K: **Human tyrosine hydroxylase in Parkinson's disease and in related disorders.** *J Neural Transm (Vienna)* 2018, **126**(4):397-409.
96. Stathakis DG, Burton DY, McIvor WE, Krishnakumar S, Wright TR, O'Donnell JM: **The catecholamines up (Catsup) protein of Drosophila melanogaster functions as a negative regulator of tyrosine hydroxylase activity.** *Genetics* 1999, **153**(1):361-382.
97. Stathakis DG, Pentz ES, Freeman ME, Kullman J, Hankins GR, Pearlson NJ, Wright TR: **The genetic and molecular organization of the Dopa decarboxylase gene cluster of Drosophila melanogaster.** *Genetics* 1995, **141**(2):629-655.
98. Hanna ME, Bednarova A, Rakshit K, Chaudhuri A, O'Donnell JM, Krishnan N: **Perturbations in dopamine synthesis lead to discrete physiological effects and impact oxidative stress response in Drosophila.** *J Insect Physiol* 2015, **73**:11-19.
99. Staveley BE, Phillips JP, Hilliker AJ: **Phenotypic consequences of copper-zinc superoxide dismutase overexpression in Drosophila melanogaster.** *Genome* 1990, **33**(6):867-872.
100. Dickson B: **Transgenic lines 1010T2 and 1010T10. Personal Communication to FlyBase.** 1996. <https://flybase.org/reports/FBBrf0086268.html>. Accessed August 22 2022.
101. True JR, Edwards KA, Yamamoto D, Carroll SB: **Drosophila wing melanin patterns form by vein-dependent elaboration of enzymatic prepatterns.** *Curr Biol* 1999, **9**(23):1382-1391.

102. Todd AM, Staveley B.E.: **Novel assay and analysis for measuring climbing ability in *Drosophila*.** *Drosophila Information Services* 87:101-107 2004.
103. Phillips JP, Tainer JA, Getzoff ED, Boulianne GL, Kirby K, Hilliker AJ: **Subunit-destabilizing mutations in *Drosophila* copper/zinc superoxide dismutase: neuropathology and a model of dimer dysequilibrium.** *Proc Natl Acad Sci U S A* 1995, **92**(19):8574-8578.
104. Gaspar P, Almudi I, Nunes MDS, McGregor AP: **Human eye conditions: insights from the fly eye.** *Hum Genet* 2018, **138**(8-9):973-991.
105. Nicholson DA, Sengupta A, Sung HL, Nesbitt DJ: **Amino Acid Stabilization of Nucleic Acid Secondary Structure: Kinetic Insights from Single-Molecule Studies.** *J Phys Chem B* 2018, **122**(43):9869-9876.
106. Smith JE, Sheng ZF, Kallen RG: **Effects of tyrosine-->phenylalanine mutations on auto- and trans-phosphorylation reactions catalyzed by the insulin receptor beta-subunit cytoplasmic domain.** *DNA Cell Biol* 1994, **13**(6):593-604.
107. Schmidt SH, Knape MJ, Boassa D, Mumdey N, Kornev AP, Ellisman MH, Taylor SS, Herberg FW: **The dynamic switch mechanism that leads to activation of LRRK2 is embedded in the DFGpsi motif in the kinase domain.** *Proc Natl Acad Sci U S A* 2019, **116**(30):14979-14988.
108. Anthony C, Ghosh M: **The structure and function of the PQQ-containing quinoprotein dehydrogenases.** *Prog Biophys Mol Biol* 1998, **69**(1):1-21.
109. Das R, Bhattacharjee S, Patel AA, Harris JM, Bhattacharya S, Letcher JM, Clark SG, Nanda S, Iyer EPR, Ascoli GA *et al*: **Dendritic Cytoskeletal Architecture Is Modulated by Combinatorial Transcriptional Regulation in *Drosophila melanogaster*.** *Genetics* 2017, **207**(4):1401-1421.
110. Sepulveda B, Mesias R, Li X, Yue Z, Benson DL: **Short- and long-term effects of LRRK2 on axon and dendrite growth.** *PLoS One* 2013, **8**(4):e61986.
111. Ng M, Diaz-Benjumea FJ, Cohen SM: **Nubbin encodes a POU-domain protein required for proximal-distal patterning in the *Drosophila* wing.** *Development* 1995, **121**(2):589-599.
112. Ross J, Kuzin A, Brody T, Odenwald WF: **Mutational analysis of a *Drosophila* neuroblast enhancer governing nubbin expression during CNS development.** *Genesis* 2018, **56**(8):e23237.
113. Lindberg BG, Tang X, Dantoft W, Gohel P, Seyedoleslami Esfahani S, Lindvall JM, Engstrom Y: **Nubbin isoform antagonism governs *Drosophila* intestinal immune homeostasis.** *PLoS Pathog* 2018, **14**(3):e1006936.
114. Jack J, Dorsett D, Delotto Y, Liu S: **Expression of the cut locus in the *Drosophila* wing margin is required for cell type specification and is regulated by a distant enhancer.** *Development* 1991, **113**(3):735-747.
115. Iyer SC, Ramachandran Iyer EP, Meduri R, Rubaharan M, Kuntimaddi A, Karamsetty M, Cox DN: **Cut, via CrebA, transcriptionally regulates the COPII secretory pathway to direct dendrite development in *Drosophila*.** *J Cell Sci* 2013, **126**(Pt 20):4732-4745.
116. Chen L, O'Keefe SL, Hodgetts RB: **Control of Dopa decarboxylase gene expression by the Broad-Complex during metamorphosis in *Drosophila*.** *Mech Dev* 2002, **119**(2):145-156.
117. Reddy KL, Wohlwill A, Dzitoeva S, Lin MH, Holbrook S, Storti RV: **The *Drosophila* PAR domain protein 1 (Pdp1) gene encodes multiple differentially expressed**

- mRNAs and proteins through the use of multiple enhancers and promoters. *Dev Biol* 2000, **224**(2):401-414.
118. Tronche F, Yaniv M: **HNF1, a homeoprotein member of the hepatic transcription regulatory network.** *Bioessays* 1992, **14**(9):579-587.
 119. Xu M, Zhu J, Liu S, Wang C, Shi Q, Kuang Y, Fang X, Hu X: **FOXD3, frequently methylated in colorectal cancer, acts as a tumor suppressor and induces tumor cell apoptosis under ER stress via p53.** *Carcinogenesis* 2020, **41**(9):1253-1262.
 120. Hu H, Tian M, Ding C, Yu S: **The C/EBP Homologous Protein (CHOP) Transcription Factor Functions in Endoplasmic Reticulum Stress-Induced Apoptosis and Microbial Infection.** *Front Immunol* 2019, **9**:3083.
 121. Maris M, Overbergh L, Gysemans C, Waget A, Cardozo AK, Verdrengh E, Cunha JP, Gotoh T, Cnop M, Eizirik DL *et al*: **Deletion of C/EBP homologous protein (Chop) in C57Bl/6 mice dissociates obesity from insulin resistance.** *Diabetologia* 2012, **55**(4):1167-1178.
 122. Lorenzo PI, Fuente-Martin E, Brun T, Cobo-Vuilleumier N, Jimenez-Moreno CM, I GHG, Lopez Noriega L, Mellado-Gil JM, Martin-Montalvo A, Soria B *et al*: **PAX4 Defines an Expandable beta-Cell Subpopulation in the Adult Pancreatic Islet.** *Sci Rep* 2015, **5**:15672.
 123. Hwang SS, Kim LK, Lee GR, Flavell RA: **Role of OCT-1 and partner proteins in T cell differentiation.** *Biochim Biophys Acta* 2016, **1859**(6):825-831.
 124. Wang J, Xiao K, Hou F, Tang L, Luo D, Liu G, Wang Z: **POU2F1 Promotes Cell Viability and Tumor Growth in Gastric Cancer through Transcriptional Activation of lncRNA TTC3-AS1.** *J Oncol* 2021, **2021**:5570088.
 125. Stepchenko AG, Portseva TN, Glukhov IA, Kotnova AP, Lyanova BM, Georgieva SG, Pankratova EV: **Primate-specific stress-induced transcription factor POU2F1Z protects human neuronal cells from stress.** *Sci Rep* 2021, **11**(1):18808.
 126. Klann M, Seaver EC: **Functional role of pax6 during eye and nervous system development in the annelid *Capitella teleta*.** *Dev Biol* 2019, **456**(1):86-103.
 127. Neyen C, Binggeli O, Roversi P, Bertin L, Sleiman MB, Lemaitre B: **The Black cells phenotype is caused by a point mutation in the *Drosophila* pro-phenoloxidase 1 gene that triggers melanization and hematopoietic defects.** *Dev Comp Immunol* 2015, **50**(2):166-174.
 128. Wright TR: **Phenotypic analysis of the Dopa decarboxylase gene cluster mutants in *Drosophila melanogaster*.** *J Hered* 1996, **87**(3):175-190.
 129. Li J, Mahajan A, Tsai MD: **Ankyrin repeat: a unique motif mediating protein-protein interactions.** *Biochemistry* 2006, **45**(51):15168-15178.
 130. Tewari R, Bailes E, Bunting KA, Coates JC: **Armadillo-repeat protein functions: questions for little creatures.** *Trends Cell Biol* 2010, **20**(8):470-481.
 131. Imai Y, Gehrke S, Wang HQ, Takahashi R, Hasegawa K, Oota E, Lu B: **Phosphorylation of 4E-BP by LRRK2 affects the maintenance of dopaminergic neurons in *Drosophila*.** *EMBO J* 2008, **27**(18):2432-2443.
 132. Neckameyer WS: **Multiple roles for dopamine in *Drosophila* development.** *Dev Biol* 1996, **176**(2):209-219.
 133. Venderova K, Kabbach G, Abdel-Messih E, Zhang Y, Parks RJ, Imai Y, Gehrke S, Ngsee J, Lavoie MJ, Slack RS *et al*: **Leucine-Rich Repeat Kinase 2 interacts with**

- Parkin, DJ-1 and PINK-1 in a *Drosophila melanogaster* model of Parkinson's disease.** *Hum Mol Genet* 2009, **18**(22):4390-4404.
134. Tzolovsky G, Deng WM, Schlitt T, Bownes M: **The function of the broad-complex during *Drosophila melanogaster* oogenesis.** *Genetics* 1999, **153**(3):1371-1383.
135. Yao C, El Khoury R, Wang W, Byrd TA, Pehek EA, Thacker C, Zhu X, Smith MA, Wilson-Delfosse AL, Chen SG: **LRRK2-mediated neurodegeneration and dysfunction of dopaminergic neurons in a *Caenorhabditis elegans* model of Parkinson's disease.** *Neurobiol Dis* 2010, **40**(1):73-81.
136. Liu G, Sgobio C, Gu X, Sun L, Lin X, Yu J, Parisiadou L, Xie C, Sastry N, Ding J *et al*: **Selective expression of Parkinson's disease-related Leucine-rich repeat kinase 2 G2019S missense mutation in midbrain dopaminergic neurons impairs dopamine release and dopaminergic gene expression.** *Hum Mol Genet* 2015, **24**(18):5299-5312.
137. Warner HR: **Superoxide dismutase, aging, and degenerative disease.** *Free Radic Biol Med* 1994, **17**(3):249-258.
138. Offer T, Russo A, Samuni A: **The pro-oxidative activity of SOD and nitroxide SOD mimics.** *Faseb J* 2000, **14**(9):1215-1223.
139. Lundell MJ, Hirsh J: **Temporal and spatial development of serotonin and dopamine neurons in the *Drosophila* CNS.** *Dev Biol* 1994, **165**(2):385-396.
140. Quintero-Espinosa D, Jimenez-Del-Rio M, Velez-Pardo C: **Knockdown transgenic *Lrrk* *Drosophila* resists paraquat-induced locomotor impairment and neurodegeneration: A therapeutic strategy for Parkinson's disease.** *Brain Res* 2016, **1657**:253-261.
141. Wang D, Tang B, Zhao G, Pan Q, Xia K, Bodmer R, Zhang Z: **Dispensable role of *Drosophila* ortholog of LRRK2 kinase activity in survival of dopaminergic neurons.** *Mol Neurodegener* 2008, **3**:3.
142. Ng CH, Mok SZ, Koh C, Ouyang X, Fivaz ML, Tan EK, Dawson VL, Dawson TM, Yu F, Lim KL: **Parkin protects against LRRK2 G2019S mutant-induced dopaminergic neurodegeneration in *Drosophila*.** *J Neurosci* 2009, **29**(36):11257-11262.
143. Arbez N, He X, Huang Y, Ren M, Liang Y, Nucifora FC, Wang X, Pei Z, Tessarolo L, Smith WW *et al*: **G2019S-LRRK2 mutation enhances MPTP-linked Parkinsonism in mice.** *Hum Mol Genet* 2020, **29**(4):580-590.
144. Rudyk C, Dwyer Z, Hayley S: **Leucine-rich repeat kinase-2 (LRRK2) modulates paraquat-induced inflammatory sickness and stress phenotype.** *J Neuroinflammation* 2019, **16**(1):120.
145. Franco JL, Posser Ts, Gordon SL, Bobrovskaya L, Schneider JJ, Farina M, Dafre AL, Dickson PW, Dunkley PR: **Expression of Tyrosine Hydroxylase Increases the Resistance of Human Neuroblastoma Cells to Oxidative Insults.** *Toxicological Sciences* 2009, **113**(1):150-157.
146. Nagatsu T, Nagatsu I: **Tyrosine hydroxylase (TH), its cofactor tetrahydrobiopterin (BH4), other catecholamine-related enzymes, and their human genes in relation to the drug and gene therapies of Parkinson's disease (PD): historical overview and future prospects.** *J Neural Transm (Vienna)* 2016, **123**(11):1255-1278.
147. Latremoliere A, Costigan M: **GCH1, BH4 and pain.** *Curr Pharm Biotechnol* 2015, **12**(10):1728-1741.

148. Shin JH, Lee WW, Lee JY, Kim HJ, Jeon B: **GCH-1 genetic variant may cause Parkinsonism by unmasking the subclinical nigral pathology.** *J Neurol* 2020, **267**(7):1952-1959.
149. Gillis EE, Brinson KN, Rafikova O, Chen W, Musall JB, Harrison DG, Sullivan JC: **Oxidative stress induces BH4 deficiency in male, but not female, SHR.** *Biosci Rep* 2018, **38**(4).
150. Anastasiadis PZ, Kuhn DM, Blitz J, Imerman BA, Louie MC, Levine RA: **Regulation of tyrosine hydroxylase and tetrahydrobiopterin biosynthetic enzymes in PC12 cells by NGF, EGF and IFN-gamma.** *Brain Res* 1996, **713**(1-2):125-133.
151. Wang Z, Ferdousy F, Lawal H, Huang Z, Daigle JG, Izevbaye I, Doherty O, Thomas J, Stathakis DG, O'Donnell JM: **Catecholamines up integrates dopamine synthesis and synaptic trafficking.** *J Neurochem* 2011, **119**(6):1294-1305.
152. Tang X, Xing S, Ma M, Xu Z, Guan Q, Chen Y, Feng F, Liu W, Chen T, Chen Y *et al*: **The Development and Design Strategy of Leucine-Rich Repeat Kinase 2 Inhibitors: Promising Therapeutic Agents for Parkinson's Disease.** *Journal of Medicinal Chemistry* 2023, **66**(4):2282-2307.
153. Ruan W, Srinivasan A, Lin S, Kara k I, Barker PA: **Eiger-induced cell death relies on Rac1-dependent endocytosis.** *Cell Death Dis* 2016, **7**:e2181.
154. Smith WW, Pei Z, Jiang H, Moore DJ, Liang Y, West AB, Dawson VL, Dawson TM, Ross CA: **Leucine-rich repeat kinase 2 (LRRK2) interacts with parkin, and mutant LRRK2 induces neuronal degeneration.** *Proc Natl Acad Sci U S A* 2005, **102**(51):18676-18681.
155. Linhart R, Wong SA, Cao J, Tran M, Huynh A, Ardrey C, Park JM, Hsu C, Taha S, Peterson R *et al*: **Vacuolar protein sorting 35 (Vps35) rescues locomotor deficits and shortened lifespan in Drosophila expressing a Parkinson's disease mutant of Leucine-Rich Repeat Kinase 2 (LRRK2).** *Mol Neurodegener* 2014, **9**:23.
156. Shannon B, Soto-Ortolaza A, Rayaprolu S, Cannon HD, Labbe C, Benitez BA, Choi J, Lynch T, Boczarska-Jedynak M, Opala G *et al*: **Genetic variation of the retromer subunits VPS26A/B-VPS29 in Parkinson's disease.** *Neurobiol Aging* 2014, **35**(8):1958 e1951-1952.
157. Ligoxygakis P, Yu SY, Delidakis C, Baker NE: **A subset of notch functions during Drosophila eye development require Su(H) and the E(spl) gene complex.** *Development* 1998, **125**(15):2893-2900.
158. Parks AL, Turner FR, Muskavitch MAT: **Relationships between complex Delta expression and the specification of retinal cell fates during Drosophila eye development.** *Mechanisms of development* 1995, **50**(2):201-216.
159. Meloty-Kapella L, Shergill B, Kuon J, Botvinick E, Weinmaster G: **Notch ligand endocytosis generates mechanical pulling force dependent on dynamin, epsins, and actin.** *Dev Cell* 2012, **22**(6):1299-1312.
160. Imai Y, Kobayashi Y, Inoshita T, Meng H, Arano T, Uemura K, Asano T, Yoshimi K, Zhang CL, Matsumoto G *et al*: **The Parkinson's Disease-Associated Protein Kinase LRRK2 Modulates Notch Signaling through the Endosomal Pathway.** *PLoS Genet* 2015, **11**(9):e1005503.
161. Xu J, Gridley T: **Notch Signaling during Oogenesis in Drosophila melanogaster.** *Genet Res Int* 2012, **2012**:648207.

162. Starble R, Pokrywka NJ: **The retromer subunit Vps26 mediates Notch signaling during *Drosophila* oogenesis.** *Mech Dev* 2018, **149**:1-8.
163. Bugarcic A, Zhe Y, Kerr MC, Griffin J, Collins BM, Teasdale RD: **Vps26A and Vps26B Subunits Define Distinct Retromer Complexes.** *Traffic* 2011, **12**(12):1759-1773.
164. Duvic B, Hoffmann JA, Meister M, Royet J: **Notch signaling controls lineage specification during *Drosophila* larval hematopoiesis.** *Curr Biol* 2002, **12**(22):1923-1927.
165. de Celis JF, Bray S, Garcia-Bellido A: **Notch signalling regulates veinlet expression and establishes boundaries between veins and interveins in the *Drosophila* wing.** *Development* 1997, **124**(10):1919-1928.
166. Conley CA, Silburn R, Singer MA, Ralston A, Rohwer-Nutter D, Olson DJ, Gelbart W, Blair SS: **Crossveinless 2 contains cysteine-rich domains and is required for high levels of BMP-like activity during the formation of the cross veins in *Drosophila*.** *Development* 2000, **127**(18):3947-3959.
167. Antson H, Tonissoo T, Shimmi O: **The developing wing crossvein of *Drosophila melanogaster*: a fascinating model for signaling and morphogenesis.** *Fly (Austin)* 2022, **16**(1):118-127.
168. Blair SS: **Wing vein patterning in *Drosophila* and the analysis of intercellular signaling.** *Annu Rev Cell Dev Biol* 2007, **23**:293-319.
169. Kim KS, Kim CH, Hwang DY, Seo H, Chung S, Hong SJ, Lim JK, Anderson T, Isacson O: **Orphan nuclear receptor Nurr1 directly transactivates the promoter activity of the tyrosine hydroxylase gene in a cell-specific manner.** *J Neurochem* 2003, **85**(3):622-634.
170. Eells JB, Rives JE, Yeung SK, Nikodem VM: **In vitro regulated expression of tyrosine hydroxylase in ventral midbrain neurons from Nurr1-null mouse pups.** *J Neurosci Res* 2001, **64**(4):322-330.
171. Crews L, Mizuno H, Desplats P, Rockenstein E, Adame A, Patrick C, Winner B, Winkler J, Masliah E: **Alpha-synuclein alters Notch-1 expression and neurogenesis in mouse embryonic stem cells and in the hippocampus of transgenic mice.** *J Neurosci* 2008, **28**(16):4250-4260.
172. Hsouna A, Lawal HO, Izevbaye I, Hsu T, O'Donnell JM: ***Drosophila* dopamine synthesis pathway genes regulate tracheal morphogenesis.** *Developmental Biology* 2007, **308**(1):30-43.